Recent Progress of Laser Processing Technology in Micro-LED Display Manufacturing: A review

Lingxiao Song[1], Xuechao Yong[1*], Peilei Zhang[1*], Shijie Song[1], Kefan Chen[1], Hua Yan[1], Tianzhu Sun[2*], Qinghua Lu[1], Haichuan Shi[1], Yu Chen[3], Yuze Huang[4]

[1] School of Materials Science and Engineering, Shanghai University of Engineering Science, Shanghai 201620, China

[2] Warwick Manufacturing Group (WMG), University of Warwick, Coventry CV4 7AL, UK

[3] Amplitude Shanghai Laser Technology Company Ltd., Shanghai 200127, China

[4] Department of Engineering, Lancaster University, Lancaster LA1 4YW, UK

[*] Correspondence authors: yongxuechao@sues.edu.cn (Xuechao Yong), peilei@sues.edu.cn (Peilei Zhang) and tianzhu.sun@warwick.ac.uk (Tianzhu Sun)

Abstract

Micro-LED undoubtedly stands out as a highly anticipated technology when it comes to the innovation of future display technologies. Micro-LED technology surpasses traditional display technologies regarding color representation, energy efficiency, and flexibility by individually assembling tiny light-emitting diodes on a substrate. Micro-LED technology, a further evolution of LED, is considered the most promising next-generation display technology due to its outstanding brightness, high contrast ratio, and extremely high pixel density. The application of laser technology in Micro-LED displays is increasingly becoming a focus of research and industry. As a highly integrated light source, lasers offer unique advantages in Micro-LED applications, including high-energy density processing, non-contact processing, precise microstructure processing and sculpting capability, efficient packaging, and improved device quality and reliability. These advantages provide a distinctive edge in achieving high-precision manufacturing and assembly of Micro-LED chips. Laser epitaxy substrate technology utilizes laser heating and material deposition to grow Micro-LED chips on a substrate. Laser etching technology achieves precise control of lasers to enable microstructure processing and sculpting of Micro-LED devices. Laser lift-off technology utilizes laser-induced decomposition of GaN to peel off the underlying material, allowing for the

separation of Micro-LEDs. Laser-based massive transfer technology uses the energy of lasers to swiftly and accurately transfer Micro-LEDs from the substrate to the target substrate, enabling rapid device transfer. Lastly, laser repair technology is employed for the detection and repair of potential defects in Micro-LEDs, enhancing device quality and reliability. By utilizing lasers, we can expect to achieve higher production efficiency, more precise device manufacturing, and superior optoelectronic performance in the field of Micro-LED, thereby presenting broader prospects for future display technology and lighting applications. These laser technologies provide new solutions for Micro-LED devices' high-precision and high-efficiency production.

Keywords: Micro-LED; laser epitaxy substrates; laser etching; laser lift-off; laser mass transfer; laser repair.

1. Introduction

1.1 Micro-LED

Micro LED technology has emerged as a frontier field in the next-generation display landscape, attracting widespread attention and research. The current mainstream display technologies include liquid crystal display (LCD), organic light-emitting diode (OLED), and micro-light-emitting diode (Micro-LED). These three display technologies exhibit significant differences in various performance metrics, such as high ambient contrast ratio (ACR), fast motion picture response time (MPRT), wide viewing angle, wide color gamut, low power consumption, high pixel density, low cost, long lifespan, and thin/flexible form factors [1–14].OLED and Micro-LED, owing to their self-emissive nature, can achieve extremely high ambient contrast ratios up to 100,000:1, far surpassing the typical 5:1 contrast ratio of conventional LCDs [3], even though the recently developed Mini-LED backlit LCDs for VR applications can reach a contrast ratio of 106:1. Additionally, Micro-LED displays have a speedy response time, typically in the nanosecond range. OLED displays can achieve a response time of 0.1ms, significantly better than the 2-8ms of LCDs, effectively mitigating motion blur[3]. The self-emissive nature of Micro-LED and OLED also grants them wide and

uniform viewing angles of more than ±80°, far surpassing the severe viewing angle dependence of LCDs [12].

In terms of color performance, quantum dot (QD)-based liquid crystal displays (LCDs) can achieve over 85% of the Rec. 2020 color gamut [15]. This allows them to match or even exceed the color range of advanced OLED televisions in certain cases [3,6,14]. Both QD-LCDs and OLEDs demonstrate wider color gamuts compared to RGB micro-LEDs, primarily due to the full width at half maximum (FWHM) of the green LEDs, which is approximately 50 nm. Although micro-LED technology is often lauded for its potential low power consumption, the actual power consumption is influenced by various factors, such as resolution, pixel size, brightness, ambient contrast ratio, and average picture level (APL) [16]. Furthermore, as the chip size of micro-LEDs decreases, their external quantum efficiency (EQE) may decline, impacting overall energy efficiency [7]. Therefore, while micro-LEDs can provide significant energy savings, these benefits depend on specific operating conditions and design choices. Regarding pixel density, both OLED and micro-LED technologies have demonstrated resolutions ranging from 5,000 to 10,000 PPI, effectively meeting the high-resolution requirements of AR/VR applications [3,5]. For LCDs, utilizing silicon-based liquid crystal on silicon (LCoS) instead of active matrix LCDs is advantageous. AR-based LCoS panels typically feature pixel pitches of less than 4 μm, resulting in pixel densities greater than 6,000 PPI, which also satisfies the demands of AR applications [17,18]. However, micro-LED technology exhibits more pronounced advantages over both OLED and LCoS technologies. The self-emissive nature of micro-LEDs enables independent control of each pixel, resulting in higher contrast ratios and faster response times, which are particularly critical for dynamic scene displays.

On the cost front, traditional LCDs are relatively low-cost, around $200 per square meter, but the introduction of mini-LED backlighting has increased the cost to $500 per square meter. OLED costs have steadily decreased with process optimization, approaching LCD levels, while Micro-LED costs remain higher at around $1,000 per square meter [7]. In terms of lifespan, Micro-LED can achieve over 100,000 hours, on par with LCDs, while OLED organic materials have a relatively shorter lifespan. However, new device structures and encapsulation techniques have extended OLED lifetimes to 30,000-50,000 hours [1,6,8,10–12,14]. Furthermore, the organic-based OLED exhibits excellent flexibility, enabling the realization of ultra-thin displays with a thickness of only 0.5mm and showcasing applications in rollable and foldable screens [2,9]. In contrast, LCDs are

limited by the backlight unit, typically 6-10mm thick. Micro-LED has also demonstrated applications on 5μm-thick flexible substrates[5]. These advantages position Micro-LED as a promising technology for televisions, smartphones, wearable devices, automotive displays, and AR/VR applications.

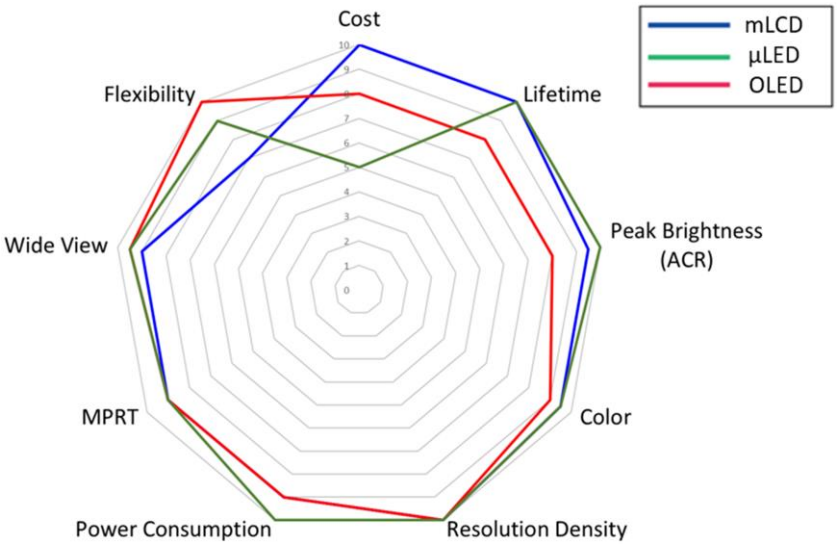

Figure 1. Display performance metrics comparison between mLCD, RGB OLED, and RGB micro-LED displays. [13]

Micro-LED is essentially a technology that miniaturizes LEDs. 1991 the first gallium nitride (GaN)--based blue LED chip was developed, laying the foundation for large-scale LED color displays [19]. Early color LED displays used a combination of RGB colors, but the package size was large, with a pixel spacing of about 20mm. With the advancement of LED miniaturization and packaging technology, the pixel spacing gradually decreased to about 3mm. Subsequently, mini-LEDs emerged, with LED sizes reduced to less than 100μm and pixel spacing of about 0.2mm. Micro-LEDs reduce the LED size to less than 50μm [20]. In 2000, Hong Xing Jiang's laboratory team at Texas Tech University successfully fabricated blue Micro-LEDs based on InGaN/GaN quantum well structures, creating a chip array with a size of 0.5mm × 0.5mm, with individual chip sizes of 12μm [21]. In 2004, Chan and other researchers fabricated the first UV Micro-LED array based on AlInGaN structures, with an emission unit size of 20μm [21]. In 2012, Hong Xing Jiang's laboratory team further fabricated a 10×10μm chip array and integrated it with a CMOS active array driver, achieving display performance [22]. In 2013, the research group LED by Liu at the Hong Kong University of Science and Technology fabricated a silicon-based light-emitting diode (LEDoS) micro-display with a size of 50μm and a pixel density of 360 ppi. One year later, they forged a blue

LEDoS with a size of 15μm and a pixel density of 1700ppi [23][24]. In 2015, Han and other researchers reported a full-color RGB LED with a size of 35×35μm and a pixel spacing of 40μm, achieving color display using aerosol jet printing of quantum dots [25]. In 2018, Liu's team fabricated a Micro-LED with a pixel density 2500ppi, driven by CMOS, and equipped with various functions such as micro-display, temperature sensing, illumination, and light detection [26]. In 2020, Smith and other researchers used self-alignment technology to fabricate Micro-LED chips with a minimum diameter of 1μm. They observed that their surface mesa structure formed a conical shape with a tilt angle 60°. The research showed that green LEDs smaller than 10μm were no longer affected by side effects, while blue LEDs still exhibited side effects [27]. In 2021, Zhang and other researchers based on silicon-based CMOS driving of Micro-LED arrays and combined with red and green quantum dot technology achieved a full-color display with a pixel density of 317ppi [28]. In the same year, Samsung Group introduced an advanced 1000-inch version of their "The Wall" product. In 2022, a research team led by H.W. Jang explored a multi-layer sapphire thin film technology, which facilitated the transfer of Micro-LEDs and significantly reduced the efficiency degradation issues encountered during the transfer process [29]. Then, in 2023, a team led by J. Kim from the Massachusetts Institute of Technology developed a vertical stacking Micro-LED technology. This approach achieved an array density as high as 5100 PPI, with a pixel size of only 4 μm [30]. Due to the size reduction, Micro-LEDs can be used to create presentations with high pixel density. Innovative fabrication techniques and advancements in equipment have also improved the optoelectronic performance of Micro-LEDs, offering broad prospects for development in the display field.

Micro-LED revolves around the fabrication and packaging of micro-sized LED chips. Each Micro-LED chip has dimensions ranging from tens to hundreds of micrometers and consists of red, green, and blue LEDs. Due to their small size, Micro-LED chips exhibit superior performance in terms of flexibility and stretchability compared to larger-sized chips. Compared to traditional LCD and OLED technologies, Micro-LED offers smaller pixel pitch and higher pixel density, enabling the display of more pixels within the same area, resulting in finer and more realistic image quality.

Like traditional large-sized LEDs, Micro-LEDs have three different device structures: flip-chip, inverted chip, and vertical chip [31]. Flip-chip Micro-LEDs are the most commonly used because they are easier to bond and integrate onto the driving backplane. They are more efficient

than their top-emitting counterparts [32]. Vertical chips are also highly efficient, but their integration is more complex due to the relative positioning of the two electrodes.

1.2 Luminescence Principle

Micro-LED is an electroluminescent device composed of P-type and N-type semiconductors. It utilizes the radiative recombination of holes generated in the P-region and electrons developed in the N-region [33]. Due to the concentration gradient, the holes caused in the P-region and the electrons generated in the N-region diffuse towards the N-region and P-region, creating a built-in electric field at the junction, forming a PN junction. Under the influence of the built-in electric field, electrons drift toward the N-region while holes drift toward the P-region. Diffusion and drift reach a dynamic equilibrium in the absence of an external electric field, as shown in Figure 2(a)；

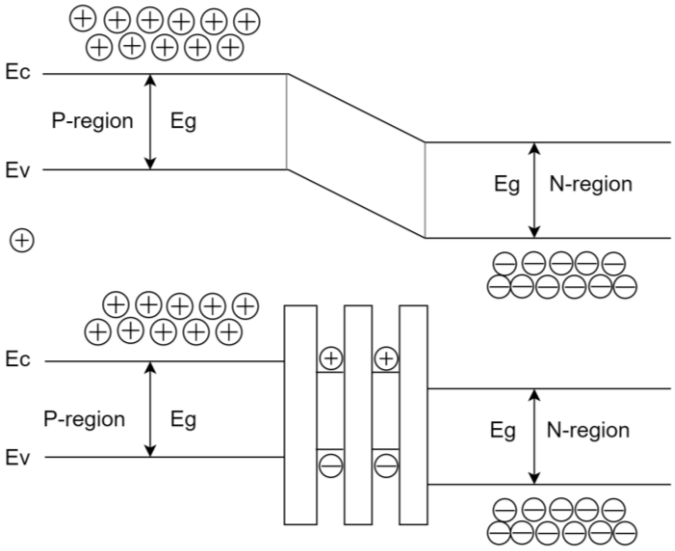

Figure 2. (a) without quantum well structure (b) with quantum well structure.

Applying a forward bias voltage weakens the strength of the built-in electric field, enhancing the diffusion motion and promoting the recombination of electrons and holes. Radiative recombination generates photons, resulting in LED emission. The region where radiative recombination occurs is known as the active region. Researchers have proposed using quantum well structures to increase the probability of electron-hole recombination, as shown in Figure 2(b). Quantum wells are formed by the periodic growth of two thin-film materials with varying band gaps. The materials with different bandgap widths include a potential barrier and a potential well, typically having a narrower bandgap and the wall having a wider bandgap. This arrangement effectively

confines electrons and holes within the potential well, increasing the probability of recombination. The emitted wavelength of the LED can be determined by the bandgap width of the semiconductor material in the quantum well layers, given by λ (nm) =1.24 / Eg. The LED wavelength can cover the ultraviolet to infrared by changing the fabric. Multiple quanta well structures can precisely control the position and structure of energy bands, enabling efficient electron-hole recombination. However, poor carrier matching and reduced radiative recombination rates can occur in multiple quantum wells under low current density injection conditions, decreasing light emission efficiency. To address this issue, recent research has found that reducing the number of quantum wells improves carrier matching, enhancing light emission efficiency. Figure 3 illustrates the relationship between the number of quantum wells and carrier matching under low current-density injection conditions. The bilayer quantum well exhibits the highest radiative recombination rate and light efficiency due to its excellent carrier-matching effect [34].

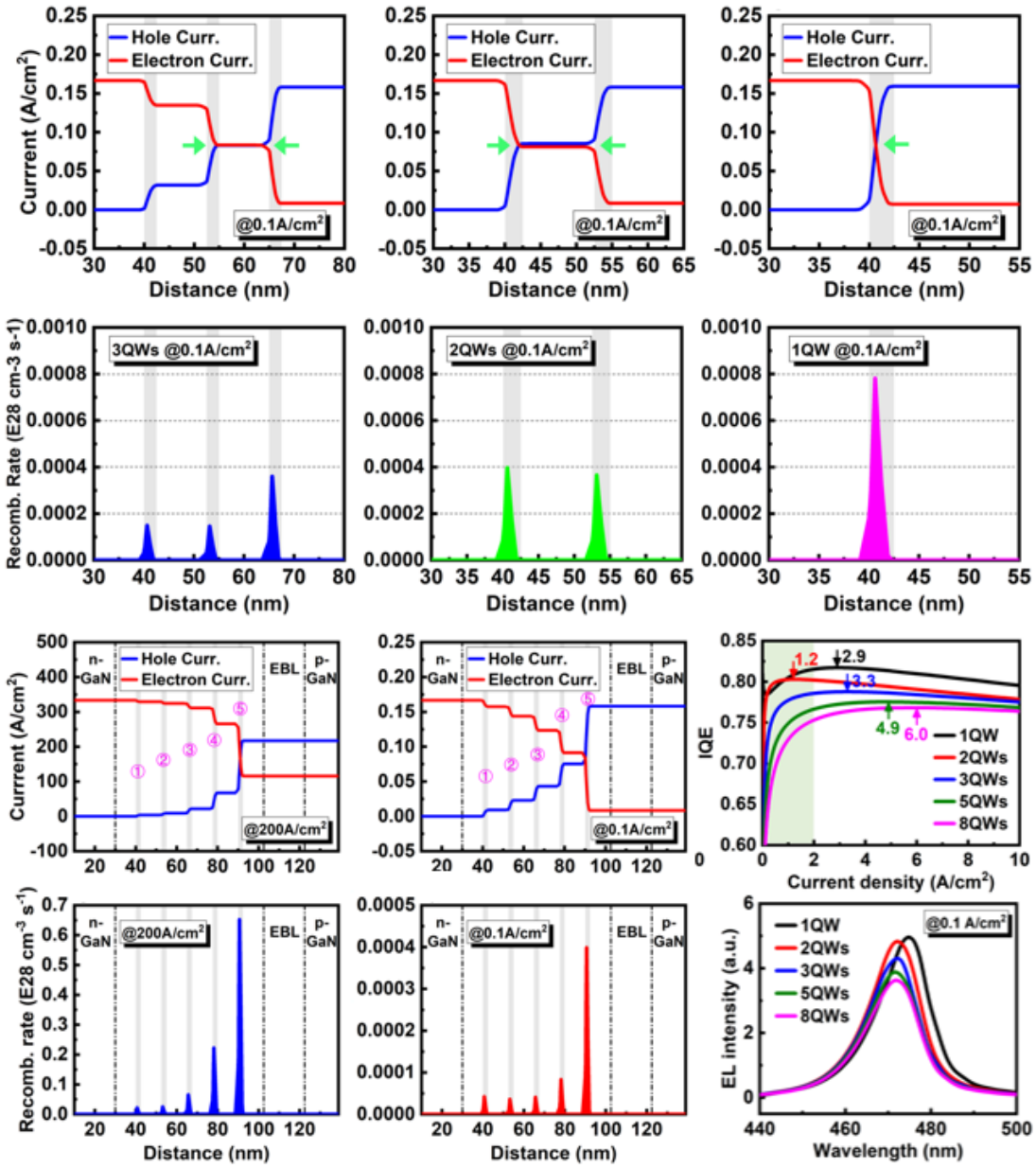

Figure 3. Matching of Quantum Well Quantity and Carrier at Low Current Density. [34]

Not all of the energy from electron-hole recombination is converted into photons. During this process, some of the recombination energy is released as heat. This energy-release process is known as non-radiative recombination, while the energy-release process in the form of light is referred to as radiative recombination. Non-radiative recombination processes include Shockley-Read-Hall (SRH) recombination, Auger recombination, carrier leakage, and others, depending on the specific circumstances [35,36]. SRH recombination refers to recombination processes that occur in defects, and dislocations, impurities, and other factors increase the likelihood of SRH recombination, affecting device performance. Auger recombination generally refers to transferring recombination energy to a third carrier, which is then dissipated in the form of photons. Compared to SRH

recombination, Auger recombination occurs with a much lower probability. Carrier leakage refers to electrons crossing over the quantum well and recombining with holes in the P region. The electron leakage from the quantum well to the P region is more likely to occur in a polarized electric field, where the energy bands are tilted and the barrier is lowered. An electron-blocking layer is added to the epitaxial layer structure to suppress carrier leakage.

Compared to LEDs, high-performance Micro-LED chips exhibit a higher probability of radiative recombination between electrons and holes, resulting in a greater likelihood of emitting photons from the surface of the device. Efficiency parameters associated with Micro-LEDs include internal quantum efficiency, light extraction efficiency, external quantum efficiency, and optoelectronic conversion efficiency. Internal quantum efficiency is the ratio of the number of photons generated per second from the active region to the number of electrons injected into the chip. External quantum efficiency is the ratio of the number of photons emitted into space per second to the number of electrons injected into the chip. Light extraction efficiency is the ratio of the number of photons emitted into the free room per second to the number of photons generated in the active region. It can be observed from the definitions that the ratio of external quantum efficiency to internal quantum efficiency gives the light extraction efficiency. Wall-plug efficiency (WPE) refers to the balance of the optical power of emitted photons to the input electrical power (product of forward voltage and forward current) after applying a forward current [37]. Optoelectronic conversion efficiency is a macroscopic concept, while external quantum efficiency is a microscopic concept.

Micro-LEDs' high-performance characteristics include increased radiative recombination probability between electrons and holes, improved photon emission probability, enhanced internal quantum efficiency, light extraction efficiency, external quantum efficiency, and optoelectronic conversion efficiency. Researchers have utilized laser processing to study and improve LED technology, leading to several advancements. Laser processing exhibits the following benefits in enhancing the light-emitting performance of Micro-LEDs:

- Laser processing enables precise micrometer-scale fabrication. By creating microstructures or optical surface treatments on the Micro-LED structure, light reflection and refraction within the device can be increased, thereby improving light extraction efficiency. By optimizing light extraction efficiency, more photons can escape from the device, resulting in higher output

brightness and efficiency.

- Laser processing helps produce more uniform and regular Micro-LED structures, reducing defects and impurities, thus lowering the probability of non-radiative recombination and improving external quantum efficiency. This means more electrons and holes will release energy through radiative recombination, generating more photons.
- Laser processing enables the fabrication of exact and consistent device structures and dimensions, ensuring similar probabilities of electron-hole recombination for each Micro-LED, thereby enhancing internal quantum efficiency.

1.3 Laser Manufacturing in Micro LED

Micro-LED, as an emerging display technology, possesses numerous advantages. However, the commercialization of Micro-LED technology still faces several challenges, including the precise operation, high efficiency, and high cost involved in Micro-LED chips' fabrication and packaging processes. To address these issues, laser technology has been introduced into the fabrication and packaging of Micro-LEDs, providing new solutions.

Firstly, the fabrication process of Micro-LEDs is highly complex and requires precise techniques. Due to the small size of Micro-LED chips, typically ranging from tens to hundreds of micrometers, micro-level positioning, alignment, and assembly operations are extremely challenging. As the size and surface area of LED chips decrease, the proportion of etch-damaged regions to active regions increases, forming more defects during the etching process. This leads to an increase in non-radiative Shockley-Read-Hall (SRH) recombination rates and a decrease in light efficiency [38]. Additionally, there is a risk of leakage current in the sidewall-damaged regions, further reducing the reliability of the chips. Moreover, the fabrication of Micro-LEDs also demands highly uniform light-emitting characteristics and color consistency, imposing higher requirements on material selection, growth condition control, and process optimization.

Secondly, the mass transfer process of Micro-LEDs also encounters difficulties. Mass transfer is crucial in transferring Micro-LED chips from the growth substrate to the target substrate. Multiple massive transfers of Micro-LED chips are required to integrate Micro-LED with circuit driving in display arrays (at least from a sapphire substrate to a temporary substrate and then to a new

substrate), and each transfer involves many chips. This process demands high stability and precision in the transfer technique [39]. For RGB full-color displays, since each process can only produce chips of one color, the R/G/B chips need to be transferred separately. This requires extremely accurate positioning of the chips, greatly increasing the difficulty of the transfer process. Micro-LED chips have a thickness of only a few micrometers, making it challenging to place them onto the target substrate precisely. Moreover, the chip sizes and spacing are small, presenting a significant challenge in connecting the chips to the circuitry [40,41].

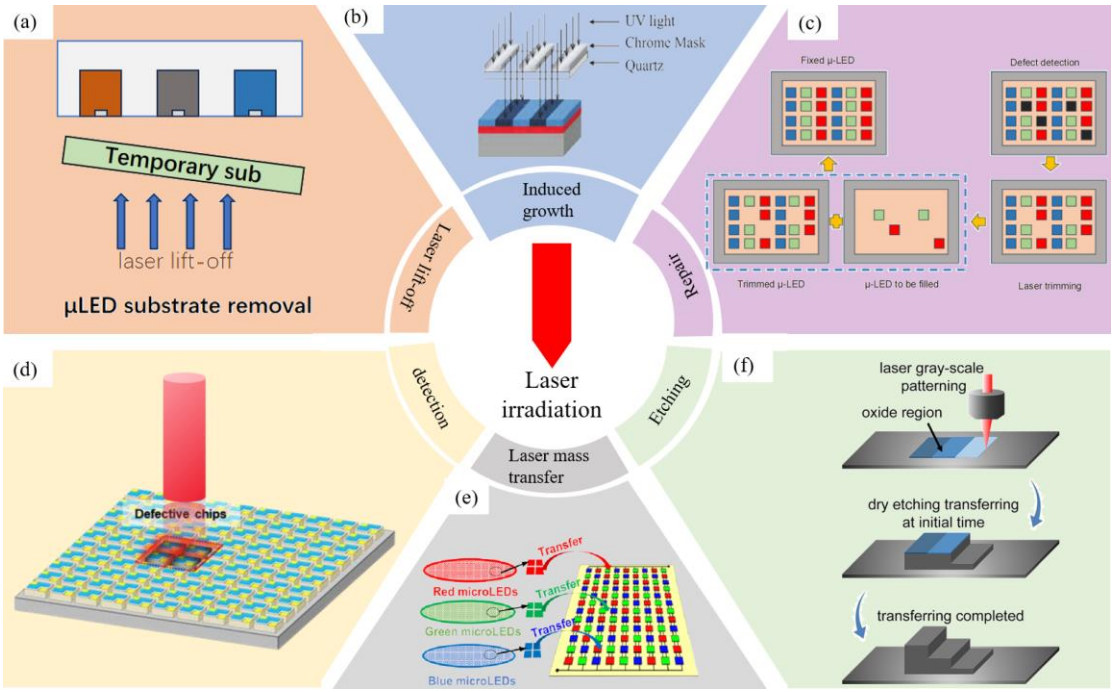

Figure 4. Application of Laser in Micro LED Manufacturing (a) Laser lift-off. (b) Induced Growth. [42] (c) Repair. [43] (d) Detection of Damaged Chips. [44] (e) Transfer [45] (f) Laser Etching. [46]

Currently, the fabrication and transfer processes of Micro-LEDs primarily rely on semiconductor processes and manual operations, which are feasible for small-scale production but present many challenges for large-scale production. Issues such as the high cost of production equipment, stability and consistency of growth processes, chip selection, and screening need to be addressed. Ensuring high efficiency, repeatability, and consistency in the production process is also challenging.

Micro-LEDs face difficulties and challenges in areas such as fabrication, mass transfer, texture treatment, and large-scale production, and laser technology plays an indispensable role in the manufacturing and processing of micro-LEDs. The technology that lasers can provide for the

manufacturing of Micro LEDs is shown in Figure 4. Laser technology offers specific applications and advantages of micro-led output, primarily in the following aspects:

- High precision: Laser technology enables high-precision fabrication of Micro-LED chips. Techniques such as laser etching and laser-induced growth allow for micro-level structural processing and precise control of crystal growth. This high-precision fabrication can improve the pixel uniformity, device performance, and display quality of Micro-LEDs.
- Efficient packaging: Laser technology has advantages in the packaging process of Micro-LEDs in terms of efficiency. Laser lift-off and mass transfer techniques enable fast and precise chip separation and transfer, improving packaging efficiency and production speed. Compared to traditional mechanical delamination and transfer methods, laser technology features non-contact, high efficiency, and high precision, reducing chip damage and enhancing packaging quality.
- High-energy density processing: Lasers possess high energy density, enabling precise processing of Micro-LED chips. Laser etching techniques can achieve micro-level texture treatment, enhancing light extraction efficiency and optical uniformity. Laser repair techniques can perform localized chip repairs, improving chip reliability and repeatability. These high-energy density processing techniques provide more flexibility and refinement to the fabrication and packaging processes of Micro-LEDs.
- Non-contact nature: Laser processing is a non-contact method that does not require physical contact with the material surface, thereby reducing damage and contamination to Micro-LED chips. This is crucial for ensuring the quality and reliability of Micro-LEDs.

The article provides an overview of various applications of laser technology in Micro-LED processing, including substrate epitaxy, laser etching, substrate removal, laser mass transfer, and laser repair. These laser techniques play a significant role in fabrication by enabling precise processing and optimization of Micro-LED chips through their high precision, efficiency, and controllability. Hopefully, these laser technologies will contribute to the development and industrial application of Micro-LED technology.

2. Laser processing method in Micro-LED manufacturing

The manufacturing process of Micro-LED includes substrate epitaxy, laser etching, substrate removal, and laser mass transfer. Firstly, GaN and other materials are grown layer by layer on the substrate through substrate epitaxy. Next, photolithography techniques transfer patterns onto the epitaxial layer, including electrodes and micro-groove structures. Subsequently, excess materials are removed through the etching process to achieve the desired structures and morphology. Then, the epitaxial layer is detached from the substrate using peeling techniques. Following that, the Micro-LED chips on the detached epitaxial layer are massively transferred onto a target substrate using laser technology. Finally, in the integration stage, the transferred Micro-LED chips undergo packaging and interconnection processes to realize their final applications.

2.1 Substrate Epitaxy

In the fabrication process of Micro-LEDs, substrate epitaxy technology plays a crucial role. Laser, as a powerful tool and method, is widely employed in the substrate epitaxy process of Micro-LEDs, providing new possibilities for achieving high-quality Micro-LED devices. The unique advantage of laser substrate epitaxy technology lies in its ability to precisely control the growth and structure of materials, thereby optimizing the performance and reliability of Micro-LEDs.

When selecting a substrate for GaN-based LED materials, several factors need to be considered, including lattice matching with GaN, matching of thermal expansion coefficient with GaN, good stability, high thermal conductivity, and low cost. Currently, most commercially available GaN-based LEDs are fabricated on sapphire substrates. This is mainly because sapphire has the same wurtzite crystal structure as GaN, and its Al_2O_3(0002) plane can serve as the epitaxial surface [47]. Additionally, sapphire exhibits good thermal stability and high mechanical strength, ensuring the stability of LED device performance.

However, there exists a significant lattice mismatch (approximately 13.2% [47,48]) and a mismatch in thermal expansion coefficients (approximately 27%) between sapphire and gallium nitride. Moreover, sapphire has lower thermal conductivity (0.25 W/(cm·K)), which poses challenges for the development of "high-performance, high-power, and low-cost" LED chips on

sapphire substrates.

Despite the limitations of sapphire's low thermal conductivity, it has the advantage of high transparency, making it suitable for visible and ultraviolet light and enabling efficient light transmission. This allows for the selection of shorter-wavelength lasers on sapphire substrates to improve material absorption efficiency. In contrast, silicon substrates have higher absorption capabilities for visible and near-ultraviolet light, requiring the selection of longer-wavelength lasers. Additionally, sapphire exhibits excellent thermal conductivity, aiding in efficient heat dissipation and temperature control during growth. However, as a semiconductor material, silicon has higher thermal conductivity, enabling better heat dissipation. The physical properties of the sapphire substrate and silicon substrate are shown in Table 2.

Table 2. Physical Properties of Sapphire and Silicon. [47,48]

	Sapphire	Si
lattice constant(nm)	A=0.4760	A=0.5431
	C=1.2991	C=0.5431
lattice mismatch(%)	0.08	17
Thermal expansion coefficient(10^{-6}/K)	9.03 // c axis	2.62
	5.0 ⊥ c axis	
thermal conductivity(W/(cm*K))	0.23 // c axis	156
	0.25 ⊥ c axis	
Bandgap(eV)	8.1-8.6	1.1
melting point(℃)	2030	1414

The preparation steps for the substrate include surface treatment, growth of the emission layer, and electrode preparation. The growth of the emission layer requires the use of substrate epitaxy techniques. Currently, the widely applied techniques for growing gallium nitride (GaN) layers include Metal-Organic Chemical Vapor Deposition (MOCVD), Pulsed Laser Deposition (PLD), and Laser Molecular Beam Epitaxy (LMBE). Both pulsed laser deposition and laser molecular beam epitaxy involve the use of lasers. Regarding the defect density and crystal quality of the epitaxial layers, the laser-assisted LMBE technique can produce the highest-quality epitaxial layers, with a defect density as low as 10^4 cm^{-2} [49]. Some advanced LMBE systems and optimization methods can even reduce the defect density to the 10^3 cm^{-2} level[50], achieving the best crystal quality. In comparison, the MBE process can also reach a defect density in the 10^4-10^5 cm^{-2} range[51–53], with

excellent crystal quality. The laser-assisted PLD [54] technique can also improve the quality of the epitaxial layers, with a defect density in the 10^4-10^5 cm^{-2} range. MOCVD [55] epitaxy has a slightly higher defect density, generally in the 10^6-10^7 cm^{-2} range[56–58].

In terms of the epitaxial growth rate, the laser-assisted PLD technique shows a clear advantage, with a high growth rate of 10-15 μm/h[59,60], significantly shortening the epitaxial preparation time [61]. MOCVD and MBE[62,63] are relatively slower, with growth rates of only around 2-3 μm/h and 1 μm/h, respectively [64]. The growth rate of laser-assisted LMBE is slightly higher compared to MBE, at around 3-5 μm/h[65,66], but still relatively slow.

From the mechanism perspective, MOCVD relies on chemical vapor deposition[67,68], MBE utilizes the precise control of molecular beams, while PLD and LMBE leverage laser technology to achieve epitaxy. The two laser-assisted methods can better control the heat input and material transport processes, thereby improving the epitaxial quality. For applications seeking high epitaxial growth rates and good epitaxial quality, the laser-assisted PLD technique is undoubtedly the optimal choice[69,70]. However, if there are higher requirements for the fine control of the epitaxial layer and the defect density, the MBE and laser-assisted LMBE processes would be more suitable[71]. As a more traditional method, MOCVD has certain advantages in terms of cost and production efficiency[72,73].

In addition to epitaxy techniques directly applied to the substrate, laser-patterned sapphire substrate (LPSS) can indirectly assist in obtaining high-quality GaN during epitaxial growth.

2.1.1 Pulsed laser deposition (PLD)

PLD is a surface treatment technique used for epitaxial growth. Figure 5 illustrates the principle of PLD. The principle of PLD involves irradiating the target material with laser pulses and transferring energy to the surface atoms and molecules of the target material. This imparts sufficient kinetic energy to them, causing them to leave the target surface at high speeds. The atoms and molecules leaving the target form a plasma plume, which deposits onto the substrate, forming a thin film.

Compared to the widely used MOCVD technique, PLD offers highly precise material control. The laser provides precise energy focusing, allowing for localized growth and deposition at the micron level, enabling more accurate structural control. PLD can be performed at relatively low

temperatures for material growth. In contrast, MOCVD typically requires high-temperature chemical reaction processes, which can lead to thermal decomposition and uneven growth of materials. PLD applies to various types of materials and substrates, including silicon, sapphire, and other substrate types.

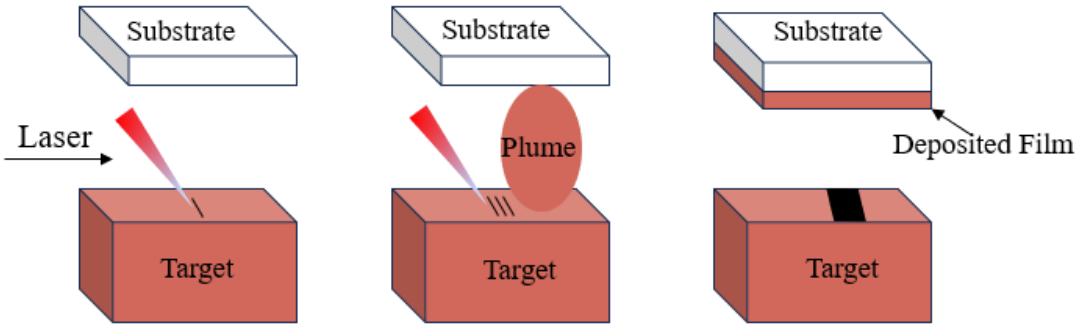

Figure 5. Schematic Diagram of PLD Principle.

The PLD technique was first employed in 1965 to fabricate optical thin films successfully [74]. However, due to limitations in laser technology, the results were not satisfactory, and the PLD technique remained stagnant for several years. It was not until the 1970s, when short-pulsed lasers, particularly the application of KrF excimer lasers, emerged that the PLD technique regained attention. Notably, Dijkkamp et al. from Bell Laboratories [75] achieved the successful fabrication of high-temperature superconducting thin films, specifically $YBa_2Cu_3O_7$-δ, using the PLD technique with KrF excimer lasers. This breakthrough propelled the rapid development of the PLD technique, making it one of the best methods for thin film fabrication within a few years. Moreover, it gradually found application in the field of epitaxial growth of GaN thin films.

The distance between the laser pulse and the substrate is a parameter that requires careful control. M. Kawwam [76] investigated the influence of different target-substrate distances and laser energy densities on substrate epitaxy. As shown in Figure 6(a), the distance between the GaN target and the sapphire substrate and the deposition axis was modified. The study revealed that, in the (0002) direction, as the working distance increased from 8 to 10 cm, the intensity increased, while the root mean square (RMS) value of surface roughness decreased to approximately 10 nm. SEM images (Figure 6(b)) demonstrated that as the working distance increased to approximately 10 cm, particle elimination occurred, resulting in improved surface smoothness.

The energy density of the laser pulse is another important parameter. By adjusting the energy density of the laser pulse, the deposition rate and quality of the material can be controlled. Higher

energy density can promote faster deposition rates, but if the energy density is too high, it may lead to structural deformation and the generation of defects in the material. While maintaining the same spot size and shape, M. Kawwam [76] increased the laser energy density from 0.75 to 1.25 J/cm^2 by raising the discharge voltage of the light source. XRD data in Figure 6(c) shows an intensity increase in (0 0 0 2) orientation of samples grown at lower fluence down to 0.75 J/cm^2. SEM images in Figure 6(d) demonstrate that as the fluence decreases, the surface roughness reduces, and the target droplets begin to disappear from the surface. The RMS surface roughness is less than 3 nm at the lowest fluence. The initial energy flux of material in PLD is typically on the order of 100 eV, significantly higher than the optimal value (≤10 eV) required for high-quality thin film growth. Therefore, increasing the distance between the target and the substrate is necessary while reducing the laser energy density. PLD has certain advantages in research and small-batch production. It uses laser pulses to evaporate source materials and deposit them onto substrates, offering high flexibility and adaptability. It enables rapid sample preparation and prototype development. However, there may be some challenges in large-scale production, such as slow growth rates and control of uniformity.

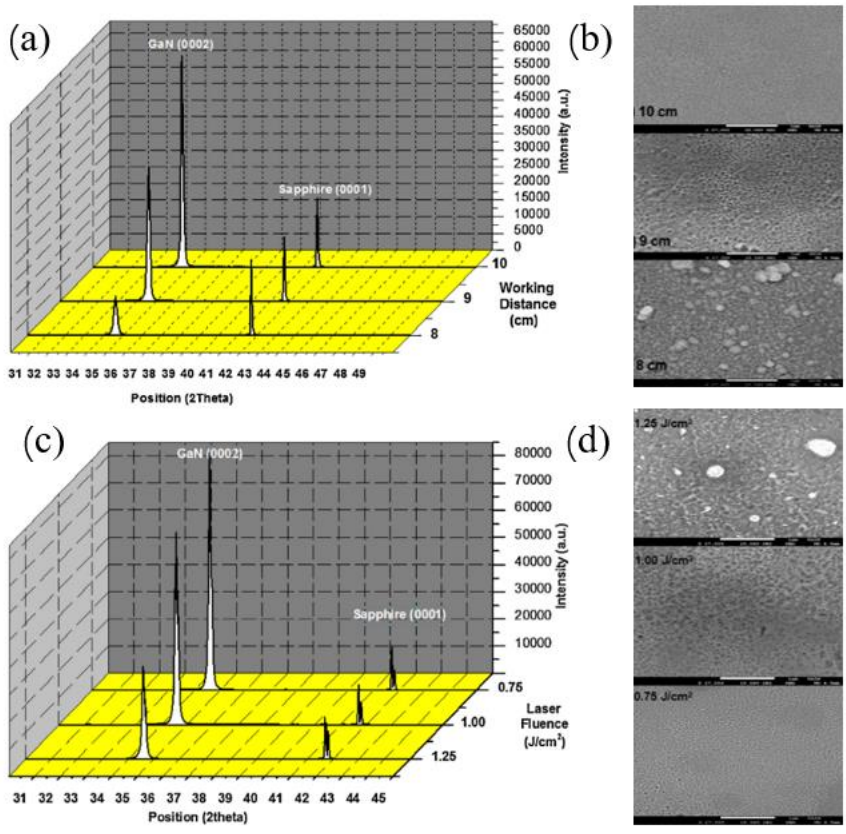

Figure 6 (a) XRD spectra were obtained for GaN thin films grown on conventional sapphire substrates at varying

target-substrate distances, ranging from 8 cm to 10 cm. (b) SEM images were taken of GaN thin films deposited on conventional sapphire substrates at different target-substrate distances. (c) XRD spectra were collected for GaN thin films grown on conventional sapphire substrates using different laser energy densities. (d) SEM images were captured of GaN thin films deposited on conventional sapphire substrates at different laser energy densities. [76]

In recent years, research on GaN thin film growth using PLD epitaxial techniques has shown two major trends. Firstly, researchers have been exploring the advantages of low-temperature growth using PLD and continuously investigating the epitaxial growth of GaN thin films on novel substrates other than sapphire and silicon, such as SiC and metallic materials [77]. Secondly, buffer layer techniques have been employed to overcome the lattice mismatch issue between GaN films and substrates, thereby improving the quality of GaN thin films. For example, Si substrates are suitable for large-scale production.

The quality of the substrate itself and its compatibility with the thin film directly impact the crystal quality and optoelectronic properties of GaN films. Therefore, selecting a suitable substrate is crucial for heteroepitaxial growth of GaN thin films. PLD technology, by providing the driving force for thin film growth through lasers, lowers the temperature requirements for substrates, thus significantly expanding the range of substrate choices. From the existing research literature on PLD-grown GaN, substrates used include not only sapphire but also SiC, metallic substrates, and others [77–80].

The lattice mismatch between SiC substrates and GaN is only 3.5%, which is much lower than that of sapphire. Additionally, SiC has good conductivity and high thermal conductivity, making it suitable for the fabrication of vertical device structures. However, SiC does not have a thermal advantage over sapphire, and the wetting behavior between GaN and SiC is poor. Although this can be improved by using an AlN buffer layer, it increases the resistance between the GaN thin film and the substrate, which is detrimental to the fabrication of vertical device structures [81].

Metal materials have good conductivity, which is beneficial for the fabrication of vertical structures. They have low resistance and heat generation. Metal materials also have excellent thermal conductivity, which is advantageous for device heat dissipation, reducing junction temperature, and improving the quantum effects within the device [82]. To overcome the drawbacks of insulating sapphire, researchers have used laser lift-off techniques to transfer GaN thin films from sapphire substrates to metal substrates before device fabrication [83]. However, the process of

transferring GaN thin films from sapphire substrates is complex and significantly increases the cost of device fabrication. With the advancement of epitaxial techniques, researchers have begun to prepare GaN thin films directly on metal substrates. PLD has the advantage of low-temperature deposition, making it an ideal epitaxial method for high-temperature reactive metals. Okamoto et al. [77,79,80] have made significant contributions in this regard. They have grown AlN buffer layers on metals such as Cu, Fe, Ni, Ag, and Ta and successfully epitaxially grown single-crystal GaN films on the AlN buffer layers. The researchers investigated the epitaxial relationship and growth mechanisms between GaN films, AlN buffer layers, and metal substrates. The results showed that GaN films on metal substrates typically exhibit a 30° rotation. Haider et al. [83], while studying the influence of annealing processes on the performance of PLD-grown GaN films, used metal Ta as one of the experimental substrates. The results indicated that the heating and cooling rates during the epitaxial growth of GaN films on Ta strongly influence the film's performance. It is recommended to anneal the films at lower temperatures (300-500°C) for longer durations (2-4 hours) to release thermal stress gradually, thereby significantly improving the crystal quality and surface smoothness of the films.

One of the research directions pursued by researchers is the use of buffer layer techniques to overcome the lattice mismatch issue between GaN films and substrates, thus improving the quality of GaN films. Silicon (Si), as one of the most abundant materials on Earth, has become an ideal substrate material for achieving high-performance, high-power, and low-cost GaN-based LEDs due to its advantages of low cost, large size, high thermal conductivity, good conductivity, and mature manufacturing processes. Therefore, the use of PLD technology to prepare GaN films on Si substrates is currently a hot research topic. However, there are challenges in the epitaxial growth of GaN on Si substrates. Si and Ga are prone to melt-back etching at high temperatures [84], there is a significant lattice mismatch [47,48], and high crystal defect density. The large coefficient of thermal expansion mismatch [47] and the susceptibility of epitaxial films to cracking pose challenges for the epitaxial growth of GaN on Si substrates.

In 1995, Vispute et al. [85] first reported the epitaxial growth of smooth AlN single-crystal films on Si(111) substrates using a combination of pulsed laser deposition (PLD) and sintered AlN ceramic targets. Jagannadham et al. [86] investigated the performance variation of AlN films grown on Si(111) substrates using PLD at different temperatures (300-750°C). The test results showed that

as the growth temperature increased from 300°C to 750°C, the grain size of AlN increased from 18 nm to 30 nm, and AlN films grown at lower temperatures exhibited higher residual compressive stress. These results demonstrated the close relationship between the stress state in AlN films and the PLD growth temperature [86]. During PLD, when a pulsed laser irradiates the AlN target, high-energy species are generated and diffuse toward the Si substrate, gradually depositing as AlN films. However, at lower substrate temperatures, the mobility of these precursors is reduced, leading to atomic misarrangements in the crystal and introducing compressive stress in the film. Ohta et al. [87] studied the interface structure of Si/AlN in AlN films grown on Si(111) substrates using PLD. The findings revealed a minimal interface roughness of 0.5 nm for Si/AlN, signifying the near absence of a SiNx interfacial layer between the AlN film grown through PLD and the Si substrate. This is in stark contrast to AlN films prepared by MOCVD [88], highlighting the superiority of PLD in epitaxially growing III-nitride films on Si substrates. To address the issue of poor film uniformity in PLD growth, Li et al. [89] employed a combined laser grating technique during PLD growth and successfully obtained crack-free AlN films with uniform thickness. The obtained 2-inch single-crystal AlN films exhibited a root mean square thickness variation of less than 3.6% and a surface roughness of only 1.4 nm, demonstrating high film uniformity and surface flatness.

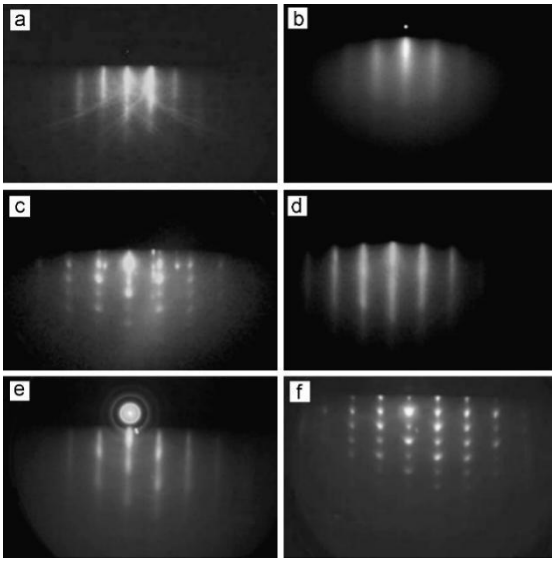

Figure 7. RHEED patterns were obtained during the growth of GaN films using an AlN buffer layer. The following patterns were observed: (a) Si(111) substrate, (b) 0.6 nm AlN, (c) 1.2 nm AlN, (d) 27 nm AlN, (e) 80 nm AlN, and (f) 45 nm GaN on an 80 nm AlN buffer layer. [87]

Research on low-temperature epitaxial growth of GaN films on Si substrates has been proposed

following the successful use of PLD to grow AlN films on Si substrates [90]. Ohta et al. [87] employed PLD to sequentially grow an AlN buffer layer and a GaN film on Si(111) substrates and elucidated the growth mechanism. As shown in Figure 7, directly growing GaN films on Si(111) substrates using PLD resulted in poor crystal quality, exhibiting an amorphous state. However, with the introduction of an AlN buffer layer, the GaN films grown on top of it were single-crystalline. This indicates that regardless of low-temperature or high-temperature epitaxy, the AlN buffer layer is a crucial factor for achieving high-quality GaN growth on Si substrates.

Tong et al. [91] employed a gas discharge-assisted PLD technique to investigate the properties of GaN films grown by epitaxy at different growth temperatures and laser energies. Figures 8 and 9 show the performance of GaN under different growth temperatures and laser energies. The experimental findings indicated that the GaN films exhibited a wurtzite crystal structure, and the crystal quality of GaN was enhanced as the growth temperature increased. This improvement was primarily attributed to the enhanced surface atom mobility and improved thermal stability of GaN films at higher growth temperatures. However, excessive growth temperatures led to a decrease in the crystal quality of GaN films due to surface evaporation at elevated temperatures. Additionally, they studied the influence of laser energy variation on the surface morphology of GaN films. At a laser energy of 220 mJ/pulse, the epitaxially grown GaN films exhibited the lowest surface roughness of 3.3 nm. However, when the laser energy was either higher or lower than 220 mJ/pulse, a multitude of large particles were observed on the surface of the GaN films. This phenomenon can be explained from two perspectives. Firstly, lower laser energy fails to provide sufficient kinetic energy, resulting in the incomplete migration of precursor particles and the subsequent formation of large particles on the film surface. On the other hand, excessively high laser energy during target bombardment produces precursor particles with larger diameters, which hinder their sufficient motion on the film surface and lead to the formation of rough film surfaces.

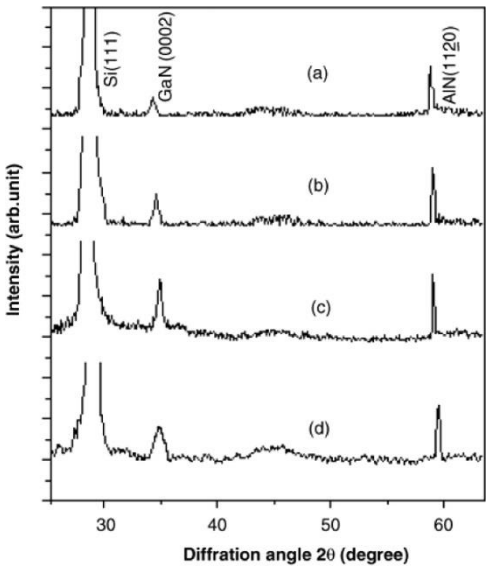

Figure 8. XRD results of the GaN grown at different temperatures of (a) 400 ℃, (b) 600 ℃, (c) 700 ℃ and (d) 800 ℃. [91]

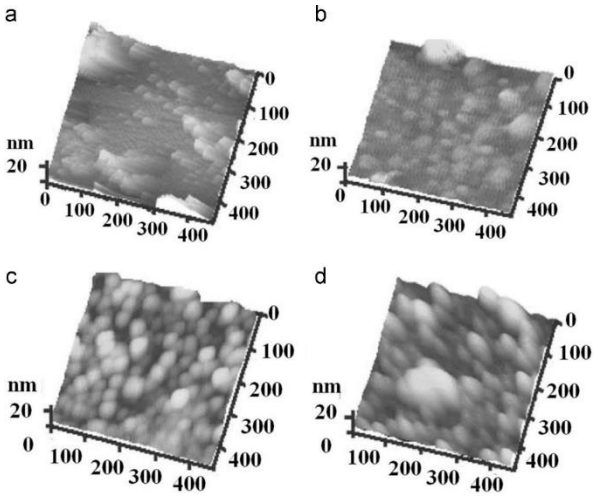

Figure 9. AFM images of GaN films grown at different laser incident energies of (a) 150, (b) 180, (c) 220, and (d) 250 mJ/pulse. [91]

Yamada et al. [92] first proposed the use of a two-step method with a low-temperature AlN interlayer for the epitaxial growth of GaN films on Si substrates. In this method, a 70 nm thick low-temperature AlN layer was deposited on the Si substrate using reactive sputter deposition at 350 ℃. Subsequently, the sample was transferred to MOCVD, where GaN was grown at a high temperature of 1100 ℃. A comparison revealed that the dislocation density in the GaN epitaxial layer grown using the two-step method was reduced by an order of magnitude compared to GaN grown using the traditional one-step method.

Similarly, Wang et al. [93] also utilized an epitaxial sputter deposition of a low-temperature

AlN layer to achieve the growth of GaN epitaxial films on Si substrates. Additionally, they investigated the influence of the GaN nucleation stage on the crystal quality of the epitaxial film. They found that by controlling the number of GaN nucleation islands and prolonging the lateral growth time of the islands, the dislocation density in GaN could be effectively reduced.

2.1.2 Laser molecular beam epitaxy (LMBE)

LMBE is an advanced technology used for the manufacturing of Micro-LEDs. Its principle is based on the precise control of atomic and molecular beams using laser beams. By employing laser evaporation techniques, metallic Ga and nitrogen gas are converted into high-energy atomic and molecular beams. The laser beam allows real-time adjustment and control of the shape, direction, and intensity of the molecular beam, which is then directed toward the surface of the substrate for deposition and growth. Through optimization of the growth conditions, high-quality crystal growth and excellent electrical and optical properties can be achieved. The core principle of LMBE lies in the ability to position atomic and molecular beams precisely using laser beam control, enabling high-precision crystal growth and improving the performance and reliability of Micro-LED devices.

Ramesh et al. [94] reported the growth of epitaxial GaN films on the a-plane sapphire using LMBE technology, achieving crystalline GaN films at temperatures close to 600°C, confirming the feasibility of LMBE for GaN film preparation. V. Aggarwal et al. [95] investigated the growth sequences of GaN film, NC-GaN, and NP-GaN under different conditions. Figure 10 illustrates the growth sequences of GaN on (11-20) plane sapphire substrates under different conditions. By carefully optimizing the process parameters of laser MBE, high stoichiometric ratio GaN crystal films can be prepared in an ammonia-free environment and at relatively moderate growth temperatures. The growth temperature, pre-nitridation, and laser scanning speed are key factors influencing LMBE.

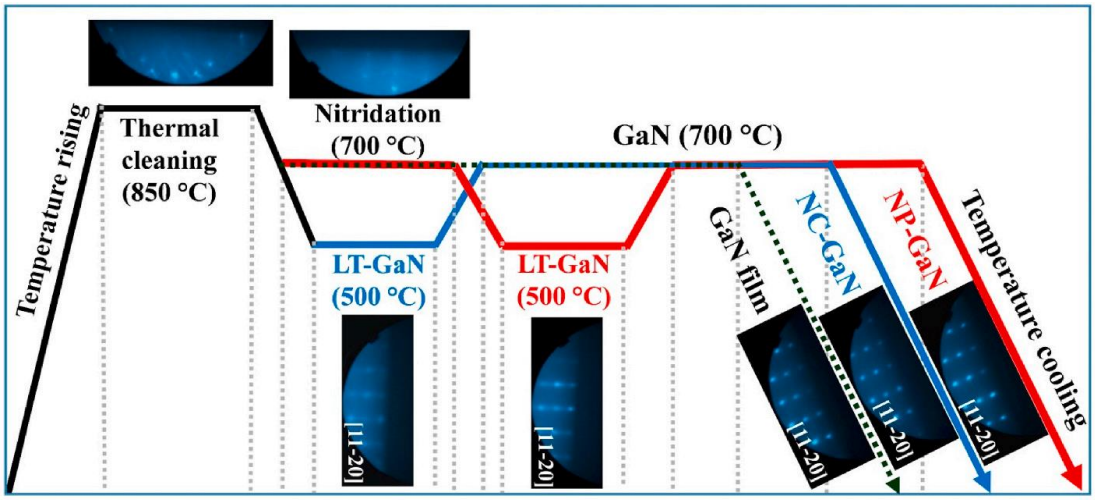

Figure 10. Schematic diagram of the growth sequence of GaN on a (11-20) plane sapphire substrate under different conditions. [95]

The growth temperature can have an impact on various aspects of the LMBE process, such as material structure, crystal quality, and growth rate [96]. The growth temperature can influence the crystallinity and crystal quality of the material. An appropriate growth temperature provides sufficient thermal energy to promote crystal growth and crystallization, facilitating the formation of high-quality crystal structures. The growth temperature also affects the growth rate. Generally, higher growth temperatures can accelerate the growth rate, but excessively high temperatures may cause material melting, increase surface roughness, or introduce impurities. Therefore, it is necessary to control the growth temperature to avoid adverse effects while maintaining the desired growth rate. The growth temperature can also influence the composition and doping behavior of the material. In the epitaxial process, an appropriate growth temperature can facilitate compositional control and doping effects to meet the specific requirements of Micro-LEDs. Low-temperature growth can reduce the formation of thick interfacial compounds. Compared to MOCVD and PA-MBE techniques, LMBE has the advantage that high-energy thin film precursors generated by laser ablation can be used to grow GaN films at lower deposition temperatures and moderate deposition rates [97,98]. Dixit [99] studied the impact of growth temperature on LMBE within the range of 500-700°C. Figure 11 shows the surface morphology and Raman spectra of GaN layers grown on sapphire substrates at different temperatures. The results showed that the growth mode of GaN significantly affects the in-plane strain of LMBE GaN layers. GaN grown at lower temperatures exhibited significantly higher in-plane stresses of around 1 GPa, while the in-plane stress values

decreased significantly for GaN grown at the highest temperature. The mechanical strength of the GaN layer grown at high temperatures also increased significantly. The influence of growth temperature should be considered in the strain reaction of the GaN layer.

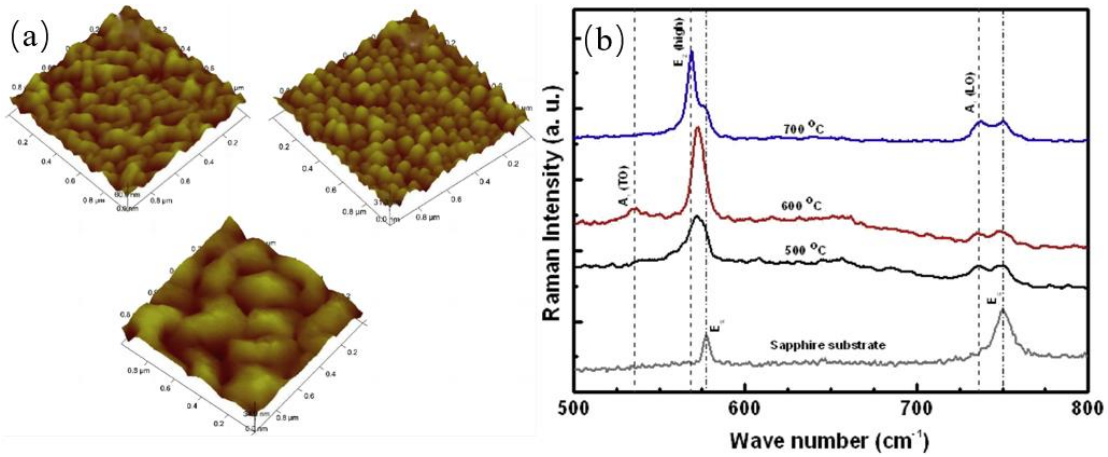

Figure 11. (a) AFM surface morphology of LMBE GaN layers grown on sapphire (0001) at various growth temperatures. (b) The Raman spectra of LMBE-grown GaN layers on sapphire (0001) substrates were recorded at room temperature under various growth temperatures. [99]

Nitrogen flow rate refers to the amount of nitrogen gas input through the gas source during the epitaxial growth process. Changes in nitrogen flow rate can impact material properties and the quality of epitaxial films in the LMBE process, particularly for nitride materials growth. Before growing GaN films, a buffer layer is formed on the Al_2O_3 surface of the sapphire substrate through intense nitrogen plasma treatment [100]. As a result of this process, the substrate undergoes nitridation, which serves as a beneficial means of compensating for the lattice mismatch (approximately 16%) between sapphire and GaN films [100]. Following the nitridation step, GaN films are grown on the modified sapphire substrate using varying nitrogen flow rates (ranging from 1 to 3 sccm), while keeping all other process parameters constant.

Sheetal Dewan prepared highly c-axis-oriented GaN films using different nitrogen flow rates [101]. The obtained GaN films exhibited point diffraction patterns in the RHEED images, indicating the growth of GaN films with LMBE (Figure 12). The AFM images showed that the surface roughness increased from 0.7 nm to 1.1 nm as the nitrogen flow rate increased from 1 sccm to 3 sccm (Figure 13). Additionally, p-n junction structures of GaN/Mg: GaN on a GaN template were achieved at a low nitrogen flow rate of 1 sccm, exhibiting characteristics similar to a rectifying diode. XRD spectra confirmed the growth of single-phase c-axis (0002) oriented wurtzite GaN films

at different nitrogen flow rates.

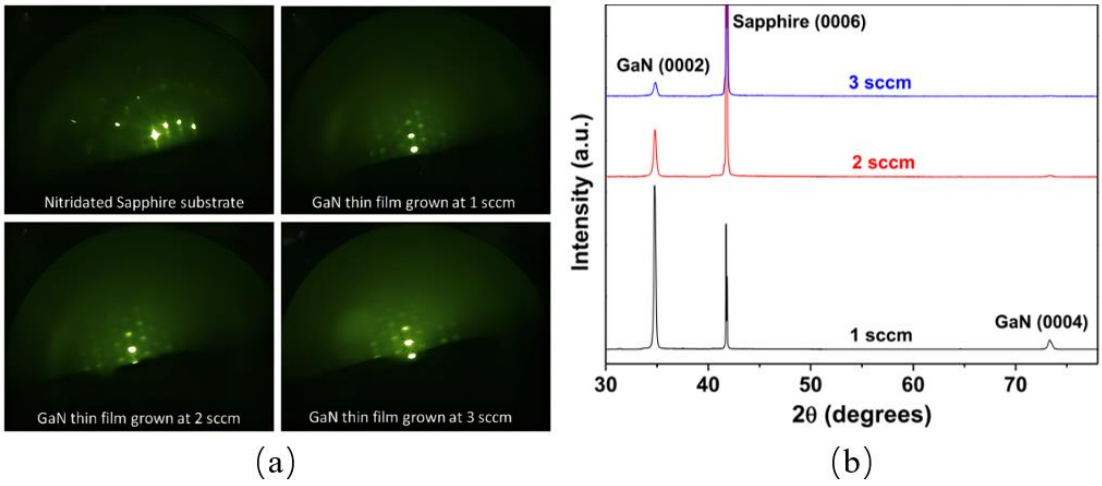

Figure 12. (a) GaN thin films grown at different nitrogen gas flows. (b) XRD pattern of the GaN thin films at varying nitrogen gas flow. [101]

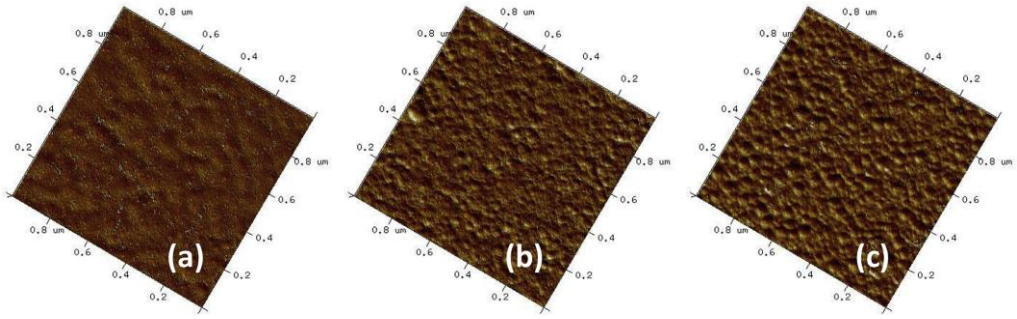

Figure 13. AFM images of GaN thin films grown at (a) 1 sccm (b) 2 sccm and (c) 3 sccm nitrogen gas flow. [101]

The nitrogen flow rate directly determines the nitrogen content in nitride materials. By adjusting the nitrogen flow rate, the proportion of nitrogen in the film can be controlled, thereby influencing the composition and properties of the material. An appropriate nitrogen flow rate enables the attainment of the desired nitride composition and enhances specific material properties such as bandgap and refractive index. The nitrogen flow rate also plays a crucial role in the crystal quality of nitride materials. Optimal nitrogen flow rate promotes crystal growth, improves crystallinity, and reduces defect formation. Excessive or insufficient nitrogen flow rates may lead to increased surface roughness or decreased crystal quality. Changes in nitrogen flow rate can also affect the growth rate. Increasing the nitrogen flow rate generally accelerates the growth rate, but excessively high nitrogen flow rates can result in increased surface roughness. Therefore, it is necessary to balance the impact of the nitrogen flow rate while controlling the growth rate.

Laser scanning frequency refers to the rate and frequency at which the laser beam scans over

the epitaxial surface. Changes in laser scanning frequency can impact material growth rate, crystal quality, and surface morphology in the LMBE process. S. S. Kushvaha [102] used an LMBE system on c-plane sapphire substrates to grow GaN layers by ablating with radio-frequency nitrogen plasma in the laser repetition frequency range of 10-30 Hz. The SEM image in Figure 14(a) demonstrates the higher crystalline quality of GaN at a laser repetition frequency of 30 Hz. Raman spectroscopy, as shown in Figure 14(c) and (d), also confirmed the growth of high-quality GaN films at 30 Hz. The AFM image in Figure 14(b) revealed the growth of three-dimensional GaN under nitrogen-rich flux conditions. GaN epitaxial layers grown at 30 Hz exhibited minimal stress and demonstrated high structural and optical performance. These results indicate that LMBE technology can produce high-quality, low-stress thin GaN layers for Micro-LED applications with minimal polarization effects.

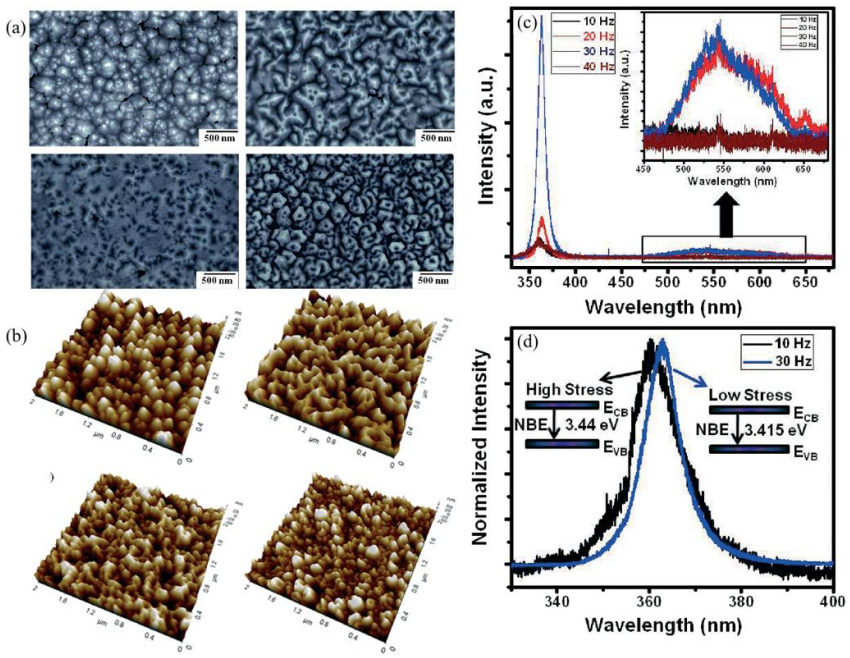

Figure 14. (a) GaN films on sapphire (0001) were imaged using plan-view FE-SEM at different laser repetition rates. (b) GaN films on sapphire (0001) were imaged using 3D AFM at varying laser repetition rates. (c) Room temperature PL spectra were obtained for GaN films on sapphire (0001) grown at different laser repetition rates. (d) Normalized NBE PL spectra were measured for GaN layers grown at 10 and 30 Hz, indicating the NBE peak position. [102]

The laser scanning frequency has several major effects on LMBE:

- Growth rate: Increasing the laser scanning frequency results in an increased growth rate

because the fast laser scanning speed reduces the amount of time the material stays on the epitaxial surface. By adjusting the laser scanning frequency, it is possible to control the growth rate and achieve the desired growth speed and thickness.

- Crystal quality: Optimal laser scanning frequency can promote crystal growth and crystallinity, thereby enhancing crystal quality. Higher scanning frequencies can reduce crystal defects and surface roughness, producing higher-quality epitaxial films.
- Surface morphology: Changes in laser scanning frequency also influence the surface morphology of the epitaxial film. Higher scanning frequencies can improve surface flatness and uniformity, reducing surface defects and roughness. This is crucial for the fabrication of Micro-LEDs as better surface morphology helps improve light emission efficiency and device performance.

LMBE, as a highly controllable growth technique, is widely considered a suitable method for large-scale production in the epitaxial growth of Micro-LEDs on sapphire substrates. LMBE offers high growth rates, excellent uniformity, and repeatability, making it an ideal choice to meet the demands of large-scale production. Current research indicates that in GaN grown on the c-plane of sapphire, the formation of GaN layers and heterostructures induces an internal electric field due to polarization-induced charges, resulting in the Quantum Confined Stark Effect (QCSE) [5,6]. This effect hampers the performance of light-emitting diodes and other optoelectronic devices as it causes spatial separation of electrons and holes, decreasing their recombination efficiency and subsequently reducing the quantum efficiency of these devices. To address this issue, researchers have turned to non-polar GaN growth surfaces. However, non-polar GaN growth surfaces face challenges due to the formation of a thick interfacial layer between a-plane GaN and r-plane sapphire caused by high-temperature growth. To overcome these limitations, Tyagi et al. [7] successfully grew flat and tightly bonded GaN layers on r-plane sapphire by introducing an HT-AlN buffer layer and using the LMBE technique. This innovative approach holds promise for improving the quality of non-polar GaN growth and providing a better foundation for the performance of optoelectronic devices.

Extensive research efforts have been dedicated to developing Gallium Nitride (GaN) films on unconventional oxide substrates as alternatives to sapphire. Conventional sapphire substrates exhibit significant lattice mismatch with GaN, leading to a high density of dislocations in the

epitaxial layer and hindering the achievement of exceptional quality in grown epilayers. This, in turn, adversely affects the performance of GaN-based optoelectronic devices and hampers further advancements. To address this issue, various unconventional oxide substrates, including $LaAlO_3$ [103], $LaSrAlTaO_6$ (LSAT) [104], and MgO [105], have been extensively studied. These substrates offer several advantages over sapphire. Firstly, they possess minimal lattice mismatch with GaN, facilitating nucleation during early growth and promoting the development of excellent crystalline quality. Secondly, nonpolar GaN-based devices can be fabricated using various oxide substrates, such as $LiGaO_2$ (1 0 0) and $LiAlO_2$ (1 0 0), which eliminates the QCSE and enhances the radiative recombination efficiency.

2.1.3 Laser-patterned sapphire substrate (LPSS)

In substrate epitaxy techniques, apart from direct epitaxy, LPSS technology can indirectly assist in obtaining high-quality GaN films, improving crystal quality, and enhancing light extraction efficiency.

Sapphire is the most widely used substrate material in the GaN-based LED industry due to its mature manufacturing process, good stability, and high-temperature performance. However, there still exists a significant lattice mismatch (16.1%) and thermal mismatch (34.7%) between sapphire and GaN. The large lattice mismatch results in the generation of a high density of dislocations (up to 10^8-10^{10} cm^{-2}) during the GaN epitaxial growth process, leading to lower crystal quality and adversely affecting the internal quantum efficiency of LEDs. The presence of thermal mismatch leads to biaxial compressive stress between GaN and sapphire substrates, making it prone to cracking in the GaN epitaxial layers. Additionally, the high refractive index of the sapphire substrate and GaN layer restricts the light extraction angle of LEDs to only 23%, resulting in lower light extraction efficiency of LED devices. Moreover, the light trapped within the device is absorbed and converted into heat, reducing the reliability of LEDs.

To address these issues of low-quality GaN epitaxial layers on sapphire substrates and low light extraction efficiency of LED devices, the use of Patterned Sapphire Substrates (PSS) is widely adopted as a solution. PSS changes the growth mode of GaN epitaxy, reducing the upward extension of dislocations in the epitaxial layer and lowering the epitaxial layer stress, thereby improving the crystal quality and internal quantum efficiency of LEDs. Additionally, PSS improves the photon

propagation path in the active region, increasing the chances of light emission from within the LED and thus enhancing the light extraction efficiency of LEDs.

The principle of LPSS involves creating micron-scale patterned structures on the surface of a sapphire substrate using laser processing. Typically, femtosecond laser pulses are utilized to achieve high precision and non-thermal damage processing. Sapphire substrates possess high optical quality and thermal conductivity, making them preferred substrates for Micro-LED devices. LPSS aims to improve substrate quality and enhance the performance of Micro-LED devices.

The origin of the patterned sapphire substrate (PSS) technology can be traced back to the Epitaxial Lateral Overgrowth (ELOG) technique. In 1994, Kato et al. [106] applied this technique to reduce the dislocation density of GaN films during epitaxial growth. ELOG is a method that reduces the dislocation density in GaN epitaxial layers through a two-step growth process. Firstly, a GaN layer with a thickness of approximately 2-3 μm is grown on a sapphire substrate. Then, a patterned mask layer, typically made of silicon nitride or silicon dioxide, is created on the GaN layer. Finally, a second growth process is performed on the GaN epitaxial layer. In this secondary growth process, GaN starts to grow from the openings of the mask layer laterally and gradually fills the gaps between the mask patterns. This approach suppresses dislocations during the lateral growth, resulting in a reduced dislocation density in the GaN epitaxial layer. With the ELOG technique, obtaining GaN epitaxial layers with lower dislocation densities is possible.

In 2005, Wang et al. [107] demonstrated the advantages of PSS in fabricating high-performance near-ultraviolet LEDs on both flat sapphire substrates and PSS. The dislocation density of GaN decreased from 1.1×10^{9} cm^{-2} to 2.8×10^{8} cm^{-2}, the internal quantum efficiency increased from 36% to 38%, and the external quantum efficiency improved by approximately 29%. This conclusion indicates that the performance enhancement of PSS is not only attributed to the improved internal quantum efficiency resulting from dislocation reduction but also to the enhanced light extraction efficiency provided by PSS. In 2006, Lee et al. [108] utilized photolithography and wet etching processes to fabricate PSS with a diameter and spacing of 3 μm. The 450 nm LED grown on these PSS substrates exhibited a 1.15-fold higher light output power compared to devices grown on flat sapphire substrates, reaching an output power of 9 mW under a 20 mA injection current. In 2008, Chen et al. [109] fabricated nano-patterned sapphire substrates (NPSS) using nanosphere lithography and dry etching techniques. They grew 450 nm GaN-based LEDs on NPSS, and under

a 20 mA injection current, the output power of LEDs grown on NPSS was 1.3 times higher than that of LEDs grown on flat sapphire substrates and 1.11 times higher than that of LEDs grown on micro-sized PSS substrates. In 2011, Park et al. [110] fabricated NPSS using nanoimprint lithography and dry etching processes. The photoluminescence and electroluminescence intensities of LEDs grown on NPSS were found to be twice and 2.8 times higher, respectively, compared to those grown on flat sapphire substrates. In 2014, Zhang et al. [111] utilized a self-assembled monolayer of SiO_2 nanoparticles as a template and employed dry etching techniques to fabricate NPSS with varying spacing. Due to epitaxial lateral overgrowth, GaN grown without spacing on the top of NPSS exhibited the best crystal quality. In the same year, Guo et al. [112] prepared NPSS using a hybrid nanoimprint soft lithography technique. They utilized a nickel mask and inductively coupled plasma (ICP) etching to create NPSS with a period of 550 nm and a conical shape. In comparison to LEDs grown on both NPSS and flat sapphire substrates, the NPSS LEDs showed a 57.9% increase in overall electroluminescence intensity and a 43.8% improvement in light output power. In 2015, Jiang et al. [113] fabricated volcano-shaped patterned sapphire substrates using imprint lithography and wet etching techniques. The larger sidewall reflection area and smaller tilt angle of the substrates enhanced the light extraction efficiency of LEDs. In the same year, Wu et al. [114] utilized a wet etching process to fabricate concave-shaped sapphire substrates with a period of 3 μm. They observed that the crystal quality of GaN grown on the concave-shaped sapphire substrates improved as the pattern spacing (c-plane percentage) decreased. However, when the pattern spacing decreased to 0.41 micrometers, the crystal quality decreased due to the difficulty in GaN film formation caused by the reduced c-plane percentage. This indicates that, while ensuring film formation is essential, a smaller c-plane percentage leads to higher crystal quality. In 2020, Hu et al. [115] fabricated patterned sapphire substrates with a silica array (PSSA) using a dry etching process. Benefiting from the reduced threading dislocation density and improved light extraction efficiency, UV LEDs based on PSSA exhibited more than a two-fold increase in external quantum efficiency compared to LEDs fabricated on flat sapphire substrates.

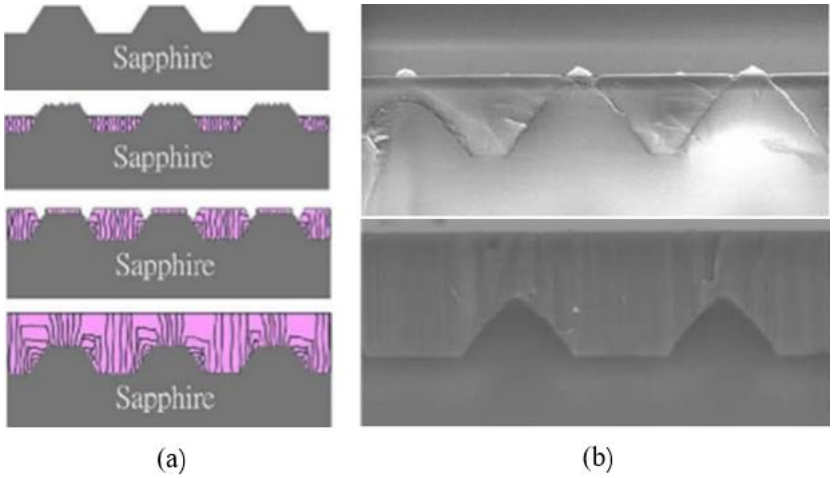

Figure 15. (a)Schematic diagram of the GaN film growth process on PSS.(b) Cross-sectional SEM micrographs of the GaN grown on PSS. [116]

By summarizing the development of PSS technology, we can conclude the following key points:

- In addition to effectively reducing threading dislocation density in the epitaxial layer, improving internal quantum efficiency (as shown in Figure 15), increasing light scattering probability, and enhancing light extraction efficiency (as shown in Figure 16), PSS technology is also applicable for the growth of visible and ultraviolet LED structures.
- Compared to ELOG techniques, PSS technology requires only a single growth step during the GaN growth process.
- PSS structures can be designed and controlled by changing structural parameters, allowing for flexibility in optimizing their performance.
- As manufacturing processes advance, PSS technology is gradually evolving towards more precise and higher-quality NPSS.

Tian[100][117] successfully fabricated green GaN-based Micro-LEDs by preparing a PSS structure and utilizing the laser lift-off (LLO) technique. Figure 17 shows the SEM image of the LLO process with PSS structure. Experimental results have demonstrated that combining the advantages of PSS epitaxy with a GaN-based LED laser lift-off process significantly enhances the performance of the chips. Therefore, PSS technology offers various advantages in improving LED performance, and with advancements in manufacturing processes, it is moving towards the development of higher-precision NPSS.

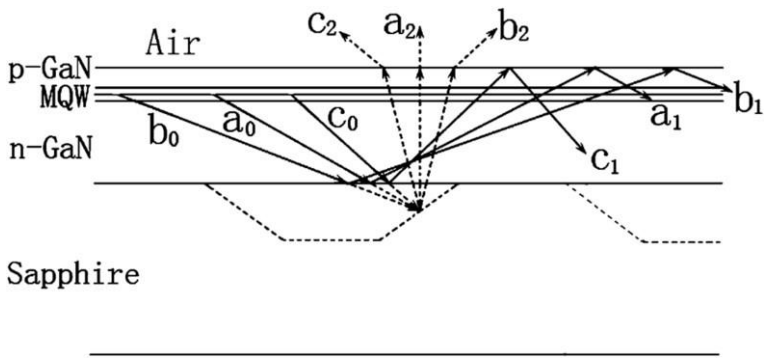

Figure 16. Schematic diagram of internal light propagation in LEDs grown on patterned substrates. [118]

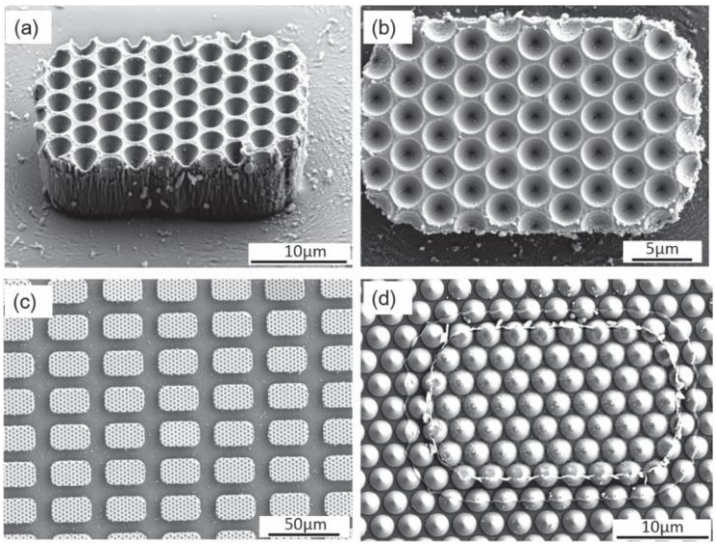

Figure 17. SEM images of PSS structure Micro-LED chip after LLO: (a) 3D diagram (b) top view (c) Local array devices diagram. (d) Sapphire interface after Micro-LED separation. [117]

Currently, the most advanced technology for PSS fabrication is femtosecond laser processing. Femtosecond laser processing technology offers capabilities for micro/nanopattern configurations, nanoscale processing accuracy, strong design flexibility, simplified process flow, and the ability to process challenging materials like sapphire. However, the main challenge in using femtosecond laser processing for PSS fabrication is the relatively low processing efficiency.

In femtosecond laser processing, material is typically processed by scanning a focused laser beam. The structures fabricated using high-precision femtosecond laser processing are typically on the micrometer scale, while sapphire substrates usually require centimeter-scale patterns. This challenges large-scale processing equipment and high-precision femtosecond laser processing efficiency.

2.2 Laser Etching

Laser etching is a process that involves focusing a high-energy laser beam onto specific areas of a chip's surface, causing the material to heat up and undergo chemical or physical changes, thereby removing it. This etching process allows for precise control by adjusting the laser's power, pulse duration, and focal point position, enabling highly controllable etching processes to meet the requirements of different structures and sizes in chip fabrication. The production of Micro-LED chips requires the definition and formation of complex microstructures at the nanoscale to achieve high precision and high-resolution etching. Figure 18 illustrates the basic etching shapes of Micro LEDs.

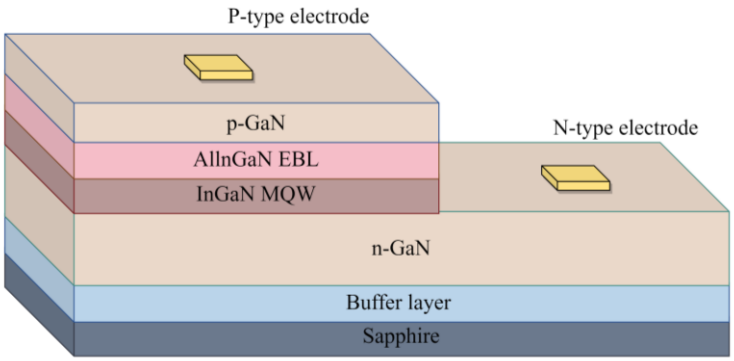

Figure 18. Schematic illustration of Micro-LED after etching.

Laser etching plays a crucial role in the manufacturing of Micro-LED devices. It is used to create the necessary structures and patterns for circuitry connections, optimizing light emission efficiency and enhancing optical performance. Precise laser etching enables high-density circuitry connections and the fabrication of micro- and nano-scale structures, thereby improving the performance and reliability of Micro-LED chips. Laser etching offers several technological advantages, including high precision, small feature sizes, excellent controllability, and non-contact processing, making it a key process for producing high-quality Micro-LED devices.

Laser processing allows for instantaneous material removal, enabling the creation of micro-sized trenches on GaN surfaces with minimal edge collapse and microcracking. Laser etching is a non-contact processing method that does not cause physical damage to the chip's surface, reducing the risks of material contamination and degradation.

2.2.1 Laser-assisted Dry Etching

Currently, dry etching technology is one of the most widely used and mature techniques for GaN processing. Dry etching, in a broad sense, refers to etching techniques that do not involve chemical solution corrosion. Currently, inductively coupled plasma (ICP) / reactive ion etching (RIE) dry etching is the most commonly used method for etching Micro LEDs, utilizing ICP or RIE techniques. Compared to the ICP/RIE process, laser-assisted dry etching exhibits clear advantages in key performance indicators. For instance, the typical etching rate of the laser-assisted process can reach 50 nm/s [119,120], while ICP/RIE is only 3 nm/s [121], making the former about 16 times faster. In terms of etching uniformity, the laser-based process can achieve a spatial uniformity of 1-3% [122], superior to the 3-5% of ICP/RIE [123], representing a 33-50% improvement. Moreover, the throughput of laser-assisted dry etching can reach 50-100 wafers/h [124], compared to 10-20 wafers/h for ICP/RIE, a 2.5-5 times enhancement. In the aspect of Micro LED device sidewall quality control, the laser-assisted process also exhibits advantages, including a sidewall verticality of 88-90° [125], outperforming the 85-87° of ICP/RIE [126], and a surface roughness (RMS) of 0.5-1 nm [127], better than the 1-2 nm of ICP/RIE. These performance advantages are crucial for improving the optical performance and reliability of Micro LEDs.

Laser-assisted dry etching essentially replaces traditional plasma etching methods with laser etching, involving laser-based micro-nano processing. Among existing dry etching techniques for semiconductor micro-nano structures, photolithography is the first and most crucial step in semiconductor micro-nano structure fabrication. It is also the most complex and technologically challenging step in dry etching processes. The photolithography process is essentially a process of pattern transfer, including the transfer of patterns from a mask to a photoresist layer and from the photoresist layer to the wafer surface. Figure 19 demonstrates the photolithography process described above. The process consists of four main steps: exposure, development, etching, and stripping. Exposure involves precise alignment of the mask and pattern on the wafer, where a laser beam is directly used to illuminate the photoresist layer. The laser beam is focused using lenses or other optical components to concentrate the light energy onto specific regions of the photoresist. Development is the step where unexposed or untreated portions of the photoresist are removed, leaving behind the desired pattern. After development, the pattern is transferred from the mask to

the photoresist layer. Etching removes the exposed portions of the photoresist layer on the wafer surface using laser etching, creating openings for pattern transfer from the photoresist layer to the wafer surface. Finally, the photoresist layer on the wafer is removed using methods such as acetone, completing the pattern transfer process.

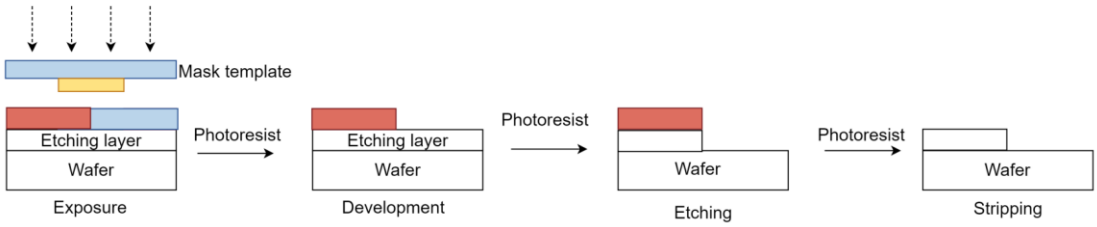

Figure 19. Laser-assisted dry etching process.

UV lasers are typically chosen as the laser source. By using UV lasers to etch the exposed material, the pattern is transferred to the underlying layers. Dai et al. [128] utilized a deep ultraviolet pulsed laser to etch a gallium nitride coating on a sapphire substrate. Figure 20 demonstrates the patterns formed by scanning with a 157 nm wavelength laser with a 20 ns pulse width. Analysis revealed that the average roughness decreased with increasing scanning speed and increased with higher laser repetition frequency. During the laser etching process, direct photodissociation or photochemical reactions played a dominant role. To achieve sharp sidewalls for microgrooves, a narrower laser spot size should be used.

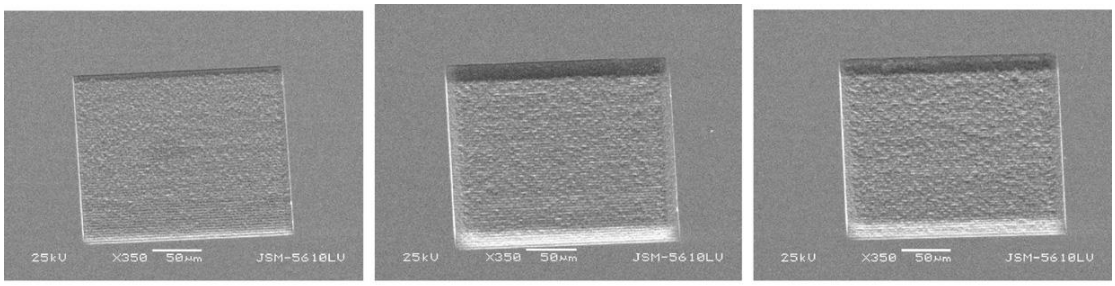

(a) (b) (c)

Figure 20. The square pattern was formed by scanning with a 157 nm laser on a gallium nitride film. [128]

Due to the shorter wavelength of UV lasers, their energy is more easily absorbed by materials and interacts with the surface. However, this results in relatively shallow etching depths. For Micro-LEDs that require greater depths, multiple processing steps or alternative methods may be necessary with UV lasers. E. Gu [129] utilized UV laser processing by employing a group of internally modulated beams that oscillate in a scanning line pattern. The beam oscillation combines circular motion with linear motion, resulting in a spiral motion of the laser beam. This technique is illustrated

in Figure 21(a). The cross-sectional image in Figure 21(b) demonstrates the fabrication of microgrooves using this method. It can be observed that the microgrooves have smooth sidewalls. However, the bottom surface is not flat, and the maximum depth is located at the bottom edges. Due to the high photon energy of UV laser processing, there is a tendency for redeposition of material on the sidewalls and bottom of the microgrooves, making it challenging to achieve deep processing of the grooves.

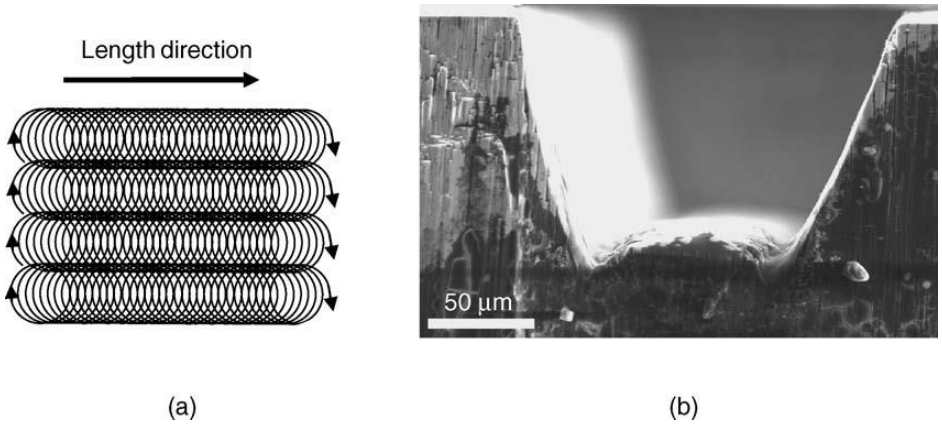

Figure 21. (a)Laser process strategy to fabricate micro-trenches in GaN. (b) SEM image of a micro-trench in GaN. [129]

Laser lithography can utilize a variety of photoresists, including photo-polymer-based and thermally sensitive photoresists. Laser-assisted dry etching enables efficient etching processes and allows for different pattern definitions by changing the mask. However, this technique requires the use of masks, making the fabrication process more complex and requiring high precision in mask preparation and alignment.

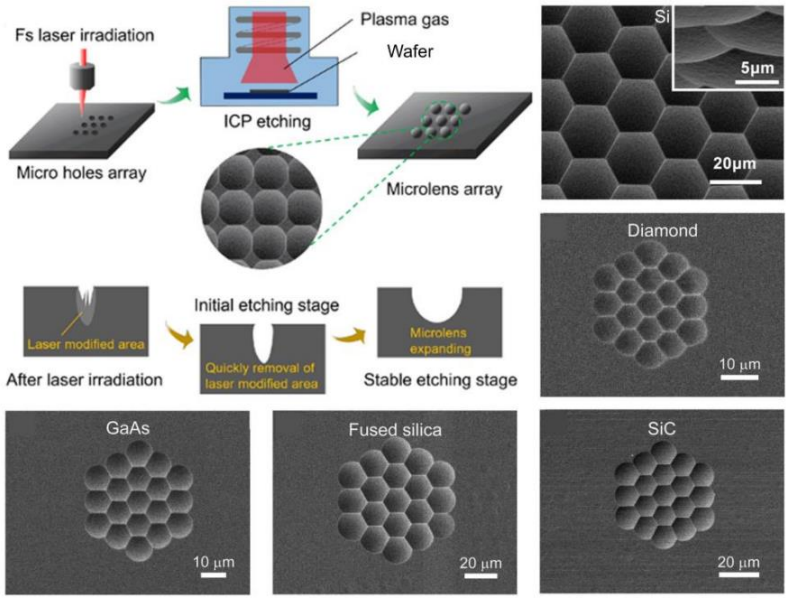

Figure 22. Dry etching-assisted femtosecond laser processing. [130,131]

The combination of femtosecond laser and dry etching has gradually attracted the attention of researchers. Liu et al. [130,131] utilized a process involving dry etching-assisted femtosecond laser processing to fabricate micro-lens structures on the surfaces of materials such as Si, sapphire, SiC, and quartz glass (as shown in Figure 22). In the case of Si material, the dry etching-assisted femtosecond laser processing was conducted using inductively coupled plasma (ICP) etching, with the oxygen content deposited on the processed surface controlled by adjusting the femtosecond laser processing parameters. The results indicated that the deposition of oxygen species from the ambient air during femtosecond laser processing had an impact on the subsequent dry etching process.

2.2.2 Laser direct writing(LDW)

LDW, also known as maskless laser etching, is a laser etching technique that directly defines patterns on the surface of a material without using traditional photolithography masks. The principle involves controlling the positioning of the laser beam to form the desired patterned structures on the material directly, utilizing the high energy density and focusing of the laser beam to induce localized chemical or physical reactions for pattern definition and etching. By adjusting the intensity, focal point, and scanning speed of the laser beam, the processing parameters during the lithography process can be controlled to achieve high-precision pattern fabrication. This technique enables the direct fabrication of small-scale micro and nanoscale patterns on materials in a single-step process with high precision and efficiency [132–138]. Therefore, it is suitable for multiple patterning and

selective patterning of GaN thin films.

Compared to laser-assisted dry etching, it enables the fabrication of smaller microstructures and does not require masks, allowing for more flexible pattern designs. It applies to various types of materials and offers faster processing speeds.

Yu et al. [139] demonstrated the fabrication of InGaN-based Micro-LEDs with feature sizes ranging from 1 to 20 μm using the LDW technique. Figure 23 illustrates the process, and the results confirmed the suitability of the LDW technique for manufacturing Micro-LEDs.

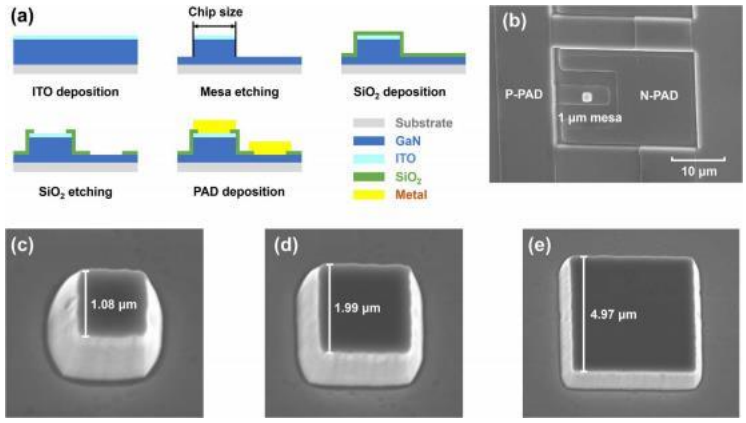

Figure 23. (a) processing scheme for GaN-based micro-LED (b) SEM micrograph of a 1 um diameter blue micro-LED, with extended positive and negative pads. (c) -(e) SEM micrographs of mesa etching with different chip sizes correspond to the second step in (a). [139]

Compared to conventional LDW, ultrafast LDW offers advantages in achieving higher precision and reduced thermal damage. Ultrafast lasers are characterized by extremely short pulse durations, typically in the femtosecond (10^{-15}) range. Because the pulses are very brief, the laser's interaction time with the material is extremely short, preventing heat from propagating significantly within the material and thus avoiding significant thermal damage. Research by C. Momma demonstrated the use of femtosecond laser processing [140], confirming that femtosecond lasers cause less thermal damage compared to other laser processing methods because they can cool down electrons and heat the lattice within femtoseconds. As a result, femtosecond lasers have become a new method for processing GaN thin films.

Extensive research has been conducted to better understand the mechanisms behind the femtosecond laser processing of GaN. Ozono et al. [141] achieved linear control over the depth of microgrooves in GaN thin films by adjusting the number of femtosecond laser pulses. The experiments demonstrated that although the effective etching rate was lower compared to

nanosecond laser ablation, a more defined ablation process could be achieved. T. Kim et al. [142] proposed the use of femtosecond laser micromachining on single-crystal GaN substrates. They found that by optimizing the laser energy density and scanning speed, ideal microgroove sizes could be obtained. G. Rice et al. [143] suggested that by adjusting the average laser power and the number of scans of the femtosecond laser, micron-scale grooves could be obtained on the surface of GaN. They observed that increasing the scanning time effectively removed the re-deposited material within the grooves. Nakashima et al. [144,145] explored a new method involving wet chemical-assisted femtosecond laser ablation. They achieved successful fabrication of well-crafted arrays of ablation holes on single-crystal GaN substrates, aiming to improve the light extraction efficiency of LEDs. Almeida and Nolasco [146,147] studied the latent period effect of the damage threshold as a function of the number of pulses during femtosecond laser micro-processing of GaN films with different wavelengths. Figure 24(a) shows the SEM image of a straight groove microfabricated on the sample surface with a fixed scanning speed. The research indicates that with the increase of laser energy density, the width of the line increases. Additionally, due to the increased generation of defects in this mechanism, higher roughness is observed in microfabrication lines with a higher impact. Wei [26][148] conducted a study on the impact and interactions of process parameters during femtosecond laser processing of single-crystal GaN substrates, focusing on microgroove depth, microgroove width, heat-affected zone (HAZ), and material removal rate (MRR). In Figure 24(b), it can be observed that increasing the laser scanning speed led to a significant reduction in microgroove depth and HAZ, while the microgroove width remained relatively stable. The MRR showed an increase. As the number of scans increased, the microgroove width initially increased rapidly until reaching a critical value, after which it stabilized. However, once the microgroove depth reached a certain critical value, it started to decrease.

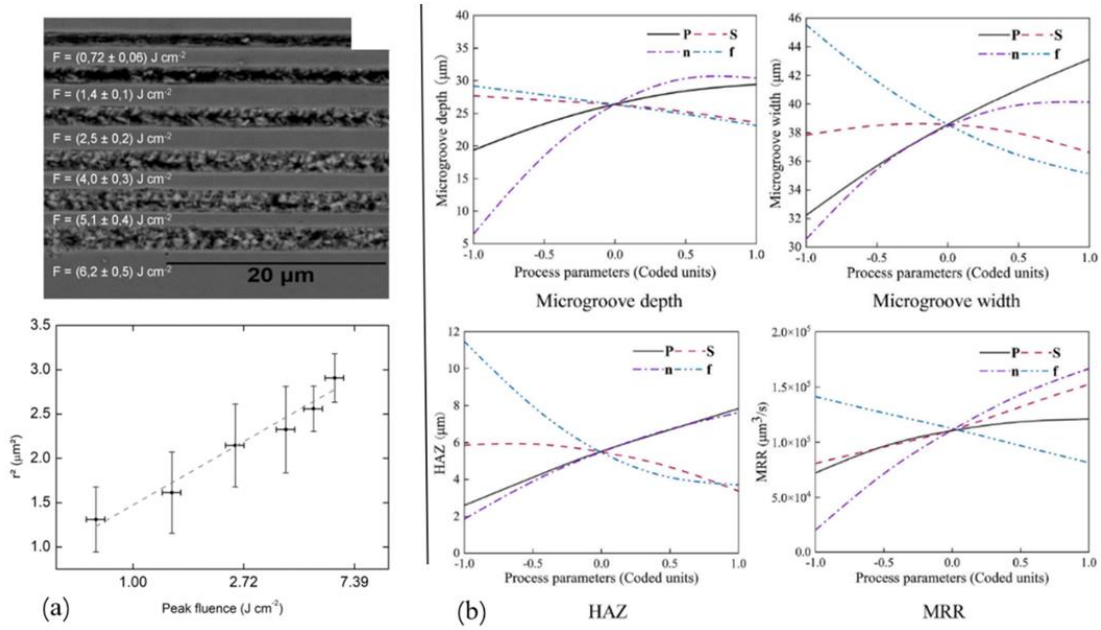

Figure 24. (a) SEM image showing the influence of micro-patterning lines on GaN film and the square half-width of the micro-patterning lines as a function of peak GaN flux. [147](b) Effects of laser power (P), scanning speed (S), scanning cycles (n), and repetition frequency (f). [148]

Based on previous research, it can be concluded that laser power, scanning speed, and scanning time have significant effects on the depth and width of microgrooves. Increasing the laser power can increase the depth of the grooves, while lower scanning speeds, more scans, and lower repetition rates can increase the width of the grooves. From previous studies, the following observations can be made:

- Laser power control: Increasing the laser power can increase the etching depth. However, it is important to avoid excessively high power that can lead to over-etching or thermal damage.
- Scanning speed and scanning time: Lower scanning speeds and longer scanning times can achieve greater etching depth and width. The etching results can be controlled by adjusting the scanning speed and scanning time.
- Repetition rate: Lower repetition rates can result in larger etching depth and width. However, it is important to note that excessively low repetition rates may lead to sintering effects or other non-ideal etching characteristics.
- HAZ: Femtosecond laser ablation has a smaller heat-affected zone, indicating less thermal damage during the etching process.

2.3 Substrate Removal

There are several reasons for removing the substrate in GaN-based LEDs grown on sapphire. Firstly, sapphire has a relatively low thermal conductivity, which hinders efficient heat dissipation and limits the performance of high-power LEDs. Secondly, due to the significant difference in refractive index between sapphire and air, a large amount of light gets trapped inside the sapphire, resulting in limited light extraction efficiency. Thirdly, the thick sapphire substrate leads to strong sidewall emission, where light leaks out from the side edges. This causes undesirable optical crosstalk during display applications, reducing the graphic quality and contrast of the displayed images. [149–151] This is particularly important for displays based on Micro-LED technology, where the substrate must be removed to mitigate these issues.

Traditional chemical [152] and mechanical [153] peeling methods can also achieve peeling, but they have obvious limitations. Chemical peeling requires a large amount of chemical reagents, which not only makes the process complex but also easily causes environmental pollution. Mechanical peeling relies on precise equipment and is very likely to damage the fragile Micro LED materials. In comparison, laser peeling technology has shown unique advantages. Laser energy is concentrated, which can achieve instant peeling [154], and the peeling speed can theoretically reach up to 10 meters per second, greatly improving production efficiency. At the same time, the energy utilization rate of laser peeling is much higher than traditional methods, which can significantly reduce material waste and lower manufacturing costs [155]. Furthermore, laser peeling has excellent controllability, allowing precise control of the peeling position and depth, avoiding problems such as chemical contamination and mechanical damage. Based on these outstanding advantages, laser peeling has undoubtedly become an indispensable key technology in Micro LED manufacturing.

In the fabrication process of Micro-LED chips, laser lift-off is a technique used to separate the epitaxial wafer from the substrate. It is commonly employed to detach Micro-LED epitaxial wafers grown on sapphire or other substrates, allowing for subsequent processing and packaging.

2.3.1 Laser Lift-Off (LLO)

Laser Lift-Off (LLO) originated in 1996 when Kelly et al. [156] discovered that short laser pulses could induce high spatial resolution decomposition of GaN. They successfully demonstrated

the removal of GaN films from sapphire substrates using 355 nm pulsed lasers. As the laser passes through the sapphire, its energy is absorbed by the GaN epitaxial layer, causing a thin layer of GaN to decompose into liquid Ga and N_2 gas. Finally, the stress generated at the interface by the decomposition products facilitates the release of the epitaxial layer from the substrate. Based on this principle, Wong et al. [157,158] utilized laser lift-off to fabricate InGaN thin-film LEDs in 1999. Since then, laser lift-off technology has been widely applied for substrate removal in both LED and Micro-LED [159] production processes.

The bandgap energies for sapphire, GaN, and AlN are 9.9 eV, 3.39 eV, and 6.2 eV, respectively. Figure 25 illustrates the principle of LLO. It involves the use of a short-wavelength laser with photon energy higher than the energy bandgap of GaN but lower than the bandgaps of sapphire and AlN. The laser irradiation starts from the sapphire side, and after passing through the sapphire and AlN layers, it is absorbed by the surface layer of GaN.

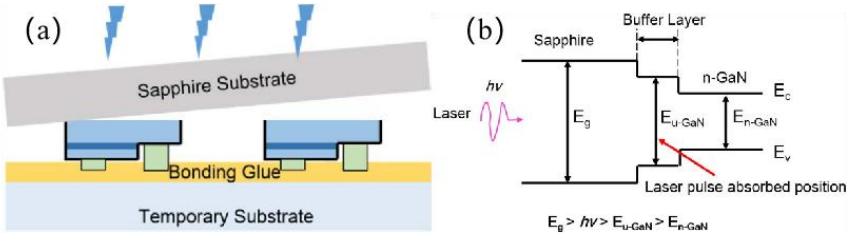

Figure 25. (a) LLO schematic diagram. (b) Schematic diagram illustrating the photon energy in the peel-off mechanism. [117]

During this process, the surface GaN undergoes thermal decomposition. Since the melting point of Ga is around 30°C, it generates N_2 gas and liquid Ga. The nitrogen gas escapes and the separation between the GaN epitaxial layer and the sapphire substrate is achieved through mechanical force [156]. The decomposition reaction occurring at the interface can be represented as follows [160,161]:

$$2GaN(s) \rightarrow 2Ga(l) + N_2\ (g)\ \uparrow$$

According to the formula for photon energy, the optimal laser wavelength that satisfies the aforementioned conditions falls within the following range: 125 nm < 209 nm $\leqslant \lambda \leqslant$ 365 nm. The laser pulse width, laser wavelength, and laser energy density are key factors in achieving the laser lift-off process. The ultraviolet range, specifically the wavelength range of 209 nm to 365 nm, is well-suited for this purpose. It should be noted that due to the thickness of GaN, a single pulse is not sufficient to achieve effective laser lift-off. Multiple pulses are often required. For example,

when using a 248 nm laser to decompose GaN with a thickness of 400 nm to 1200 nm, it is recommended to use 10 to 30 pulses. Currently, various laser sources can be used for laser lift-off, including wavelengths such as 194 nm [162], 248 nm [162], 266 nm [163], 308 nm [164], 355 nm [156], 532 nm [165], and 1030 nm [166]. Different types of lasers and process parameters have a significant impact on the Micro-LED transfer process. To better understand and optimize this technology, we have summarized the key parameters of the typical LLO processes reported in the recent literature, such as the laser type, pulse energy and width, carrier materials, and bonding methods, as shown in the table below. The selection of these parameters directly determines the efficiency and quality of Micro-LED transfer, which is crucial for the performance and reliability of Micro-LED devices.

Table 3. Various Micro-LED Transfer Methods Based on LLO [167]

Laser type	Pulse energy	Pulse width	Handing carrier	Bonding method	Lift-off area	Reference
248 nm KrF laser			PET	Wafer bonding (Ti/Au/AuSn/Au)	20 × 20 mm^2	[168]
248 nm KrF laser	900 mJ cm^{-2}	5 ns	Si	Wafer bonding (Cr/Pd)		[169]
266 nm Nd: YAG laser			/	/	11.3 × 0.46 mm^2	[170]
266 nm DPSS laser	>600 mJ cm^{-2}	10 ns	Glass	Adhesive bonding using polyimide	4-inch	[171]
266 nm DPSS laser	300 mJ cm^{-2}	5 ns	UV tape	Adhesive bonding using UV tape		[172]
266 nm DPSS laser	<600 mJ cm^{-2}		Glass	Adhesive bonding using polyimide		[173]
248 nm KrF	>950 mJ cm^{-2}	20 ns	Glass	PDMS glue bonding	14 × 14 Array	[174]

A reliable LLO process not only requires achieving complete separation at the interface but also avoiding the occurrence of electrical/optical performance defects. The bonding strength between GaN and sapphire is closely related to the laser energy density, which has a threshold value. High-energy lasers can induce certain thermodynamic effects such as crack formation, bending due to thermal stress, vapor pressure of nitrogen, thermal shock, etc., making the damage-free lift-off process a challenging task. Whether LLO can avoid defects depends on the optimization of various laser processing parameters. Specifically, it includes laser energy density [175], laser scanning method [176], laser parameters [163], etc. Among them, the appropriate energy threshold is a key parameter for the success of the delamination process. To expand the process window for the energy threshold, Tang et al. [175] inserted sacrificial layers composed of InN/InGaN superlattices at the interface when preparing GaN films on sapphire substrates. This approach resulted in GaN films with greater thickness and lower defects, reducing laser-induced damage. The laser scanning method

also affects the performance of GaN films [176]. Delmdahl et al. [176] used two laser scanning methods, namely, the linear scanning method (line beam) and the step-and-repeat scanning method (rectangular spot beam). They found that the linear scanning method caused less damage to the GaN film compared to the step-and-repeat scanning method.

Laser scanning speed is an important parameter that significantly affects the outcome of LLO. XLTong [177] conducted a study on the influence of laser scanning speed on LLO performance. The threshold laser energy density for LLO of GaN films is approximately 400 mJ/cm^2 [178]. To investigate the impact of laser scanning speed on the structural and optical properties of LLO GaN films, samples were scanned at speeds of 0.5 mm/s and 1.0 mm/s, respectively, at the same laser energy density of 600 mJ/cm^2. Increasing the laser scanning speed leads to a shorter thermal annealing time, which results in a reduction in grain size. When the thermal annealing time is too long, GaN grains can overgrow, becoming larger and agglomerated. GaN separated from sapphire at a laser scanning speed of 1.0 mm/s exhibits better surface morphology.

The laser scanning speed is also an important parameter that significantly affects the results of LLO. XLTong[177] studied the influence of laser scanning speed on the performance of LLO. The threshold laser energy density for laser ablation of GaN films is approximately 400 mJcm^{-2} [178]. To investigate the impact of laser scanning speed on the structural and optical properties of LLO GaN films, the samples were scanned at speeds of 0.5 mm/s and 1.0 mm/s, respectively, with the same laser energy density of 600 mJcm^{-2}. Figure 26 shows the corresponding Raman spectra. Increasing the laser scanning speed leads to a shorter annealing time, resulting in a reduction in grain size. When the annealing time is too long, GaN grains tend to overgrow and become coarse and agglomerated. Figure 26 presents the AFM image of GaN grains, showing that the GaN separated from the sapphire substrate at a laser scanning speed of 1.0 mms^{-1} exhibits a better surface morphology.

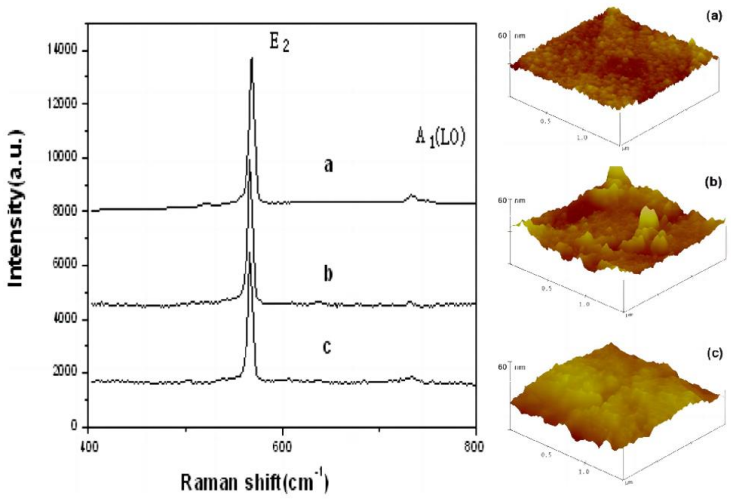

Figure 26. Raman spectroscopy and AFM images of sample scans before scanning (a), at a speed of 0.5 mms^{-1} (b), and a speed of 1.0 mms^{-1} (c). [177]

In addition to laser scanning speed, the laser pulse width also has an important influence on the LLO process. Wu et al. [179] observed that GaN films were damaged at a laser energy density of 300 mJ/cm^2 with a pulse width of 5 ns. However, they also found that at a pulse width of 35 ns, a laser energy density of 900 mJ/cm^2 was required to cause damage to the GaN film. This is because lower energy density and narrower pulse width can generate the same temperature and pressure as higher energy density and wider pulse width.

CHEN et al. [180] systematically studied the effects of laser pulse width on the GaN LLO process and performance. Under narrower pulse widths, picosecond lasers showed superior peel-off effects compared to nanosecond lasers, and they had less thermal impact on the LED chip region. This is attributed to the reduced energy required for peel-off due to the shorter pulse width and wavelength. Additionally, narrower pulse widths resulted in less damage to the GaN film due to the smaller heating area, lower transient temperature, and lower nitrogen vapor pressure during the LLO process. Understanding the temperature distribution of GaN films during the LLO process is crucial since the vapor pressure of nitrogen (N_2) is temperature-dependent [60]. Taking into account optical losses and substrate temperature rise, the temperature can be calculated using a one-dimensional heat equation. The heat equation can be expressed as (1).

$$\frac{\partial T}{\partial t} = \frac{a}{\rho C_P}\frac{\partial}{\partial_Z}\left(k\frac{\partial T}{\partial t}\right) \quad (1)$$

where the thermal diffusivity factor a is defined as $a = k/\rho \cdot Cp; k$, C_{p}, T are the thermal

conductivity, density, specific heat and temperature, respectively; $I(z,\ t)$is the incident power density at a depth z and time t, and it can be written as (2).

$$I(z,t) = I_0(t)(1-R_s)\exp(-a_s d_s)\cdot(1-R_{GaN})\exp(-a_{GaN}z) \quad (2)$$

Where αs、α_{GaN} are the optical absorption coefficients of sapphire and GaN, respectively;Rs and R_{GaN} are the surface reflectivities at the air/sapphire and sapphire/GaN interfaces, respectively;ds is the thickness of the sapphire substrate, $I_0(t)$ is the output laser power density per pulse.

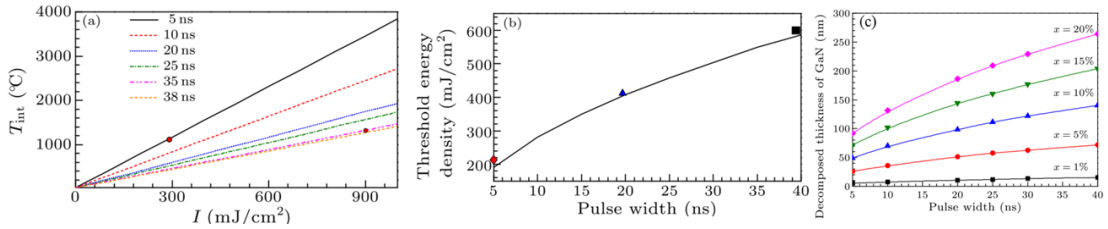

Figure 27. (a) Temperature distribution at the GaN/sapphire interface under different pulse widths and laser energy densities during quasi-continuous wave laser irradiation. (b) Threshold energy density for the LLO process as a function of the pulse width. (c) The decomposed thickness of the GaN film as a function of pulse width for different fluctuations of the pulsed laser energy. [180]

As shown in Figure 27(a), with the increase of laser energy density I_{o}, the interface temperature T_{int} shows a linear increase. Furthermore, when the pulse width is narrower, the increment of T_{int} is greater compared to wider pulse widths. In ideal conditions, for double-polished sapphire substrates, optical scattering can be neglected. As illustrated in Figure 27(b)and(c), emission can be achieved under the threshold energy density condition when the decomposition thickness of GaN is only a monolayer. However, in actual experiments, the laser energy density used is consistently higher than the threshold energy density, and the decomposition thickness can reach 100 nm [181]. These fluctuations may arise from the non-uniformity of energy distribution within the irradiation area and variations between pulses [181,182]. Only when the temperature of the entire irradiation area reaches the decomposition temperature T_{d} the GaN film be completely delaminated. LLO with shorter pulse widths causes less damage to GaN crystals. Due to the characteristics of narrow pulse widths, the laser energy is delivered to the crystal in an extremely short time, leaving almost no time for thermal conduction effects. This reduces the possibility of thermal diffusion and thermal damage, thereby minimizing the potential risks of damage to Micro-LED chips and ensuring the performance and integrity of GaN crystals to the maximum extent.

As the laser energy density I_o increases, the interface temperature T_{int} exhibits a linear increase, especially with narrower pulse widths, and under experimental conditions exceeding the threshold energy density, the decomposition thickness of GaN can reach 100 nm [181] for double-polished sapphire substrates. These fluctuations may arise from the non-uniformity of energy distribution within the irradiation area and variations between pulses [181,182]. Only when the temperature of the entire irradiation area reaches the decomposition temperature T_d can the GaN film be completely delaminated. LLO with shorter pulse widths causes less damage to GaN crystals. Due to the characteristics of narrow pulse widths, the laser energy is delivered to the crystal in an extremely short time, leaving almost no time for thermal conduction effects. This reduces the possibility of thermal diffusion and thermal damage, thereby minimizing potential risks of damage to Micro-LED chips and ensuring the performance and integrity of GaN crystals to the maximum extent.

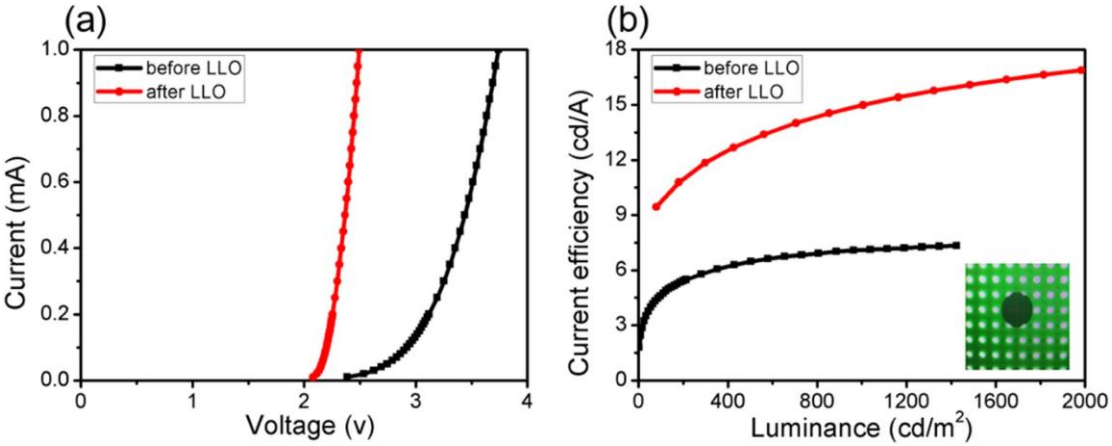

Figure 28. (a) Comparison of typical forward I–V characteristics before and after LLO. (b) Comparison of typical current efficiency-luminance characteristics of LED array device. The inset shows the typical picture of light emission. [117]

Tian et al. [117] fabricated GaN-based micro-LEDs on PSS and analyzed their I-V characteristics, as shown in Figure 28(a) and (b). The results showed that the reduction in LED forward voltage (VF) after LLO can be attributed to significant improvements in current spreading and rapid heat dissipation caused by Joule heating and PN junction temperature. Another reason is that the LLO process caused partial damage to the epitaxial lattice, opening a pathway in the original PN MQW layers. The decrease in operating voltage of the chip device implies a reduction in power consumption of the display at a fixed brightness level, meeting the demand for low-power display products.

Stephan KRAUSE et al. [183] used femtosecond laser pulses of different wavelengths to study the ultrafast non-thermal ablation-induced LLO of ultrathin layers at the interface of two materials. They determined a non-damaging processing window and confirmed the suitability of femtosecond lasers for LLO. Femtosecond lasers in LLO exhibit the following characteristics:

- Non-thermal damage: The extremely short pulse duration of femtosecond lasers results in minimal heat transfer to the material. As the pulse duration is too brief, there is almost no time for thermal conduction to occur.
- High precision and controllability: Femtosecond lasers offer high spatial and temporal resolution, enabling precise and controlled ablation processes. By adjusting laser parameters such as power and focal depth, the interaction between the laser and the chip interface can be precisely controlled, resulting in high-quality and consistent ablation outcomes.
- High efficiency: Femtosecond laser ablation typically employs micrometer-sized spots, allowing for the processing of large chip areas in a short amount of time.
- Wide applicability: Femtosecond laser ablation is suitable for various types of materials and structures, including thin films, multilayer structures, and complex devices.

However, LLO technology is only applicable to ultraviolet-transparent substrates, such as sapphire substrates; for non-transparent substrates, like silicon or gallium arsenide, mechanical grinding, and wet chemical etching techniques are feasible options.

2.3.2 Selective Laser Lift-Off (SLLO)

To achieve full-color emission in Micro-LED displays, it is necessary to precisely arrange and integrate red, green, and blue Micro-LED chips on the same substrate, creating small and high-resolution color display pixels. However, the LLO process is based on the full-area delamination of chips of the same color. Complex transfer processes are required to achieve three-color integration, which is not suitable for the selective integration of non-uniform red, green, and blue micro-LED devices. Moreover, selective repair of a small number of damaged Micro-LED chips is crucial for improving the yield of display products. Therefore, laser-based selective transfer technology has emerged. This technology is applicable for heterogeneous integration and selective repair [183,184] without requiring complex batch processing. It allows for the selective transfer of specific pre-defined LEDs and repair of damaged LEDs. Figure 29(a) illustrates the scanning strategy for SLLO.

Selective Laser Lift-Off (SLLO) is a technique that uses laser irradiation to selectively delaminate the interface between Micro-LED chips and the substrate. Typically, UV light is used as the light source. Shorter wavelengths of light have stronger interactions with the material, enabling a more precise delamination process. Additionally, UV light generates relatively less heat during the delamination process, reducing the risk of thermal damage. Jaegu Kim [184] utilized a 266nm diode-pumped solid-state laser irradiation technique to study the relationship between light intensity distribution and defocus length, as shown in Figure 29(b). SLLO of GaN-based Micro-LED on the sapphire substrate was performed, and it was found that a larger beam size with a laser intensity of approximately 37 kW/cm^2 provided better surface quality compared to a smaller beam size. The feasibility of SLLO was validated by selectively lifting off the Micro-LED onto a release layer, as depicted in Figure 29(c).

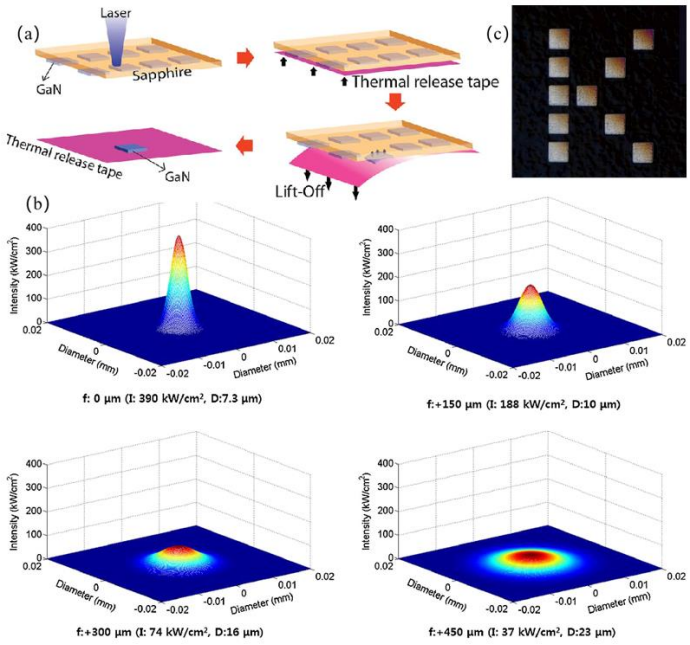

Figure 29. (a) Schematic diagram of selective laser lift-off (SLLO). [184] (b) Variation of light intensity distribution with defocusing length when the power is 150 mW and the focused beam size is 7.3 μm. [184] (c) Selective emission onto the letter "K". [184]

To determine the feasibility of complete delamination in SLLO, it is necessary to investigate the relationship between laser power density and substrate material adhesion. Junsu Park [185] studied the impact of laser energy density on SLLO performance. An ultraviolet laser with a wavelength of 266 nm, a pulse width of 20 ns, average power of 3 W, repetition rate of 30 kHz, and a beam diameter of 2 mm was used. The laser power density was varied from 64 to 108 kW/cm^2,

with changes occurring every 6 kW/cm^2. Figure 30 (a) shows that the material adhesion strength remains relatively unchanged at laser power densities of 64-76 kW/cm^2. However, at a laser power density of 83 kW/cm^2, the adhesion strength initially decreases to 43.2 MPa and then gradually increases. Figure 30 (b) analysis reveals that at laser power densities greater than 83 kW/cm^2, a significant amount of Ga residues on the surface, resulting in increased surface roughness and enhanced micro contact area between the LED and sapphire substrate, thereby increasing the friction and adhesion forces between the materials. There is a significant variation in adhesion strength within the laser power density range of 64-108 kW/cm^2. To reliably separate GaN-based LEDs from sapphire substrates, a higher power density is required than for Ga decomposition to ensure sufficient Ga precipitation through laser irradiation. On the other hand, even with Ga precipitation, higher power densities can lead to thermal damage and roughening of the interface, hindering the separation of GaN LEDs from the sapphire substrate.

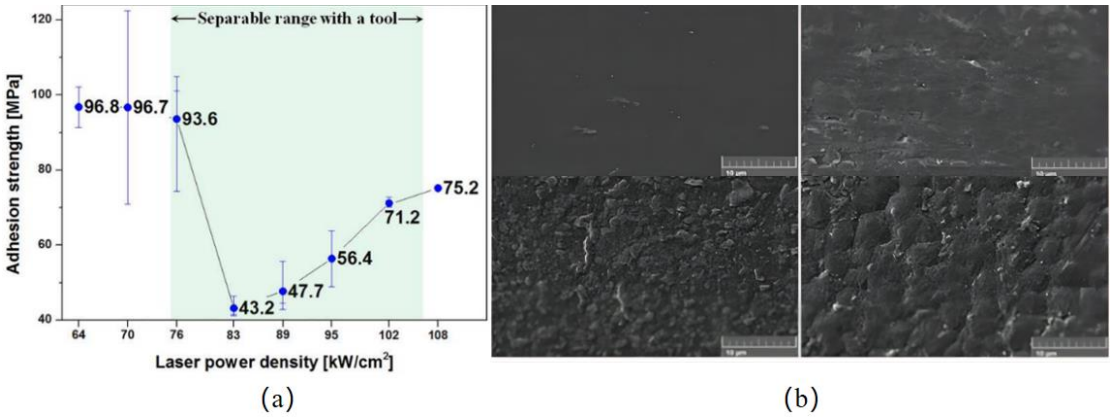

Figure 30. (a) Influence of laser power density on adhesion strength. (b) SEM images at different laser power densities. [185]

It can be concluded that laser power density has a direct impact on the separation efficiency of Micro-LEDs. Higher laser power density provides more energy, making the separation process more efficient. Laser power density has a complex influence on the separation quality. An appropriate laser power density can achieve high-quality separation, resulting in smooth separation surfaces and intact Micro-LED chips. However, excessively high laser power density may cause excessive absorption and localized melting, leading to increased roughness of the separation surface, edge burning, and cracks, thereby reducing the separation quality. The choice of laser power density is also closely related to temperature control. During the SLLO process, laser power density can cause localized heating of the material, requiring appropriate temperature control to avoid damage caused

by overheating. By combining appropriate laser power density and temperature control, good separation efficiency and quality can be achieved. Excessive laser power density may cause damage to the substrate material. Excessive focusing and absorption of laser energy can result in thermal damage, melting, and fracturing of the substrate. Therefore, it is crucial to choose an appropriate laser power density that is high enough to achieve effective separation while avoiding damage to the substrate.

Similar to LLO, SLLO with short pulse widths causes minimal damage to GaN crystals. Therefore, it is necessary to investigate the capability of femtosecond laser SLLO. Steffen Bornemann et al. [186] successfully fabricated independent Micro-LED chips with a thickness of less than 5 μm using a two-step process. Figure 31 presents a two-step process flow, where the selected separation area is scanned using a high-energy femtosecond laser, and high-quality boundaries are obtained through laser-induced cracking. Then, in the second step, a lower pulse energy was used to delaminate the selected areas to avoid chip damage. This two-step process strategy fully utilizes the high power and fine control of a high-energy femtosecond laser with lower pulse energy, demonstrating the successful fabrication of independent Micro-LED chips with a thickness of less than 5 μm through femtosecond laser delamination. Femtosecond lasers, due to their small heat-affected zone, high processing precision, and absence of thermal stress, are particularly suitable for thin-film delamination applications in Micro-LED manufacturing. SLLO is currently not in mass production and requires further research and development.

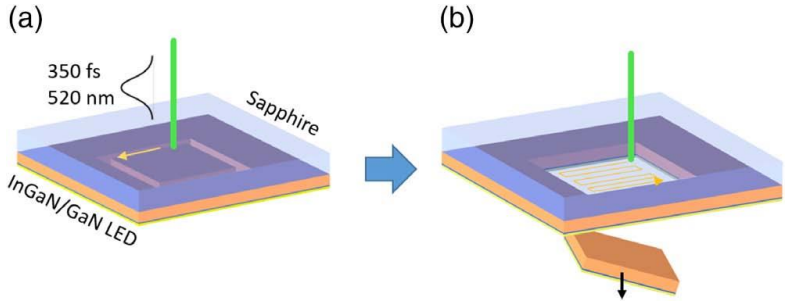

Figure 31. Two-step process flow for an area-selective LLO.[186]

2.4 Laser mass transfer

LLO is a crucial step in separating Micro-LEDs from sapphire substrates. However, after delamination, the Micro-LEDs still need to be transferred onto another substrate to complete the

final device fabrication. This involves the chip transfer process.

To achieve precise and efficient bonding of millions or even tens of millions of Micro-LED chips on a few square centimeters of a driver backplane, with a fault tolerance rate of one in a million and a positional deviation between chips controlled within ±0.5 μm, it is necessary to meticulously control each step of the process. With the current equipment and process methods, it is challenging to accomplish such a massive number of transfers. Taking a 4K television as an example, it requires the transfer of up to 26 million chips (calculated based on 4096×2160×3, where 4096×2160 represents the number of pixels, and each pixel contains R/G/B three-color chips). Assuming a transfer of 20,000 chips per cycle, it would still require 1,300 cycles. Even with a transfer yield of 99.999%, it would still necessitate the repair of 260 LED defects, and the repair of Micro-LED defects is extremely difficult.

Laser transfer is a technology that involves separating Micro-LEDs from the source substrate, picking them up in batches, and then transferring them individually or in groups to the corresponding pixel electrodes on the display substrate [187]. It can be applied to different sizes and materials of display substrates. Compared to other non-laser transfer processes, laser-assisted transfer technology performs more excellently in multiple key indicators. First, in terms of transfer efficiency, laser transfer can reach an extremely high level of 99.99%, an almost perfect transfer rate [188]. In contrast, other non-laser processes such as electrostatic [189] and fluid assembly [190] generally have transfer efficiencies in the range of 50-90%. In terms of transfer speed, laser transfer is far ahead, capable of an astonishing speed of 100 million chips per hour, over 100 times faster than non-laser processes. For example, electrostatic transfer is only about 1 million chips/hour, and fluid assembly is around 500,000 chips/hour. In chip size, laser transfer applies to chips of 1 micron and above, covering most application areas, while non-laser processes are typically limited to the 10 - 100 micron range. In addition, laser transfer does not introduce any contaminant impurities, ensuring device performance, which is difficult for non-laser processes to achieve. Of course, laser transfer also has some limitations, such as the laser source potentially damaging the stability of chip transfer. In comparison, non-laser processes like electrostatic transfer have better flexibility and repeatability. The comparison between laser massive transfer and other transfer methods is shown in table 4.

Table 4. Comparison of various mass transfer technologies.

Transfer method	Performance	Advantages	Disadvantages	Chip size	Used by companies	Reference
Laser-based	Transfer yield 99.99%. The transfer rate is ≈100 million per hour.	No impurities transfer on the substrate surface.	Laser source can damage their transfer stability.	>1 μm	Optovate/Uniqarta	[188]
Electrostatic	The transfer rate is ≈1 million per hour.	Flexible to use and have perfect repeatability.	Due to electrostatic, the charges are induced which can degrade device performance	1–100 μm	Apple/Luxvue	[189]
Fluidic-based assembly	Transfer yield ≈65%. The transfer rate is ≈50 million per hour.	Economical, easy to operate, and minimal parasitic effect.	Inefficient, the probability of pixel damage during transfer is high.	>20 μm	Foxconn/eLux	[7]
Elastomer stamp (van der Waals)	Transfer yield 99.99%. The transfer rate is ≈1 million per hour.	It can be transferred efficiently and economically because of its stickiness (elastomer stamp) nature.	It has poor repeatability because the stamp adhesion force is controlled by peeling speed. It is optimized by a magnetorheological stamp	>10 μm	X-Celeprint	[190]
Roll-to-Roll/R2R	Transfer yield 99.99%. The transfer rate is ≈10,000 per second.	Economical, high efficiency, and high throughput	The probability of device damage is high.	≈less than 100 μm	Korean institute of machinery and materials	[191,192]

By generating certain interface phenomena through photothermal or photochemical reactions, the microdevices adhered to the responsive layer material overcome adhesion forces and are transferred to the target substrate. Based on the differences in laser parameters and responsive layer materials, interface phenomena can be classified into three categories: direct delamination, bubble formation, and stress-assisted transfer.

Direct delamination refers to the complete decomposition of the responsive layer material

(such as GaN material) at the interface after absorbing laser energy, leading to a weakening of the adhesion force between the device and the interface, thereby enabling transfer. Bubble formation refers to the ablative reaction of the responsive layer material (such as metal films [193], polymers [194], or thermally releasing adhesive layers [195]) at the interface, resulting in the generation of gas products that form bubbles. The device attaches to the bubbles, and the chip is detached and transferred to the receiving substrate due to the raised interface, reducing the surface contact area. Stress-assisted transfer refers to the thermal expansion effect of the responsive layer material (such as PDMS [196], SMP [197]) after absorbing laser energy, causing deformation under thermal or shear stress. Interface cracks propagate, leading to the transfer of the chip to the target substrate.

Although these transfer techniques are based on different interface phenomena, they all utilize laser pulses to control the adhesion forces between the laser-responsive layer material and the microdevice interface, achieving chip detachment and transfer. The direct transfer method is similar to laser lift-off and will not be reiterated. The large-scale manufacturing of Micro LED displays hinges on the effective mass transfer of individual LED elements. Various laser-assisted transfer techniques have emerged as promising solutions, each exhibiting distinct advantages and tradeoffs across critical performance metrics.

The LLO approach leverages the direct decomposition of the GaN-sapphire interface under 266nm laser irradiation, enabling the peeling of individual GaN-based LED elements onto flexible substrates [198]. This method demonstrates exceptional transfer efficiency, reaching an impressive 99.9%. However, the LLO process is limited by a relatively coarse transfer precision of ±10 μm.

In contrast, the [199] LIFT method stands out for its remarkable transfer speed, achieving rates exceeding 100 parts per second or over 100 M/hour. Remarkably [200], the LIFT process also attains a high transfer precision of ±1.8 μm [201]. These speed and precision attributes make LIFT a compelling solution. Nevertheless, its transfer efficiency is lower, at 64% [202].

Other laser-assisted techniques, such as laser-driven microstructure transfer and laser-driven SMP [203] transfer, exhibit more moderate performance profiles. Their transfer efficiencies range from 50-70%, transfer precisions around ±35 μm, and relatively slower speeds [204].

The tradeoffs between these key parameters - transfer efficiency, speed, and precision - must be carefully weighed when selecting the optimal laser-assisted Micro LED mass transfer technique for a given application. The LLO method excels in throughput, while the LIFT process offers

unparalleled speed and precision. The other techniques present more balanced performance characteristics. The comparison of laser transfer methods and technologies is shown in Table 4.

Table 4. Comparison of Laser Transfer Methods Technology.

method	Interfacial Phenomena	interface	mechanism	laser	Transfer Object	Results	References
laser lift-off	direct decomposition	Sapphire-GaN	GaN decomposes into Ga and N^2	266nm solid-state laser	100 μm × 100 μmGaN LED	Realize the peeling of a single LED onto a flexible substrate	[198]
Laser-induced forward transfer	Bubble formation at the interface	Quartz-DRL	DRL-restricted ablation forms a bubbling impact	355 nm Nd: YAG laser	680 μm × 680 μm×65 μ m silicon wafer	Yield: 64% Deviation angle: 3.5 °	[199]
		Quartz - Double-layered DRL		1064 nm Nd: YAG laser	300 μm × 300 μm× 130 μ m silicon wafer	Accuracy: ± 35 μ m. Speed: 100 pieces/s	[200]
		Transparent substrate DRL layer		UV laser	50 μm× 50 μm× 6 μm μLEDs	Accuracy: ± 1.8 μ m. Speed:>100 M/h	[201]
Laser-assisted microcavity transfer		Elastic Stamp - Air	Closed cavities expand due to heat, reducing surface contact area and reducing interface adhesion	808 nm fiber laser	400 μm × 200 μmLED	Low-temperature non-contact transfer of MicroLEDs to different substrates	[202]
Laser-driven microstructure transfer		Elastic stamp - adhesive layer microspheres	The thermal effect causes the microspheres wrapped inside the viscous layer	808 nm fiber laser	285 μm × 285 μm× 4.6 μm LED10	Providing a strong-to-weak adhesion ratio of>1000, successfully	[205]

			to rapidly expand, causing deformation of the flat surface and bubbling at the interface, significantly reducing surface adhesion		×10 array	transferring Micro LEDs to different substrates	
Laser-driven micro transfer placement	Interface stress assistance	Elastic stamp - Microdevices	Interface thermal mismatch forms local shear force	805 nm infrared laser	100 μm × 100 μm× 3 μ m silicon wafer	Silicon wafers successfully picked up and released	[203]
Laser-driven SMP transfer		Shape Memory Polymers - Microdevices	During transfer, the laser thermal effect causes SMP to recover, thereby releasing mechanical stress	808 nm fiber laser	167 μm × 167 μm× 95 μm LED	Implementing transfer printing of complex shaped components at the mesoscale	[204]

2.4.1 Blister

The origin of laser transfer technology can be traced back to the Laser-Induced Forward Transfer (LIFT) technique. LIFT is a technology that enables the precise placement of various functional materials and structures into user-defined patterns, allowing for the large-scale placement of structures or devices with tiny feature sizes. LIFT technology was first proposed by Bohandy et al. in 1986 [206]. In LIFT, a laser is directed through a transparent substrate to interact with the interface material on the source substrate, causing it to melt or ablate. The resulting vapor pressure transfers the interface material and the attached device to the target substrate.

For laser-induced forward transfer of microdevices, a Dynamic Release Layer (DRL) is introduced between the transparent substrate and the microdevice [207]. The laser interacts with the DRL on the transparent substrate, causing localized energy absorption, ablation, and decomposition in the shallow region of the DRL at the interface. The remaining portion of the DRL remains intact, confining the generated gas products within the undecomposed film. When the gas pressure exceeds

the yield limit of the confined film due to the stress generated by the gas, the film deforms and forms a bubble. As the volume of the bubble increases, the gas pressure decreases until reaching a steady state. The curvature change of the bubble reduces the adhesion between the device and the sacrificial layer interface, while the instantaneous impact provides the kinetic energy for chip transfer.

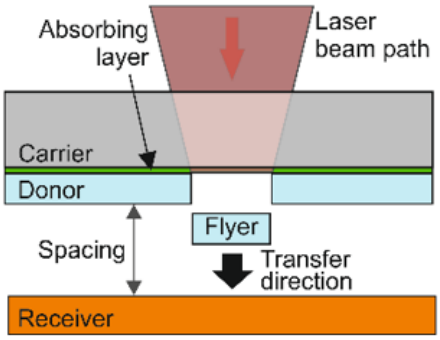

Figure 32. LIFT principle diagram. [208]

LIFT technology has successfully transferred electronic components ranging in size from 0.1 to over 6 mm^2. This technology enables reliable picking and releasing of micro-objects by controlling the adhesion forces of the stamp. Figure 32 illustrates a typical LIFT process. In the LIFT process, the laser passes through the transparent substrate and is absorbed by the dynamic release layer. Through laser ablation or vaporization, the dynamic release layer generates high pressure, quickly transferring the chip from the stamp to the receiving substrate.

The key to LIFT technology lies in selecting a DRL material that exhibits adhesion and can release the chip after laser interaction. Among them, a monolayer metal film [209] is one of the simplest DRL materials, and it has been used to transfer phosphor powders to fabricate phosphor screens [210] through Au-DRL. However, metal DRLs may result in residual material on the device surface, potentially contaminating the device. To address this issue, monolayer polymer materials with volatile decomposition products can be employed, such as photo-decomposable triazene polymers [211] (TP) or polyimide [212] (PI). These polymer materials have high absorption peaks under laser irradiation and decompose into volatile products upon irradiation, generating a shockwave that facilitates device transfer. Research by Fardel et al. [194] demonstrated the successful transfer of OLED pixels using TP as a sacrificial layer. However, the shockwave generated by ablation may cause device collision on the receiving substrate, potentially damaging the devices. Further studies have shown that significant improvements in transfer efficiency can be

achieved under smaller gaps and negative pressure conditions. Therefore, the use of polymer materials with volatile decomposition products can minimize the contamination issues associated with metal DRLs.

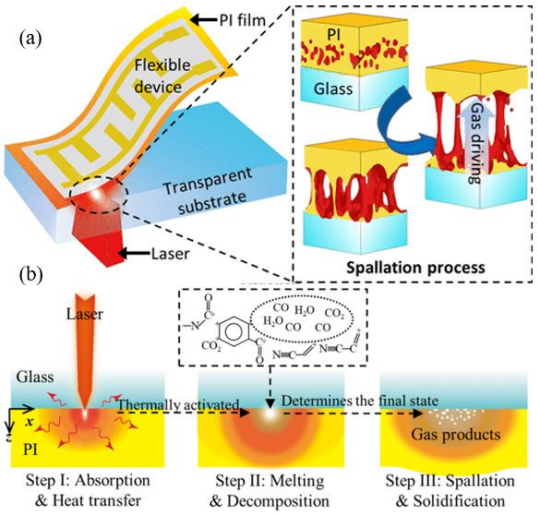

Figure 33. (a) Schematic diagram of the PI ablation model. [212] (b) Principle diagram of laser ablation-induced bubble generation in PI. [212]

PI is another commonly used DRL polymer material that achieves high-efficiency and high-precision mass transfer by generating gas products and mechanical energy through thermal decomposition under laser irradiation. Bian et al. [212] researched the foaming mechanism of PI and found that, upon laser absorption, localized high temperatures at the interface between the PI film and the glass substrate cause it to enter a molten state. As the temperature further increases, chemical bonds decompose thermally, resulting in gas products, as shown in Figure 33(a). Due to the shallow absorption depth of PI under ultraviolet light, the gas products can be encapsulated by the remaining PI, forming a bubble enclosure, as shown in Figure 33(b). The chemical energy generated during laser ablation is converted into mechanical energy, driving the device transfer and achieving high-efficiency transfer. Additionally, PI possesses a low thermal diffusivity, which helps to prevent thermal damage to devices attached to the outer surface of the bubble. By precisely controlling parameters such as incident laser energy, spot size, and material thickness, this technique enables high-efficiency and high-precision mass transfer that is only limited by the laser repetition rate.

The effectiveness of this technology for microdevice transfer has been experimentally validated. Karlitskaya et al. [200] successfully transferred silicon wafers with dimensions of

300μm×300μm and 95% of the transferred wafers achieved rotation angles within a 9° error range at a receiving gap of 195μm. Miller et al. [213] proposed a thermomechanical selective laser-assisted mold transfer technique. By introducing a dual-layer DRL and an additional adhesive layer to provide the necessary adhesion for picking up the chips, as shown in Figure 34, they transferred silicon wafers with dimensions of 680μm×680μm×65μm at a receiving gap of 195μm. The transfer yield was 64%, and the average errors for rotation and release angles were 3.5° and 14°, respectively. To optimize the transfer performance, Hong et al. [214] studied the dynamic process of crack propagation at the substrate/polymer interface during bubble formation. They found that bubble height and crack length are sensitive to the laser energy density parameter. Higher laser energy density tends to generate higher bubbles. When the laser energy density exceeds the critical value, cracks will propagate, leading to chip detachment.

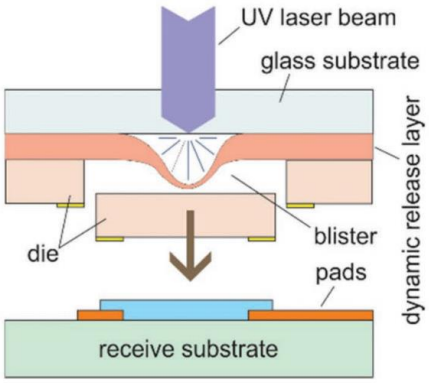

Figure 34. Dual-layer DRL structure. [213]

Uniqarta has introduced the Massively Parallel Laser-Enabled Transfer (MPLET) technology [215], building upon the LIFT technique. The working principle is depicted in Figure 35(a), where a diffraction optical element is used to diffract a single laser beam into multiple sub-beams. The number of sub-beams depends on the laser energy density, and each sub-beam corresponds to the transfer of a Micro-LED. This significantly reduces the time required for scanning and transferring with a single beam. Currently, the MPLET technology enables transfer speeds of up to 100 million units per hour for large panels and exceeds 500 million units per hour for small panels. The transfer accuracy is within ±1.8 μm.

The Coherent company has developed the UV transfer process [216], which is based on the principles shown in Figure 35(b)(c). By projecting a UV laser beam through a photomask onto a sapphire wafer, the beam's shape is transformed into a rectangular beam with a "flat top." This

uniform intensity ensures the application of equal force at every point within the processing area. Optical devices are configured to enable the detachment of large chip areas with each high-energy pulse. UV transfer provides both high precision (±1.5 pm) and high throughput, allowing the transfer of thousands of chips with a single laser irradiation. To achieve uniform and consistent grain transfer within the processing area, highly uniform laser irradiation is required. This results in the formation of a highly uniform 2D field, which is then reshaped optically into a square or rectangular beam with a large aspect ratio. As a result, the force is always perpendicular and does not cause lateral displacement due to the Gaussian distribution or tilted shape of the beam profile. Having a uniform beam intensity across a larger range (wafer width) is equally important to ensure the application of equal-sized forces to each grain. In fact, due to the shorter wavelength of UV light, micrometer-level resolution can be achieved in the future. Smaller grains only require a different projection mask.

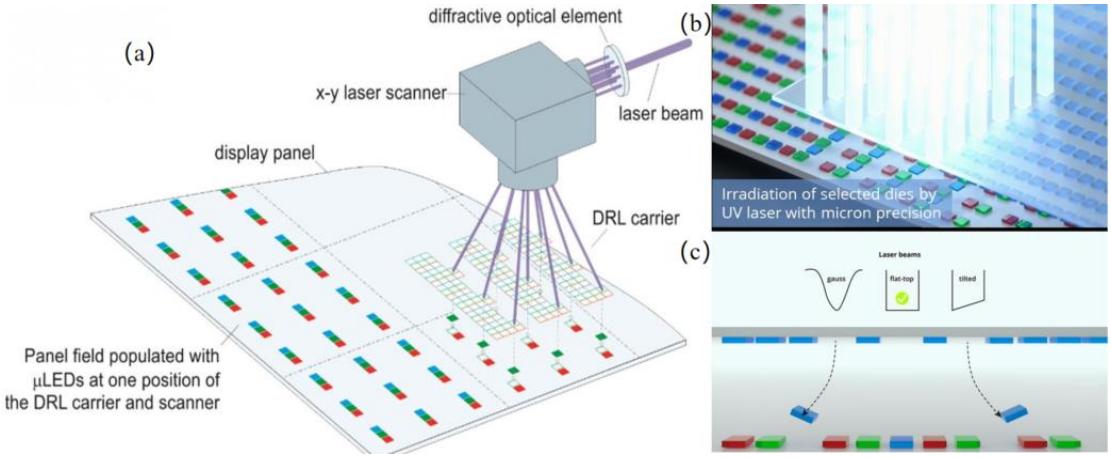

Figure 35. (a) MPLET schematic diagram. [215](b) UV transfer process. [216] (c) High placement accuracy of TopHat beams. [216]

However, due to the influence of gas dynamics and flight instability, this technology suffers from the issue of low placement accuracy. Additionally, the shockwaves generated during the LIFT process can potentially cause chip damage. Interface damage is permanent [217]; therefore, this transfer technique requires continuous replacement of the response layer

Despite the significant role played by LIFT in device transfer, it also has some limitations. To overcome these issues, researchers have started exploring new transfer techniques. One of the highly promising methods is laser-induced thermal bubble transfer. This technique utilizes the thermal effects of lasers to achieve efficient and precise device transfer by controlling temperature changes

and expansion effects during the process. Compared to traditional LIFT, laser-induced thermal bubble transfer offers better transfer control and higher success rates. When applied to massive transfers, laser-induced thermal bubble transfer initially employs the van der Waals forces of a stamp or the adhesive force of a sticky layer to pick up MicroLEDs from the source substrate or temporary substrate onto the stamp. Then, laser-induced thermal bubble transfer is used to release the Micro-LEDs from the stamp selectively onto the target substrate.

Compared to LIFT, the key difference in laser-induced thermal bubble transfer is that during laser irradiation, only a small portion of the DRL is ablated, generating gas to provide the impact energy. The DRL can create an expanding bubble shield that encapsulates the shockwave, acting as a soft ejector to gently push the chip towards the receiving substrate, thereby improving transfer accuracy and reducing damage.

The non-reusability of the stamp is a significant limitation for the application of laser-induced thermal bubble transfer. To enhance cost-effectiveness, Luo et al. [202] developed a reusable laser-induced thermal bubble transfer technique based on a clever design of reusable molds, as shown in Figure 36. The mold is moved to the surface of the microdevice and pressed against it to maintain a flat interface and contact with the device. Then, it is moved above the receiving substrate and aligned to the desired position. With the action of the laser beam, the metal layer adhered to the cavity wall absorbs heat, leading to rapid expansion of the air inside the cavity. This thermal expansion effect causes the microstructure thin film to protrude, reducing the adhesion force with the device, thereby enabling device transfer onto the substrate. To quantify the relationship between the expansion pressure inside the cavity and the deflection of the membrane with increasing temperature, researchers established a theoretical mechanical model. It was found that as the temperature increases, the height of the bubble inside the cavity increases, thereby reducing the contact area and decreasing the interfacial adhesion force. This technique can provide a conversion ability of up to 1000 times stronger or weaker adhesion when the temperature rises to 100°C. The feasibility of this technique in Micro-LED applications has been demonstrated by transferring LED chips with dimensions of 400 μm×200 μm onto different display substrates.

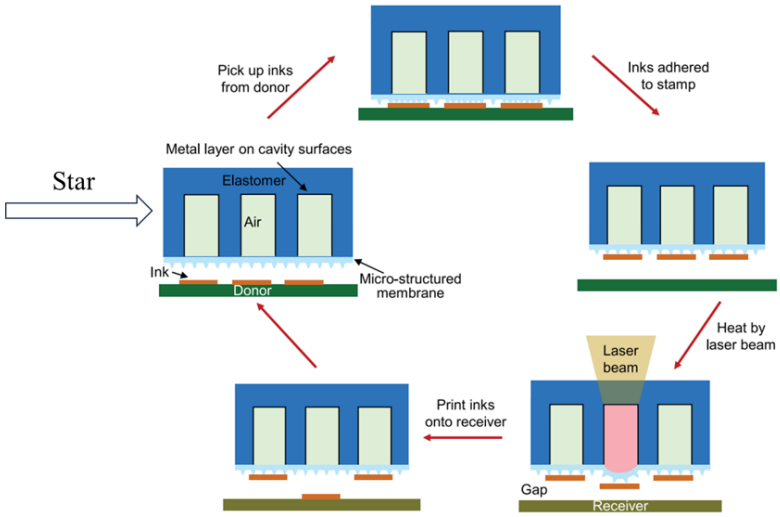

Figure 36. Schematic diagram of the programmable non-contact transfer printing process driven by an active elastic microstructure stamp using a laser. [202]

In massive transfers, strong adhesion is required during the picking process to ensure reliable pickup, while minimal adhesion is desired during placement to enable transfer. Therefore, the key to the technology lies in improving the adhesion switching ratio. Wang et al. [205] embedded expandable microspheres into the adhesive layer and utilized a laser heating system to generate external thermal stimulation. During the picking process, the small-sized embedded expandable microspheres ensure a smooth surface of the adhesive layer, while the influence of strong adhesion on the adhesive layer can be neglected. During the transfer process, the external heat stimulus generated by the laser heating system at 90°C is rapidly transmitted to the adhesive layer, resulting in the rapid expansion of internal microspheres, as shown in Figure 37(a). This leads to the formation of a hierarchical micro-bump structure on the surface, significantly reducing the surface adhesion and enabling reliable release. However, selecting the appropriate laser power is a key challenge as it needs to reach the thermal stimulation temperature for the embedded microspheres without causing performance degradation of the microdevices. To further demonstrate the applicability of this method for Micro-LED transfer, researchers successfully selectively transferred a 10×10 array of Micro-LEDs from a thermal release adhesive (TRA) mold to a temporary PDMS receiving substrate, proving the feasibility of the technique in large-scale transfers.

To achieve large-scale transfers, researchers have employed the thermal release tape (TRT) laminating technique. The study conducted by Yan et al. [195] revealed the principle of TRT (Thermo-Releasing Transfer) for microdevice transfer, where the successful transfer depends on the

variation of adhesion force between TRT and the functional device, controlled by temperature parameters, as shown in Figure 37(b). When the temperature is below the critical temperature (Tr), the energy release rate between TRT and the functional device exceeds the critical energy release rate between the functional device and the source substrate. As a result, cracks tend to propagate at the interface between TRT and the functional device, enabling the pickup of the functional device. During the transfer process, the temperature is increased beyond the Tr through laser heating. This leads to a lower energy release rate between TRT and the functional device compared to the critical energy release rate between the functional device and the target substrate. Consequently, the functional device is successfully transferred onto the target substrate. The variation in adhesion force during this transfer process and the control of temperature parameters provide a feasible solution for large-scale transfers, demonstrating the potential of the TRT laminating technique in microdevice transfer.

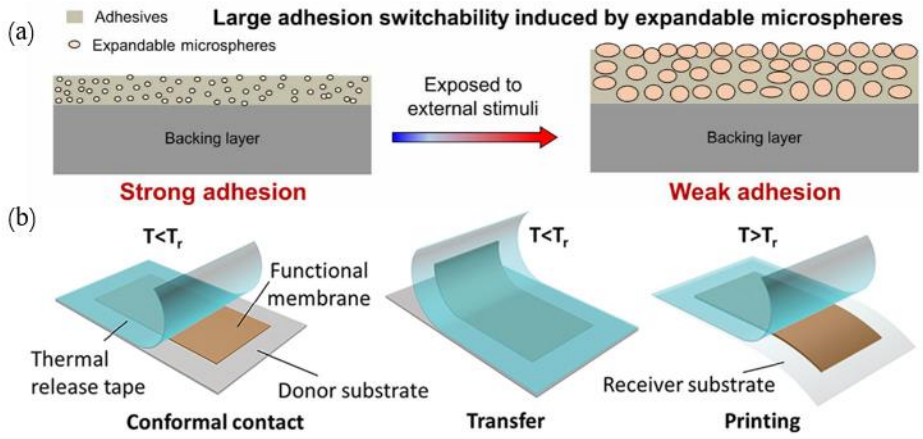

Figure 37. (a)Schematic illustration of embedded microsphere bubbling [205] (b) Schematic illustration of thermal release tape for batch transfer of micro-devices [195]

2.4.2 Laser stress-assisted transfer

To control the formation of bubbles in stamping for device transfer, it is necessary to control the surface microstructures to adjust the adhesion energy and achieve proper pick-up and placement. However, this method requires ensuring good contact between the device and the receiving substrate surface. To overcome the limitations imposed by the characteristics and geometry of the receiving substrate during the transfer process, Saeidpourazar et al. [218] introduced a laser-induced imprint thermal stress response mismatch transfer technique called Laser-Driven Micro-Transfer Placement (LMTP) technology. Figure 38 illustrates the steps of LMTP, the principle involves using a laser of

a specific wavelength to pass through a transparent stamp and act on the device. The microdevice (Si or GaAs) absorbs the laser energy, causing its temperature to rise. Due to the low thermal conductivity of the stamp, a localized hot region is formed near the device-stamp interface. The stamp, having a higher coefficient of thermal expansion (CTE), is constrained by the microdevice and the surrounding unstressed regions of the stamp. As a result, localized interface shear forces are generated at the contact interface under stress, leading to bending or protrusion. The driving force generated by this bending strain energy exceeds the adhesive strength at the device-stamp interface, causing the propagation of delamination cracks around the microdevice [219], thereby achieving the purpose of microdevice transfer and release. When the stamp interface temperature decreases, it can return to its original state, allowing for reuse. The introduction of LMTP technology eliminates the limitations imposed by the characteristics and geometry of the receiving substrate, providing a highly controllable and precise solution for microdevice transfer.

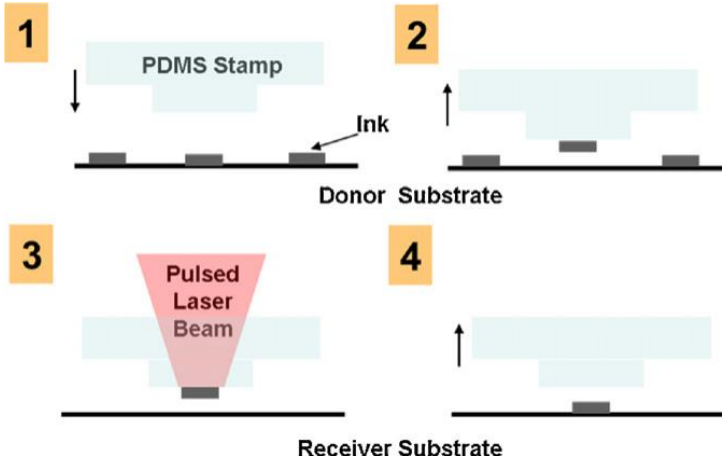

Figure 38. Schematic of the LMTP steps [218]

The core challenge of laser-driven micro-transfer printing technology lies in effectively controlling the thermodynamic properties and interface thermal stress between the stamp and the device to avoid unpredictable deformations and cracks. The success of this technique depends on precise control and adjustment of these factors. By adjusting process parameters such as laser energy and transfer distance, non-contact transfers with small errors, high success rates, and reusability can be achieved. However, it should be noted that to increase the release rate of strain energy, the technique raises the chip interface temperature by increasing the laser power. This operation may potentially cause thermal damage and have adverse effects on the stamp interface or the device. Therefore, cautious operation is necessary during the application of the technology to ensure the

integrity and performance of the devices are not compromised.

Currently, laser-driven micro-transfer printing technology has successfully demonstrated the transfer of a limited number of Micro-LEDs. However, for its application in large-scale transfers, further research is needed on factors such as chip spacing and beam organization and their impact on the transfer performance. This will help improve the scalability and reliability of the technology to meet the requirements of mass transfers.

In large-scale transfers, PDMS is commonly used as a transfer head. Although PDMS stamps can adapt well to complex geometric shapes of microdevices under compression, they quickly undergo elastic reconfiguration after the removal of compression preload, making them unable to maintain their shape in the long term. This requirement necessitates a relatively large flat area on the contact surface of micro devices to ensure effective contact and picking.

To overcome the limitations of elastic PDMS stamps in large-scale transfers, researchers have explored the use of shape memory polymers (SMP) as alternative materials for transferring and printing microdevices with different surface morphologies. SMPs exhibit shape-changing characteristics triggered by external stimuli such as light [220] or temperature variations [221]. Temperature-based SMPs undergo deformation when subjected to external pressure above their shape memory transition temperature (Tg), allowing them to conform to the shape of the device during picking. Subsequently, the SMP is cooled below Tg to remove the external pressure and retain its deformed shape. During the transfer process, when the temperature exceeds Tg, the SMP undergoes a shape recovery to its original undeformed state due to the shape memory effect, enabling the release of the picking force. The shape memory transition process of SMP is illustrated in Figure 39(a).

Laser-driven SMP transfer technology utilizes laser pulses to heat the SMP, and by controlling the laser parameters, the temperature variation can be controlled to induce the deformation transition of the SMP. The typical process of laser-driven SMP transfer technology [222] is illustrated in Figure 39(b). Firstly, the SMP stamp is uniformly heated to Tg and pressed onto the microdevices on the substrate. Under the applied preload force, the SMP stamp is deformed and then cooled to room temperature, maintaining the picking shape. Next, the SMP film with the picked devices is moved above the receiving substrate, bonded to the desired position by applying a certain load, and then the laser beam is directed onto the SMP interface to heat the deformed region, causing it to recover

to its original state, thus releasing the microdevices.

The key to laser-driven SMP transfer technology lies in the deformation transition of the stamp controlled by temperature. By utilizing the change in interface adhesion force caused by deformation, the picking and release of microdevices can be achieved. By precisely controlling the laser parameters and temperature variation, an efficient and accurate transfer process can be realized.

To better regulate adhesion force, improvements can be made in the deformation shape of the stamp or through enhanced temperature control methods to achieve better transfer results. In terms of improving the shape of the deformation, some SMP stamps have been fabricated with microstructures such as cones [223], as shown in Figure 39(c) and (d). In the initial state, only the tip of the cone or pyramid makes contact, resulting in a small contact area. However, upon deformation, a larger surface contact area is generated, providing reliable adhesion and picking force. After returning to its original shape, the device can be transferred due to the reduced contact area and the force exerted by the elastic material.

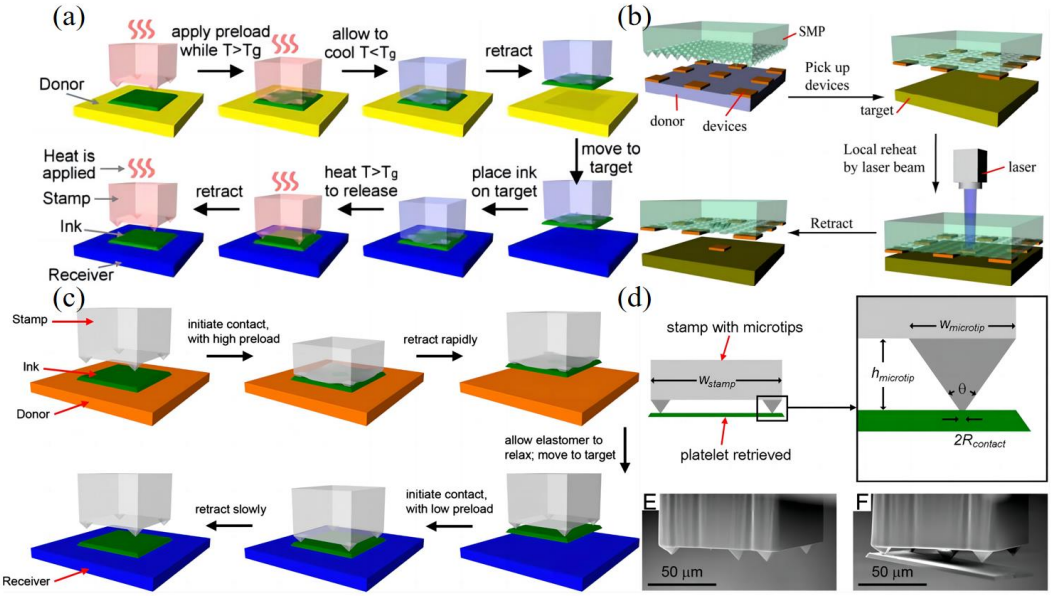

Figure 39. (a) SMP transformation process. [221] (b) Process of laser-driven SMP transfer technology. [222] (c) Deterministic assembly achieved by the implementation of elastomeric micro tips. [223] (d) SMP cone structure. [223];

To handle microdevices with more complex surfaces, Linghu et al. [204] proposed a gripper structure, as shown in Figure 40. During picking, deformation is induced primarily through stiffness variation, creating a mechanical hand structure that embeds the microdevice, thereby increasing picking reliability without relying on interfacial adhesion. However, during release, the adhesion

force on the microdevice surface plays a crucial role in the transfer process, especially as the device size decreases. Surface treatments or increased surface roughness can be utilized to reduce adhesion force and improve transfer reliability.

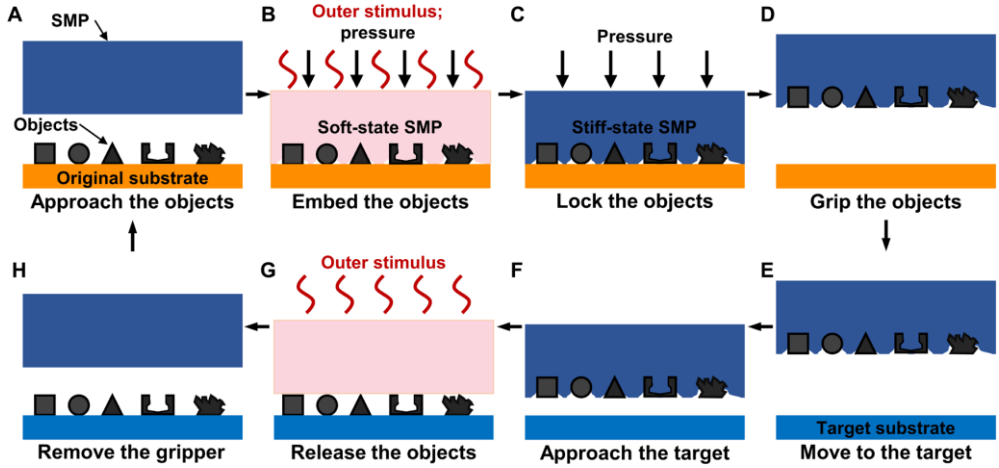

Figure 40. Schematic illustration of the gripping and release process of the universal SMP gripper. (A to D) Gripping process (E to H) Releasing process. [204]

In terms of improving temperature control, Eisenhauer et al. [197] embedded carbon black particles into the contact surface between the stamp and microdevice, as shown in Figure 41(a). These particles possess strong near-infrared absorption properties. By using near-infrared laser irradiation, localized heating of the SMP stamp is achieved. Figure 41(b) displays its 2D cross-sectional view. This composite carbon black-SMP (CBSMP) system enhances the material's absorption of laser energy, greatly expanding the range of applicable materials and optimizing temperature control methods. Serial transfer of individual wafers and parallel transfer of patterned wafers were both achieved. Linghu et al. [204] successfully transferred an array of 20x8 LEDs (167 μm x 167 μm x 95 μm), as shown in Figure 42. The transferred LEDs were validated through light emission and current-voltage characteristics, confirming the device's performance was unaffected.

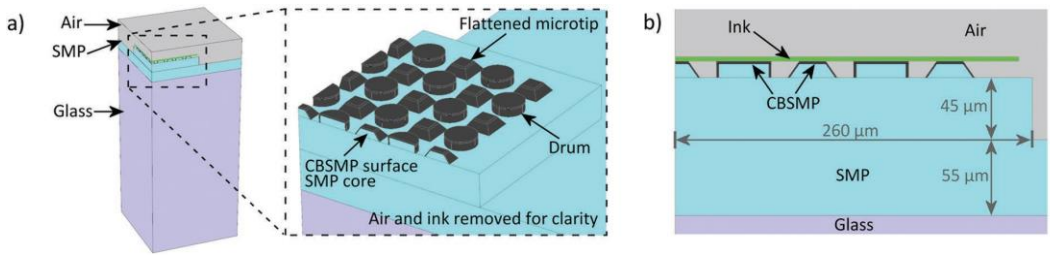

Figure 41. (a) SMP is filled with carbon black particles. (b) 2D cross-sectional view. [197]

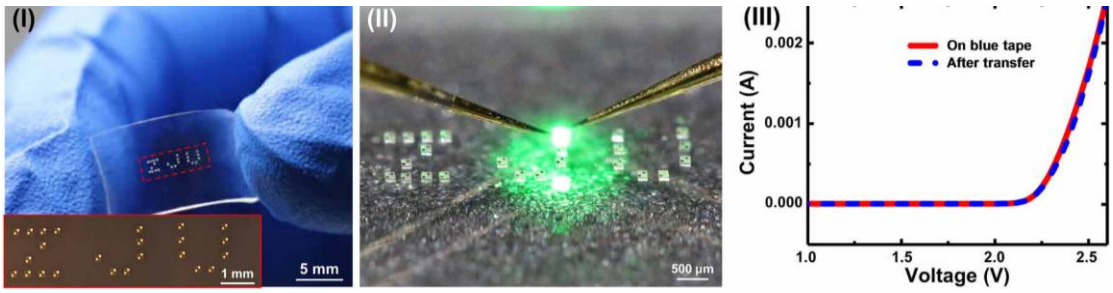

Figure 42. The transferred LEDs were characterized by their illumination and current-voltage (IV) characteristics.

[204]

Based on SMP-assisted laser-assisted transfer, a polymer mold with reversible adhesion force is used as the manipulator. The mold is heated and cooled through laser irradiation at its glass transition temperature, while the dynamic stiffness control of the SMP mold provides significant adhesion enhancement during device picking. Additionally, SMP materials' shape-fixing and shape-recovery properties offer considerable design flexibility for the stamp, allowing for more complex surface patterns and heterogeneous surface features, further reducing adhesion forces during release. This laser-based heating method offers superior speed and convenience, allowing for precise alignment of the material to be transferred.

2.5 Laser-assisted bonding（LAB）

For the reliable connection between the chip and the backplane in Micro LED technology, in addition to chip transfer, subsequent bonding processes [224–226] are crucial. Traditional methods such as reflow soldering (RS)/thermocompression bonding [227,228] and anisotropic conductive film (ACF) bonding [229,230] have been widely applied to relatively large-sized chips in conventional semiconductor devices. However, these methods face significant technical challenges when it comes to bonding Micro-LEDs with fine spacing. Difficulties in accurate alignment and bonding non-uniformity are major issues. Prolonged heating and large-area bonding can result in severe thermal stress and wafer warpage. Solder balls used for conventional flip-chip bonding may exhibit height inconsistency, both of which contribute to non-uniformity in the bonding area. Reducing the spacing and pixel size significantly increases the risk of wire short-circuits. On the other hand, ACF bonding may lead to high contact resistance or open circuits in Micro-LED bonding. The polymer particles in ACF are comparable in size to Micro-LEDs, which means only a limited number of particles can be used for bonding Micro-LEDs. Additionally, ACF bonding is not

repairable.

In contrast, LAB offers advantages such as selective bonding, localized heating, and rapid temperature control [231,232], making it highly suitable for bonding Micro-LEDs with fine spacing. LAB technology involves the use of a high-intensity laser beam to irradiate the metal surface, causing its melting and facilitating electrical connection. LAB utilizes the high positional accuracy and focusing capability of the laser beam to achieve selective heating and bonding in specific areas, thereby enhancing bonding precision and stability. Localized heating reduces the risks of thermal stress and wafer warpage [233,234], minimizing thermal impacts on sensitive components and improving bonding stability and reliability. LAB enables rapid temperature control [235,236], minimizing the influence of thermal stress and enhancing production efficiency. Its high bonding precision ensures accuracy and consistency, reducing non-uniformity in the bonding area and improving the reliability of the bonding interface. Additionally, LAB is a non-contact bonding technique, reducing mechanical stress and pressure on the chips, thereby lowering the risks of damage and contamination and improving bonding reliability and yield.

In the die-to-die bonding of Micro LEDs, LAB utilizes precisely focused laser irradiation to locally heat the chip surface, forming a molten layer and enabling controllable chip-to-chip bonding. By finely tuning key parameters such as laser power density, scanning speed, bonding temperature, and pressure, the bonding strength and reliability can be ensured. [235,236] This precise local heating characteristic makes LAB a prominent advantage in the integration of Micro LED at the individual particle level. For chip-to-chip bonding, LAB can be employed to integrate individual Micro LED chips with driver circuits, connectors, and other companion components [236]. The key lies in the reasonable control of laser irradiation parameters, where reliable bonding is achieved while also considering the potential impact of heat on the performance of Micro LED devices, ensuring the overall integration reliability. In wafer-to-wafer bonding, LAB enables the large-area bonding integration of entire epitaxial wafers with backplanes or substrates [231,232]. This requires precise control of the laser irradiation uniformity to ensure consistent temperature distribution across the bonding area, thereby improving production yield. LAB's advantage in this large-scale bonding lies in its ability to achieve localized and precise heating without causing thermal damage to the whole.

Joo et al. [237] developed a LAB process for integrating Micro-LEDs onto a driver board, as

shown in Figure 43(a). The Micro-LEDs are aligned to the receiving substrate using a vacuum bonding head, and the bonding pads on the receiving substrate are coated with anisotropic conductive paste (ACP). Subsequently, an IR laser beam is applied to the bonding head. The laser is transmitted through the intermediate layer and absorbed at the bonding junction, causing rapid melting (<1s). After retracting the bonding head, the Micro-LEDs are integrated into the receiving substrate. Using this method, a 20×20 array of Micro-LED was successfully integrated into the driver board, as shown in Figure 43(b). PMMA balls in the ACP serve as spacers, forming Sn58Bi solder joints between the Micro-LED electrodes and the substrate pads. The epoxy resin in the ACP enhances bonding strength and acts as a filler between the Micro-LEDs and the substrate, as illustrated in Figure 43(c).

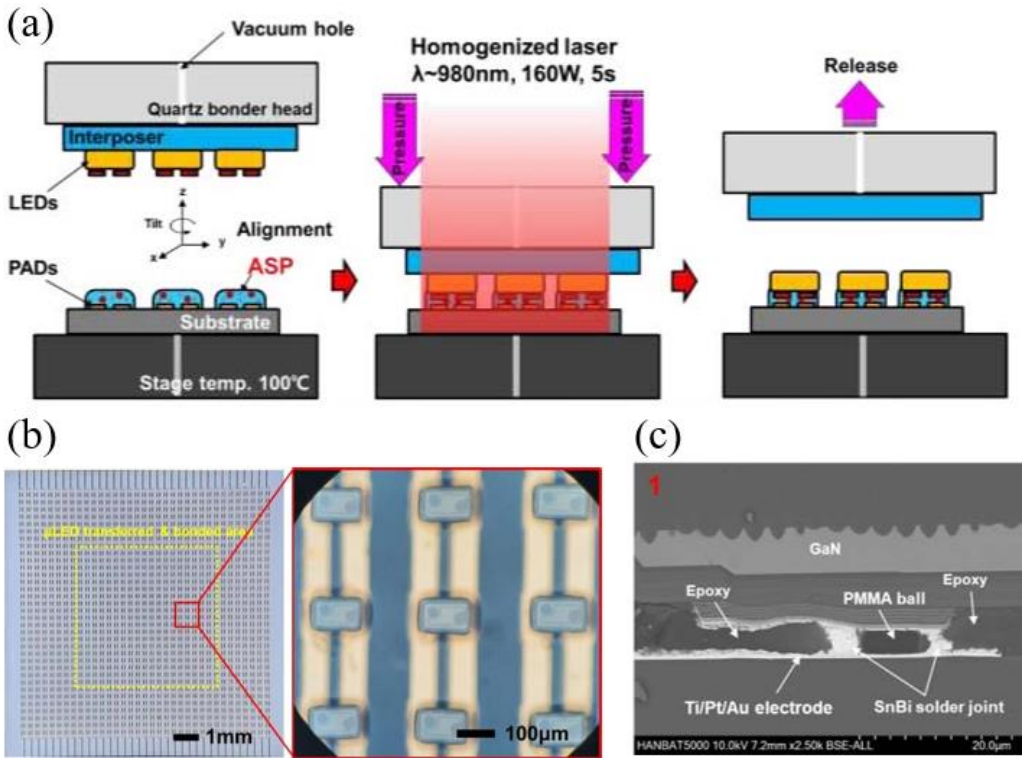

Figure 43. Laser-assisted bonding. (a) Working mechanism, (b) laser bonded Micro-LED array, (c) cross-sectional SEM image of the bonded Micro-LED onto the circuit using solder bumps.[237]

Kwang-Seong Choi et al. [234] conducted a study on two bonding materials for LAB processes. They introduced flux-filled underfill (FU) and hybrid underfill (HU), as shown in Figure 44(a) and Figure 44(b), respectively. FU is a non-conductive paste (NCP) composed of polymer materials, specifically designed for devices or packaging with solder balls or protrusions. Figure 44(c) illustrates the top and cross-sectional optical images of FU after LAB treatment. On the other hand, HU contains commercially available solder powder and is suitable for passive devices or packaging

without solder balls or protrusions, such as Micro-LEDs. Figure 44(d) presents the top and cross-sectional optical images of HU after LAB treatment.

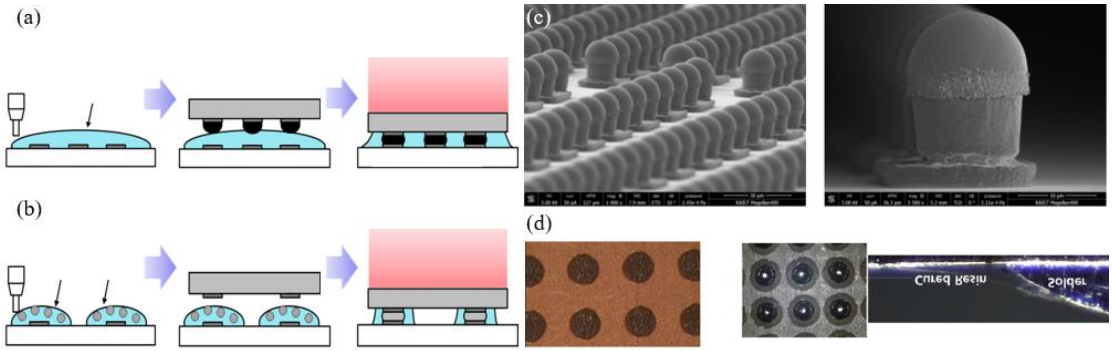

Figure 44. Process flow of the two bonding materials and SEM images after LAB treatment (a) LAB-FU (fluxing underfill) process (b) LAB-HU (hybrid underfill) process (c) Printed FU on Cu substrate and cross-sectional optical images of HU after LAB process Printed FU on Cu substrate and cross-sectional optical images of HU after LAB process (d) Printed HU on Cu substrate and cross-sectional optical images of HU after LAB process.[234]

Due to the differences in production efficiency between the transfer and bonding processes, various challenges arise during the configuration of production lines, leading to different issues. As the yield of each process is not 100%, inspections are required after each step, which can be time-consuming and challenging due to the small size of Micro-LEDs. Additionally, both the transfer and bonding processes require separate equipment and space investments. The overall yield of the entire process is determined by multiplying the yields of the transfer and bonding processes, which can result in a lower overall yield. Furthermore, the complexity of the repair process may increase, requiring significant time and hindering efforts to reduce manufacturing costs. Therefore, a new technology called simultaneous transfer and bonding (SITRAB) was introduced by SID 2021 [236], which combines the laser-assisted bonding with compression (LABC) process and SITRAB adhesive to achieve high-yield transfer and bonding of Micro-LEDs. Figure 45 illustrates the SITRAB process.

In the SITRAB process, SITRAB paste or film is deposited on the display panel substrate at room temperature through processes such as screen printing, dispensing, or lamination, as shown in Figure 45(a). The SITRAB paste and film consist of epoxy resin as the base resin, reducing agents to remove oxide on the solder surface, curing agents, catalysts to control the chemical reaction rate, and some additives to optimize processing performance. The top surface of the Micro-LEDs aligns with the sticky PDMS on the glass intermediate layer, forming a constant area of an n×n matrix, as shown in Figure 45(b). The glass intermediate layer with LEDs fixed by a quartz chuck is aligned

with the display panel substrate. After alignment between the LED and the display panel substrate, the solder pads below the LED move downward and make contact with the display panel substrate. Subsequently, a laser is applied to the area of transparent quartz and PDMS on the glass intermediate layer for a few seconds, as illustrated in Figure 45(c). In the SITRAB process, the temperature of the metal phase is maintained at 80-100°C to minimize laser power. The laser penetrates through the transparent quartz and PDMS on the glass intermediate layer, reaching the opaque metal pads below the LED and heating the solder pads and adjacent SITRAB material to the solder point's melting temperature. When the temperature reaches the melting point of the solder pads, the activated SITRAB material removes the oxide on the solder surface and wets the solder pads to the metal pads on the display panel substrate. Then, the LED is separated from the PDMS in the glass intermediate layer because the bonding strength between the LED and the metal pads on the display panel substrate is greater than the adhesive bonding strength between the LED and the PDMS, as shown in Figure 45(d).

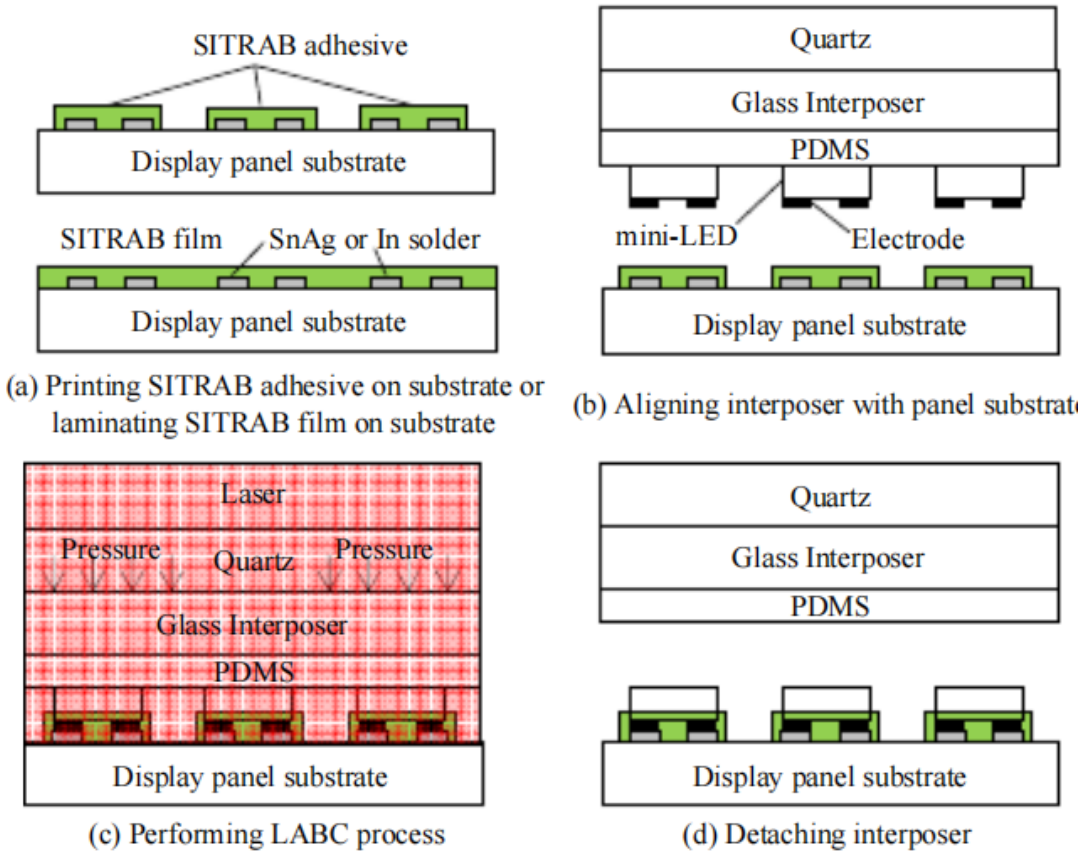

Figure 45 Schematic diagram of the SITRAB process.[236]

SITRAB technology was developed based on the SITRAB adhesive technology. A tile-type SITRAB process was adopted by Yong-Sung EOM et al. [238], and the process window of the

SITRAB material was determined for a stable SITRAB process. The process window was identified based on three different pot life: room temperature pot life (RPL), stage pot life (SPL), and laser pot life (LPL).

Tian et al. [239] proposed a novel laser-assisted bonding process using pure metal Au/Sn for high yield and cost-effective production, as illustrated in Figure 46(a). This technique was applied to a 62×78 pixel full-color Micro-LED display. The Au-Sn solder alloy exhibits high yield strength, corrosion and creep resistance, good wetting properties, as well as excellent thermal and electrical conductivity. It achieved a low-temperature solid-liquid bonding method below 280°C for the first time, ensuring reliable metal electrical connections between microscale LED devices and the backplane, thus ensuring the normal operation of the driving backplane. Figures 46(b) and (c) depict the morphology of Micro LEDs before and after the LABC process.

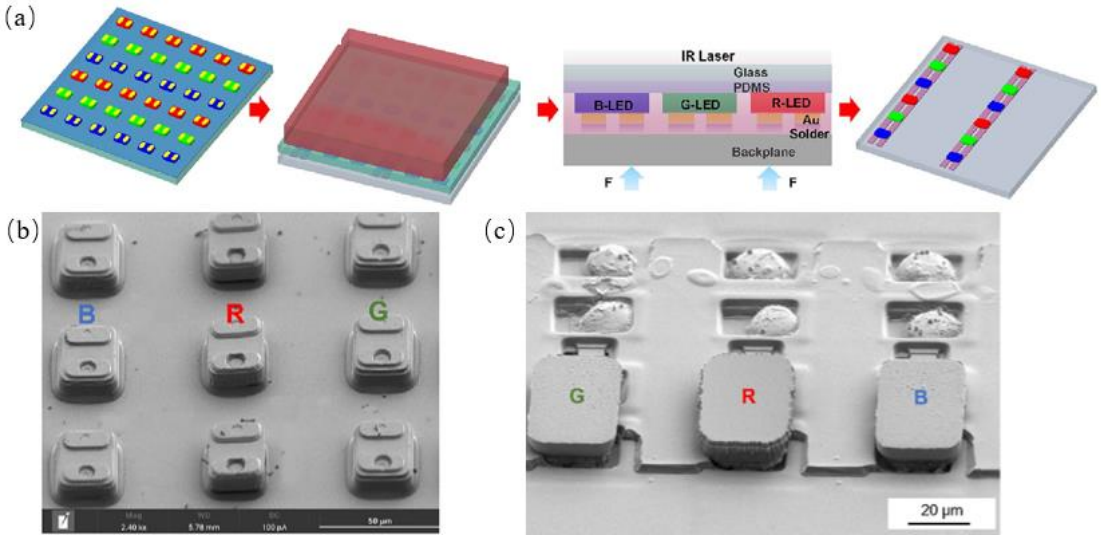

Figure 46. Pure metal Au/Sn laser-assisted bonding process (a) Schematic diagram of the process flow (b) SEM image of RGB micro-led chips on the donor substrate after soldering before laser-assisted bonding (c) SEM image of RGB micro-LED chips on substrate after welding.[239]

Despite its numerous advantages, there is still room for improvement in the bonding efficiency of LAB technology, particularly when bonding a large number of LED chips for display panels. There is a need to enhance the bonding efficiency to meet the requirements of high-volume production. One crucial factor is ensuring the uniformity of the laser beam across the entire bonding area. If the distribution of the laser beam is inconsistent or non-uniform, it may result in bonding failures, thereby affecting the overall quality and reliability of the bonding process. Therefore, precise control and optimization of laser beam parameters are essential for achieving reliable and efficient LAB bonding.

3. Laser detection and repair

During the manufacturing process of Micro-LEDs, defects or failures can affect their performance and reliability due to their small size and complex structure. Therefore, it is necessary to detect and repair defective Micro-LED devices. Traditional methods for detecting Micro-LEDs can be challenging because their size is extremely small, and the dimensions of conventional probes may exceed the size of the tested devices. High-resolution detection methods are required to assess the light-emitting performance of Micro-LED devices.

3.1 Photovoltaic Detection

In LED chips, side-wall damage during the etching process can lead to the generation of parallel resistance, resulting in unwanted leakage currents. While high-power LEDs designed for general lighting operate at higher voltage and current levels, their internal resistance is relatively small, causing minimal impact from parallel resistance. However, micro-LEDs have smaller dimensions compared to conventional LEDs and operate at much lower voltages, typically only slightly above the turn-on voltage (around 0.2V). This low operating voltage increases the internal resistance, making it easier for carriers to find leakage paths and magnifying the effects of leakage current compared to high-voltage LEDs. Thus, accurately evaluating the influence of this leakage current on the photoluminescence (PL) characteristics in micro-LED devices is crucial due to their unique operating conditions.

Among the parameters associated with the self-emissive display performance of Micro-LEDs, the emission wavelength, emission intensity, and emission uniformity are crucial for achieving a wide color gamut and high brightness. PL is a promising detection technique due to its non-contact nature. When Micro-LEDs are excited by a high-energy focused laser beam, photoluminescence occurs as a result of radiative transitions from the conduction band to the valence band. Figure 47 shows the schematic diagram of PL. Considering that the excitation energy from the laser should be higher than the expected emission energy, ultraviolet laser diodes are preferred as the laser source to detect defects in the visible light wavelength range.

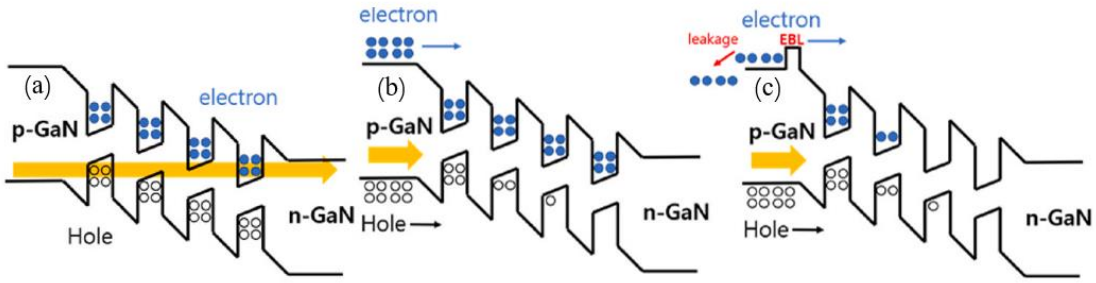

Figure 47. The schematic diagram of PL. [240]

Park et al. [44] conducted a performance analysis on a manufactured array of blue Micro-LEDs using a micro-pulsed laser. They employed a 375 nm micro-pulsed laser diode to emit and irradiate p-GaN on the chip surface, resulting in radiative transitions in multiple quantum wells (MQWs). The recombination of electrons and holes generates emission at 450 nm, which can be detected through spectroscopic methods. By comparing the spectra with those of high-quality chips, it was easy to identify defective chips when the PL intensity was low, as shown in Figure 48(a). Due to the adjustable spot size of the laser, which can be reduced to below 2 μm, photoluminescence techniques hold promise for precise analysis of Micro-LEDs. Additionally, photoluminescence offers the advantage of scanning detection for Micro-LED arrays. Figure 48(b) provides an example of a PL intensity mapping image. Four chips with lower intensities were identified compared to the others, and the positions of these chips were further determined using an optical microscope. As shown in Figure. 48(c), the LED chip defects were confirmed, leading to leakage current and a decrease in luminous intensity.

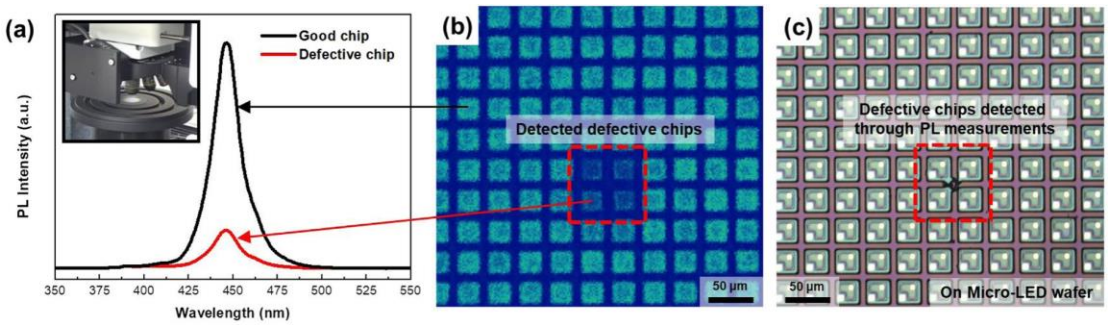

Figure 48. (a) PL intensity of good and defective chips detected by micro-pulsed laser (inserted image: Schematic illustrating how to measure adhesion; after a 1.5×1.5 cm^2 GaN piece on sapphire and the functional layer on the PI substrate are attached, the force generated by detaching these samples was measured). (b) Mapping image of the detected PL intensity after micro-pulsed laser irradiation. (c) Optical microscopy image of defective chips on a real μLED wafer found using a PL intensity map. [44]

Chen et al. [251,252] proposed a method that combines PL detection with confocal Raman microscopy for non-destructive testing and in-depth analysis of LED chip electrical characteristics. This approach can reveal damage-related information in LED chips related to electronic performance, including dislocation density [241], stress distribution [242], carrier concentration [243], and more. Photoluminescence techniques provide information about the optical properties by measuring the emitted light signal from the LED chip under excitation. On the other hand, confocal Raman microscopy measures the scattered spectra to obtain Raman signals from the LED device, which can provide insight into the device's depth distribution. By analyzing both the PL and Raman spectra, a comprehensive understanding of the LED device's performance can be obtained from both optical and electronic perspectives. This approach offers the advantages of non-destructive testing, simplicity, fast analysis, and accurate results.

3.2 Laser Repair

After identifying defects in Micro-LED chips, the key task is to remove these defective Micro-LEDs and replace them with high-quality ones. However, efficiently repairing the damaged Micro-LED chips among millions or even tens of millions of micron-sized chips is a challenging task. Researchers and engineers have been exploring various repair techniques for Micro-LEDs to address this issue, with laser repair technology being a commonly used method. Recognized techniques include ultraviolet irradiation repair technology from Konica Minolta in Japan, non-contact EL testing and Beam Assisted Removal (BAR) transfer method from TESORO in the United States, and laser melting repair technology from Toray in Japan. In March 2020, South Korean company KOSES officially delivered large-scale Micro/Mini LED repair equipment for mass production to Samsung, which utilizes laser repair technology. It can be said that most mainstream Micro-LED repair equipment adopts laser repair technology. Therefore, achieving efficient and high-quality repair work requires precise and responsive control provided by laser repair technology. Common laser repair methods include ultraviolet laser irradiation, laser micro-annealing, and massive laser selective repair.

The repair of defective micro-LEDs can be achieved by using UV laser irradiation, which involves ablating the defect area under high-energy conditions. This technique offers the advantages

of speed and efficiency, allowing for the removal or repair of defects in micro-LEDs within a shorter timeframe.

Thorsten Passow et al. [244] used a UV laser to repair defects in GaN-based LEDs. Figure 49(a) provides a schematic representation of the laser repair process, showing the LED before (left) and after (right) laser repair. The study revealed that the low current density brightness distribution image exhibited large dark areas corresponding to local defects, as shown on the left in Figure 49(a). However, after using 248nm nanosecond pulse irradiation, the local defects in the low current brightness distribution image were removed, and the repaired defects are indicated by red circles, as shown on the right in Figure 49(b). The research demonstrated the successful repair of Micro-LED chips using UV laser irradiation.

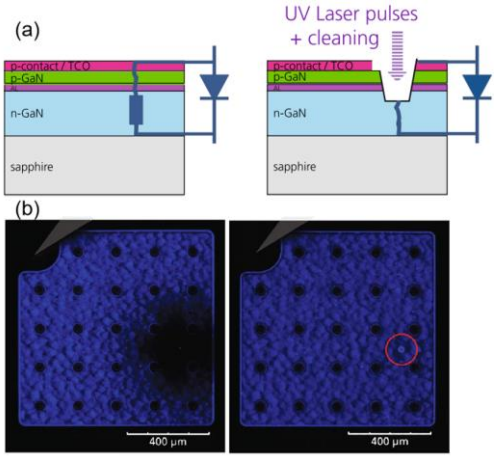

Figure 49. (a) illustrates the schematic representation of the LED before and after laser repair. [244] (b) shows the low current density brightness distribution images of a GaN-based LED chip before (left) and after (right) defect repair. [244]

Laser Micro-Annealing (LMA) is a process that involves localized heating of the defective micro-LED using a laser, inducing small structural changes in the material and thereby repairing the defects. Figure 50 (a) illustrates the principle of the LMA process. This technique offers high precision and control, enabling precise repair of microchip-level devices. For instance, LMA can induce the crystallization of amorphous silicon thin films into low-temperature polysilicon (LTPS) films with high carrier mobility, without heating the substrate.

LMA is primarily used for the formation of low-resistance ohmic contacts in III-nitride LEDs. [245–248] Forming ultra-low resistance ohmic contacts is crucial for improving the electrical and optical performance of such devices, as high voltage drops at the GaN contact interfaces can lead to

poor device reliability. Jang et al. [247] demonstrated that laser irradiation can effectively reduce p-contact resistance and n-contact resistance. In the case of n-type[167] gallium nitride, pulsed KrF excimer laser annealing was utilized to achieve ohmic contacts with a specific contact resistance of 1.7×10^{-6} Ωcm^2. The reduced contact resistance is attributed to the presence of nitrogen vacancies, which induce a degenerated GaN layer near the surface. This mechanism enables efficient electrical conduction through the contacts. Regarding p-type GaN, laser irradiation was found to increase the acceptor concentration and enhance the activation efficiency of Mg dopants. This resulted in a significant reduction in p-contact resistance to 3.6×10^{-4} Ωcm^2. The laser treatment effectively improves the electrical properties of the p-type GaN, facilitating better current flow through the contacts. Recently, M. Mikulics et al. [245] employed LMA technology for precise local tuning of nano-LEDs, as shown in Figure 50(b). Experimental data confirmed a reduction in defect layer depth from 17 nm to 5 nm determined by the LMA process. After laser annealing treatment, the devices exhibited significantly improved I-V characteristics and electroluminescence (EL) performance. Laser annealing offers the advantage of selective irradiation, allowing the formation of local contacts without affecting other areas. While laser annealing has made progress in enhancing device performance, it is considered a more expensive process. Compared to traditional thermal annealing methods, laser annealing has practical limitations in achieving widespread formation of good electrical contacts.

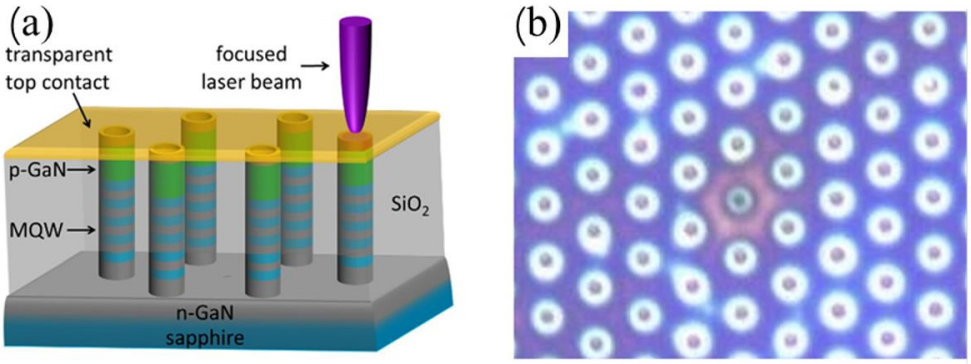

Figure 50. (a) depicts the schematic representation of the LMA process. [245] (b) illustrates the localized annealing of individual nano-LEDs using the LMA technique. [245]

Massive laser selective repair is an efficient laser repair technique that can simultaneously repair multiple defective Micro-LEDs. It utilizes a laser irradiation system and a high-precision optical system to selectively repair multiple defect areas. This technology allows for the rapid repair of a large number of defects, thereby improving repair efficiency.

Uniqarta, a company specializing in LED array repair, has developed a highly efficient technology called massively parallel laser-enabled transfer (MPLET) [215] for large-scale repair. This technique utilizes a combination of single-beam (SB) and multi-beam laser systems for the removal of defective chips and the transfer of good chips, respectively. The process is illustrated in Figure. 51, begins with the transfer of LED chips from the source wafer to a DRL carrier using the LLO method. During this transfer, even the identified defective LEDs are still transferred to the DRL carrier. The MPLET equipment operates in SB mode to selectively remove defective LED chips from the DRL carrier. Then, in a multi-beam mode, the remaining functional chips are transferred onto display panels, followed by filling the vacant positions with good LED chips using the SB mode of the MPLET system. This laser-based selective release technology enables pre-transfer detection, selective mass transfer, and improved transfer yield. Uniqarta's MPLET technology[249] offers a highly efficient approach to large-scale repair of LED arrays. By combining single-beam and multi-beam laser systems, it achieves selective removal of defective chips and successful transfer of good chips, resulting in improved transfer yield and overall performance.

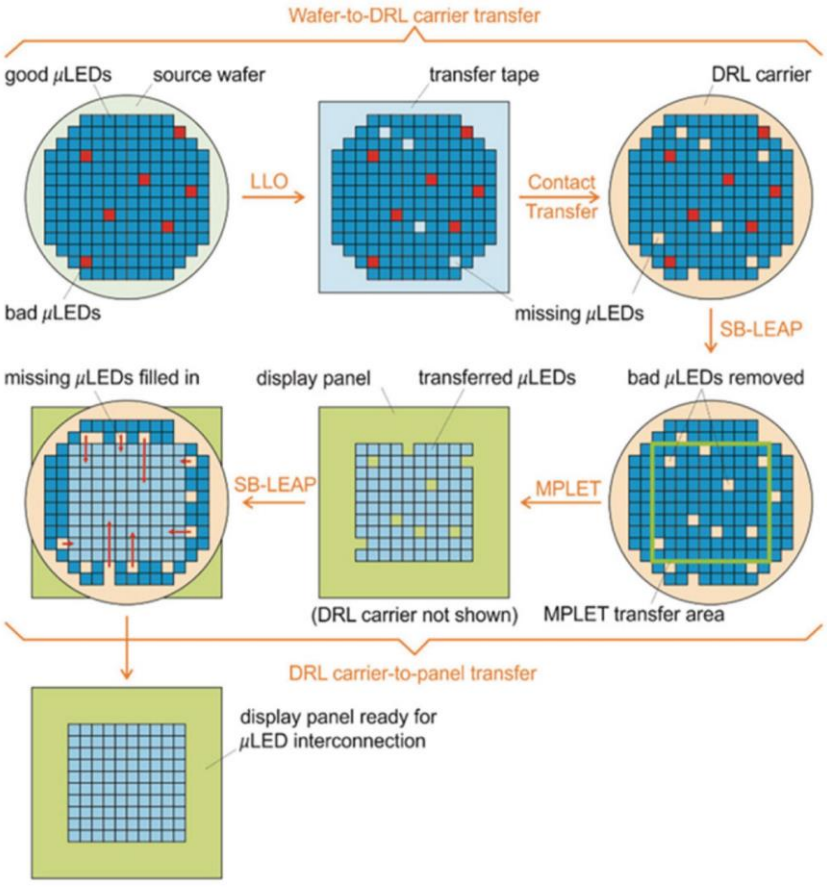

Figure 51. Schematic illustration of Uniqarta's laser repairing strategy. [215]

4. Conclusion and outlook

Due to its high reliability, fast response time, and long lifespan, micro-LED display technology holds tremendous potential across various application domains. However, several manufacturing and technological challenges must be overcome before consumer-oriented micro-LED display products can enter the market. This paper provides a comprehensive review of the latest research advancements in laser-based micro-LED display technology, discussing the working principles, advantages, and limitations of different laser techniques.

As the first step in Micro-LED production, the quality of the substrate epitaxial layer determines the performance of Micro-LEDs. Traditional epitaxial techniques involve additional steps such as low-temperature buffering or lateral epitaxy, which increase manufacturing complexity and cost. Laser processing can reduce epitaxy time by bypassing these steps, leading to a significant cost reduction. Research by Tanya Paskova et al. [250] demonstrates that using GaN as a local substrate during epitaxy can improve the quality of epitaxial films and crystal structures. GaN also possesses important optoelectronic device characteristics such as low refractive index and high anti-reflection. Therefore, it is necessary to investigate the feasibility of utilizing laser processing to achieve GaN as a local substrate. Conventional etching methods involve mask lithography and chemical etching, which generate waste and chemical substances that may cause environmental pollution. Laser-based etching techniques offer a viable alternative, enabling high precision and speed. LDW is a maskless approach that writes Micro-LED chips directly on the target substrate. However, challenges in precise beam control and scanning strategies may result in surface roughness and sidewall damage. Improvements in stable beam focusing and scanning strategies are needed to enhance the stability of LDW.

The yield of LLO needs to be improved for industrial-scale production of Micro-LEDs. Currently, achieving a yield of 99.9% is relatively easy, but defects in laser parameter selection and beam uniformity control during the scanning process make it difficult to achieve a yield of 99.99% or even higher for Micro-LED chips. Therefore, further improvement in the controllability and stability of the delamination process is required to ensure the quality and integrity of the separated

chips and substrates. This includes optimizing the selection of laser parameters, strengthening monitoring and control of temperature and beam during the delamination process, and researching delamination methods suitable for different types of bonding layers. laser-assisted massive transfer techniques are widely regarded as the most capable for large-scale transfer due to the highly localized laser action. For example, QMAT and Uniqarta [249] utilize laser-guided release technology to achieve high-volume, rapid transfer of Micro-LEDs from the original substrate, with transfer capacities up to 100 KK/h. However, laser-induced damage (such as photothermal damage and photochemical shock damage) can easily occur to the devices. Improving the controllability of transfer-induced damage can be achieved by providing uniform energy output through optical shaping systems. Additionally, changing the response layer material or structural system, using sacrificial layers or intermediate structures as buffers for laser-induced forces, can reduce damage defects and improve transfer yield.

Laser inspection techniques can effectively detect defects and faults, improving production efficiency. Improvements in accuracy and sensitivity are needed to detect smaller defects more precisely. Integration of image processing algorithms and machine learning can enhance the efficiency and reliability of defect detection. Laser repair techniques can rectify defects in Micro-LED chips during the manufacturing process. By employing laser repair techniques, damaged areas can be restored to normal functionality, enhancing chip performance and usability. These repair techniques are significant for improving product yield and reducing scrap rates. However, laser repair techniques require better control of the repair process to ensure matching and consistency with the surrounding areas.

With the continuous development and refinement of laser technology, it is believed that this will further drive the progress of Micro-LED display technology, enabling higher-quality and more reliable products while expanding the applications of Micro-LED in various fields.

Acknowledgments

This research was supported by the Foundation of Natural Science Foundation of China (52075317), Class III Peak Discipline of Shanghai—Materials Science and Engineering (High-Energy Beam Intelligent Processing and Green Manufacturing).

Conflicts of Interest: The authors declare no conflict of interest.

Authors' contributions:

Lingxiao Song: Methodology, Writing-original Draft. **Xuechao Yong:** Supervision. **Peilei Zhan**g: Funding acquisition. **Shijie Song:** Conceptualization. **Kefan Chen**: Project administration. **Hua Yan:** Formal analysis. **Tianzhu Sun:** Writing-review and editing. **Qinghua Lu:** Investigation. **Haichuan Shi:** Visualization. **Yu Chen:** Data curation. **Yuze Huang:** Data curation. All authors have read and agreed to the published version of the manuscript.

References

[1] S. Scholz, D. Kondakov, B. Lüssem, K. Leo, Degradation mechanisms and reactions in organic light-emitting devices, Chem Rev 115 (2015) 8449–8503. https://doi.org/10.1021/cr400704v.

[2] J. Liang, L. Li, X. Niu, Z. Yu, Q. Pei, Elastomeric polymer light-emitting devices and displays, Nat Photonics 7 (2013) 817–824. https://doi.org/10.1038/nphoton.2013.242.

[3] Z. Gao, H. Ning, R. Yao, W. Xu, W. Zou, C. Guo, D. Luo, H. Xu, J. Xiao, Mini-LED Backlight Technology Progress for Liquid Crystal Display, Crystals (Basel) 12 (2022). https://doi.org/10.3390/cryst12030313.

[4] E.-L. Hsiang, Z. Yang, Q. Yang, P.-C. Lai, C.-L. Lin, S.-T. Wu, AR/VR light engines: perspectives and challenges, Adv Opt Photonics 14 (2022) 783. https://doi.org/10.1364/aop.468066.

[5] Y.-T. Liu, K.-Y. Liao, C.-L. Lin, Y.-L. Li, PixeLED Display for Transparent Applications, 2018.

[6] Y. Zhang, J. Lee, S.R. Forrest, Tenfold increase in the lifetime of blue phosphorescent organic light-emitting diodes, Nat Commun 5 (2014). https://doi.org/10.1038/ncomms6008.

[7] K. Ding, V. Avrutin, N. Izyumskaya, Ü. Özgür, H. Morkoç, Micro-LEDs, a manufacturability perspective, Applied Sciences (Switzerland) 9 (2019). https://doi.org/10.3390/app9061206.

[8] B.Y. Lin, C.J. Easley, C.H. Chen, P.C. Tseng, M.Z. Lee, P.H. Sher, J.K. Wang, T.L. Chiu, C.F. Lin, C.J. Bardeen, J.H. Lee, Exciplex-Sensitized Triplet-Triplet Annihilation

in Heterojunction Organic Thin-Film, ACS Appl Mater Interfaces 9 (2017) 10963–10970. https://doi.org/10.1021/acsami.6b16397.

[9] Y. Huang, E.L. Hsiang, M.Y. Deng, S.T. Wu, Mini-LED, Micro-LED and OLED displays: present status and future perspectives, Light Sci Appl 9 (2020). https://doi.org/10.1038/s41377-020-0341-9.

[10] D.Y. Kondakov, J.R. Sandifer, C.W. Tang, R.H. Young, Nonradiative recombination centers and electrical aging of organic light-emitting diodes: Direct connection between accumulation of trapped charge and luminance loss, J Appl Phys 93 (2003) 1108–1119. https://doi.org/10.1063/1.1531231.

[11] B.-Y. Lin, M.-Z. Lee, P.-C. Tseng, J.H. Lee, T.-L. Chiu, C.-F. Lin, J. Hsieh, S. Chen, 6.1-times Elongation of Operation Lifetime in a Blue TTA-OLED by using New ETL and EML Materials, 1928.

[12] J.S. Lewis, M.S. Weaver, Thin-film permeation-barrier technology for flexible organic light-emitting devices, IEEE Journal on Selected Topics in Quantum Electronics 10 (2004) 45–57. https://doi.org/10.1109/JSTQE.2004.824072.

[13] E.L. Hsiang, Z. Yang, Q. Yang, Y.F. Lan, S.T. Wu, Prospects and challenges of mini-LED, OLED, and micro-LED displays, J Soc Inf Disp 29 (2021) 446–465. https://doi.org/10.1002/jsid.1058.

[14] J. Lee, C. Jeong, T. Batagoda, C. Coburn, M.E. Thompson, S.R. Forrest, Hot excited state management for long-lived blue phosphorescent organic light-emitting diodes, Nat Commun 8 (2017). https://doi.org/10.1038/ncomms15566.

[15] H.W. Chen, J.H. Lee, B.Y. Lin, S. Chen, S.T. Wu, Liquid crystal display and organic light-emitting diode display: present status and future perspectives, Light Sci Appl 7 (2018) 17168. https://doi.org/10.1038/lsa.2017.168.

[16] E.L. Hsiang, Z. He, Y. Huang, F. Gou, Y.F. Lan, S.T. Wu, Improving the power efficiency of micro-led displays with optimized led chip sizes, Crystals (Basel) 10 (2020) 1–15. https://doi.org/10.3390/cryst10060494.

[17] Z. Luo, Y. Ding, F. Peng, G. Wei, Y. Wang, S.-T. Wu, Ultracompact and high-efficiency liquid-crystal-on-silicon light engines for augmented reality glasses, Opto-Electronic Advances 0 (2024) 240039–240039. https://doi.org/10.29026/oea.2024.240039.

[18] Z. Yang, Z. Luo, Y. Ding, Y. Qian, S.-C. Chen, C.-L. Lin, S.-T. Wu, Advances and challenges in microdisplays and imaging optics for virtual reality and mixed reality, Device 2 (2024) 100398. https://doi.org/https://doi.org/10.1016/j.device.2024.100398.

[19] Y. Nanishi, Nobel Prize in Physics: The birth of the blue LED, Nat Photonics 8 (2014) 884–886. https://doi.org/10.1038/nphoton.2014.291.

[20] S.X. Jin, J. Li, J.Z. Li, J.Y. Lin, H.X. Jiang, GaN microdisk light emitting diodes, Appl Phys Lett 76 (2000) 631–633. https://doi.org/10.1063/1.125841.

[21] C.W. Jeon, H.W. Choi, E. Gu, M.D. Dawson, High-density matrix-addressable AlInGaN-based 368-nm microarray light-emitting diodes, IEEE Photonics Technology Letters 16 (2004) 2421–2423. https://doi.org/10.1109/LPT.2004.835626.

[22] J. Day, J. Li, D.Y.C. Lie, C. Bradford, J.Y. Lin, H.X. Jiang, Full-scale self-emissive blue and green microdisplays based on GaN micro-LED arrays, in: Quantum Sensing and Nanophotonic Devices IX, SPIE, 2012: p. 82681X. https://doi.org/10.1117/12.914061.

[23] Z.J. Liu, W.C. Chong, K.M. Wong, K.M. Lau, 360 PPI flip-chip mounted active matrix addressable light emitting diode on silicon (ledos) micro-displays, IEEE/OSA Journal of Display Technology 9 (2013) 678–682. https://doi.org/10.1109/JDT.2013.2256107.

[24] W.K.C.J.L.C.H.W. Wing Cheung Chong*, Compound Semiconductor Integrated Circuit Symposium (CSICs), 2014 IEEE., [publisher not identified], 2014.

[25] H.-V. Han, H.-Y. Lin, C.-C. Lin, W.-C. Chong, J.-R. Li, K.-J. Chen, P. Yu, T.-M. Chen, H.-M. Chen, K.-M. Lau, H.-C. Kuo, Resonant-enhanced full-color emission of quantum-dot-based micro LED display technology, Opt Express 23 (2015) 32504. https://doi.org/10.1364/oe.23.032504.

[26] Institute of Electrical and Electronics Engineers, 2018 IEEE International Electron Devices Meeting (IEDM) : 1-5 Dec. 2018., n.d.

[27] J.M. Smith, R. Ley, M.S. Wong, Y.H. Baek, J.H. Kang, C.H. Kim, M.J. Gordon, S. Nakamura, J.S. Speck, S.P. Denbaars, Comparison of size-dependent characteristics of blue and green InGaN microLEDs down to 1 μ m in diameter, Appl Phys Lett 116 (2020). https://doi.org/10.1063/1.5144819.

[28] X. Zhang, L. Qi, W.C. Chong, P. Li, C.W. Tang, K.M. Lau, Active matrix monolithic micro-LED full-color micro-display, J Soc Inf Disp 29 (2021) 47–56. https://doi.org/10.1002/jsid.962.

[29] J. Oh, D. Kim, D. Yang, K. Hwang, J. Hwang, J. Kim, S. Lee, J. Ryu, S. Park, J.K. Shin, Y. Kim, Y. Park, E. Yoon, H.W. Jang, Self-Assembled Size-Tunable Microlight-Emitting Diodes Using Multiple Sapphire Nanomembranes, ACS Appl Mater Interfaces 14 (2022) 25781–25791. https://doi.org/10.1021/acsami.2c05483.

[30] J. Shin, H. Kim, S. Sundaram, J. Jeong, B.I. Park, C.S. Chang, J. Choi, T. Kim, M. Saravanapavanantham, K. Lu, S. Kim, J.M. Suh, K.S. Kim, M.K. Song, Y. Liu, K. Qiao, J.H. Kim, Y. Kim, J.H. Kang, J. Kim, D. Lee, J. Lee, J.S. Kim, H.E. Lee, H. Yeon, H.S. Kum, S.H. Bae, V. Bulovic, K.J. Yu, K. Lee, K. Chung, Y.J. Hong, A. Ougazzaden, J. Kim, Vertical full-colour micro-LEDs via 2D materials-based layer transfer, Nature 614 (2023) 81–87. https://doi.org/10.1038/s41586-022-05612-1.

[31] M.R. Krames, O.B. Shchekin, R. Mueller-Mach, G.O. Mueller, L. Zhou, G. Harbers, M.G. Craford, Status and future of high-power light-emitting diodes for solid-state lighting, IEEE/OSA Journal of Display Technology 3 (2007) 160–175. https://doi.org/10.1109/JDT.2007.895339.

[32] J.B. Park, W.S. Choi, T.H. Chung, S.H. Lee, M.K. Kwak, J.S. Ha, T. Jeong, Transfer printing of vertical-type microscale light-emitting diode array onto flexible substrate using biomimetic stamp, Opt Express 27 (2019) 6832. https://doi.org/10.1364/oe.27.006832.

[33] Y. Boussadi, N. Rochat, J.P. Barnes, B. Ben Bakir, P. Ferrandis, B. Masenelli, C. Licitra, Investigation of sidewall damage induced by reactive ion etching on AlGaInP MESA for micro-LED application, J Lumin 234 (2021). https://doi.org/10.1016/j.jlumin.2021.117937.

[34] S. Lu, J. Li, K. Huang, G. Liu, Y. Zhou, D. Cai, R. Zhang, J. Kang, Designs of InGaN Micro-LED Structure for Improving Quantum Efficiency at Low Current Density, Nanoscale Res Lett 16 (2021). https://doi.org/10.1186/s11671-021-03557-4.

[35] M. Meneghini, N. Trivellin, G. Meneghesso, E. Zanoni, U. Zehnder, B. Hahn, A combined electro-optical method for the determination of the recombination parameters in InGaN-based light-emitting diodes, J Appl Phys 106 (2009). https://doi.org/10.1063/1.3266014.

[36] X. Jia, Y. Zhou, B. Liu, H. Lu, Z. Xie, R. Zhang, Y. Zheng, A simulation study on the enhancement of the efficiency of GaN-based blue light-emitting diodes at low current density for micro-LED applications, Mater Res Express 6 (2019). https://doi.org/10.1088/2053-1591/ab3f7b.

[37] S.S. Konoplev, K.A. Bulashevich, S.Y. Karpov, From Large-Size to Micro-LEDs: Scaling Trends Revealed by Modeling, Physica Status Solidi (A) Applications and Materials Science 215 (2018). https://doi.org/10.1002/pssa.201700508.

[38] J. Kou, C.-C. Shen, H. Shao, J. Che, X. Hou, C. Chu, K. Tian, Y. Zhang, Z.-H. Zhang, H.-C. Kuo, Impact of the surface recombination on InGaN/GaN-based blue micro-light emitting diodes, Opt Express 27 (2019) A643. https://doi.org/10.1364/oe.27.00a643.

[39] G. Zhu, Y. Liu, R. Ming, F. Shi, M. Cheng, Mass transfer, detection and repair technologies in micro-LED displays, Sci China Mater 65 (2022) 2128–2153. https://doi.org/10.1007/s40843-022-2110-2.

[40] Y. Wu, J. Ma, P. Su, L. Zhang, B. Xia, Full-color realization of micro-led displays, Nanomaterials 10 (2020) 1–33. https://doi.org/10.3390/nano10122482.

[41] J. El Ryu, S. Park, Y. Park, S.W. Ryu, K. Hwang, H.W. Jang, Technological Breakthroughs in Chip Fabrication, Transfer, and Color Conversion for High-Performance Micro-LED Displays, Advanced Materials 35 (2023). https://doi.org/10.1002/adma.202204947.

[42] C.C. Yeh, H.W. Zan, O. Soppera, Solution-Based Micro- and Nanoscale Metal Oxide Structures Formed by Direct Patterning for Electro-Optical Applications, Advanced Materials 30 (2018). https://doi.org/10.1002/adma.201800923.

[43] S.L.Z.L.Z.Z.Z.C.R.Z.H.-C.K. and T.W. Shouqiang Lai, Applications of lasers: A promising route toward low-cost fabrication of high-efficiency full-color micro-LED displays, Opto-Electronic Science (2022).

[44] J.B. Park, K.H. Lee, S.H. Han, T.H. Chung, M.K. Kwak, H. Rho, T. Jeong, J.S. Ha, Stable and efficient transfer-printing including repair using a GaN-based microscale light-emitting diode array for deformable displays, Sci Rep 9 (2019). https://doi.org/10.1038/s41598-019-47449-1.

[45] F. Chen, J. Bian, J. Hu, N. Sun, B. Yang, H. Ling, H. Yu, K. Wang, M. Gai, Y. Ma, Y.A. Huang, Mass transfer techniques for large-scale and high-density microLED arrays, International Journal of Extreme Manufacturing 4 (2022). https://doi.org/10.1088/2631-7990/ac92ee.

[46] X.Q. Liu, L. Yu, Q.D. Chen, H.B. Sun, Mask-free construction of three-dimensional silicon structures by dry etching assisted gray-scale femtosecond laser direct writing, Appl Phys Lett 110 (2017). https://doi.org/10.1063/1.4977562.

[47] L. Liu, J. Edgar, Substrates for gallium nitride epitaxy, n.d.

[48] G. Li, W. Wang, W. Yang, H. Wang, Epitaxial growth of group III-nitride films by pulsed laser deposition and their use in the development of LED devices, Surf Sci Rep 70 (2015) 380–423. https://doi.org/10.1016/j.surfrep.2015.06.001.

[49] P. Tyagi, B.K. Pradhan, A.K. Mauraya, D. Mahana, V. Aggarwal, G. Gupta, S.S. Kushvaha, S.K. Muthusamy, Effect of substrate nitridation and a buffer layer on the growth of a non-polar a-plane GaN epitaxial layer on an r-plane sapphire substrate by laser molecular beam epitaxy, Mater Adv 3 (2022) 8317–8322. https://doi.org/10.1039/d2ma00782g.

[50] P. Tyagi, B.K. Pradhan, A.K. Mauraya, D. Mahana, V. Aggarwal, G. Gupta, S.S. Kushvaha, S.K. Muthusamy, Effect of substrate nitridation and a buffer layer on the growth of a non-polar a-plane GaN epitaxial layer on an r-plane sapphire substrate by laser molecular beam epitaxy, Mater Adv 3 (2022) 8317–8322. https://doi.org/10.1039/d2ma00782g.

[51] V. Kirchner, R. Ebel, H. Heinke, S. Einfeldt, D. Hommel, H. Selke, P.L. Ryder, Influence of buffer layers on the structural properties of molecular beam epitaxy grown GaN layers, 1999.

[52] O. Brandta, H. Yangb, J.R. Miillh%user, A. Tramperta, K.H. Ploog, MATERIALS SCIENCE & ENGlWEERiNG B Properties of cubic GaN grown by MBE, 1997.

[53] R. Hentschel, J. Gärtner, A. Wachowiak, A. Großer, T. Mikolajick, S. Schmult, Surface morphology of AlGaN/GaN heterostructures grown on bulk GaN by MBE, J Cryst Growth 500 (2018) 1–4. https://doi.org/10.1016/j.jcrysgro.2018.07.026.

[54] X. Wang, A. Yoshikawa, Molecular beam epitaxy growth of GaN, AlN and InN, Progress in Crystal Growth and Characterization of Materials 48–49 (2004) 42–103. https://doi.org/10.1016/j.pcrysgrow.2005.03.002.

[55] F. Kwong, Y. Li, L. Low, S.A. Oh, Z. Hassan, 4 Gallium Nitride: An Overview of Structural Defects, n.d. www.intechopen.com.

[56] J.L. Weyher, P.D. Brown, A.R.A. Zauner, S. Muk, C.B. Boothroyd, D.T. Foord, P.R. Hageman, C.J. Humphreys, P.K. Larsen, I. Grzegory, S. Porowski, Morphological and structural characteristics of homoepitaxial GaN grown by metalorganic chemical vapour deposition (MOCVD), 1999.

[57] A. Hierro, M. Hansen, J.J. Boeckl, L. Zhao, J.S. Speck, U.K. Mishra, S.P. Denbaars, S.A. Ringel, Carrier Trapping and Recombination at Point Defects and Dislocations in MOCVD n-GaN, n.d.

[58] M. Sumiya, Y. Kurumasa, K. Ohtsuka, K. Kuwahara, Y. Takano, S. Fuke, Reduction of defect density in GaN epilayer having buried Ga metal by MOCVD, 2002.

[59] M. Niehus, P. Sanguino, T. Monteiro, M.J. Soares, E. Pereira, M. Vieira, S. Koynov, R. Schwarz, Optical properties and transport in PLD-GaN, n.d. www.elsevier.com/locate/sse.

[60] W.K. Wang, S.Y. Huang, M.C. Jiang, D.S. Wuu, Optoelectronic properties and structural characterization of GaN thick films on different substrates through pulsed laser deposition, Applied Sciences (Switzerland) 7 (2017). https://doi.org/10.3390/app7010087.

[61] E. Hwang, J. Choi, S. Hong, Emerging laser-assisted vacuum processes for ultra-precision, high-yield manufacturing, Nanoscale 14 (2022) 16065–16076. https://doi.org/10.1039/d2nr03649e.

[62] S. Porowski, Near defect free GaN substrates, in: MRS Internet Journal of Nitride Semiconductor Research, Materials Research Society, 1999.

https://doi.org/10.1557/s1092578300002210.

[63] H. Heinke, V. Kirchner, S. Einfeldt, D. Hommel, Analysis of the Defect Structure of Epitaxial GaN, 1999.

[64] A. Chatterjee, S. Acharya, S.M. Shivaprasad, Morphology-Related Functionality in Nanoarchitectured GaN, in: Annu Rev Mater Res, Annual Reviews Inc., 2020: pp. 179–206. https://doi.org/10.1146/annurev-matsci-081919-014810.

[65] S.S. Kushvaha, M. Senthil Kumar, B.S. Yadav, P.K. Tyagi, S. Ojha, K.K. Maurya, B.P. Singh, Influence of laser repetition rate on the structural and optical properties of GaN layers grown on sapphire (0001) by laser molecular beam epitaxy, CrystEngComm 18 (2016) 744–753. https://doi.org/10.1039/c5ce02257f.

[66] S.S. Kushvaha, M. Senthil Kumar, A.K. Shukla, B.S. Yadav, D.K. Singh, M. Jewariya, S.R. Ragam, K.K. Maurya, Structural, Optical and Electronic properties of Homoepitaxial GaN Nanowalls grown on GaN Template by Laser Molecular Beam Epitaxy, n.d. www.rsc.org/advances.

[67] O. Abdullaev, M. Mezhenny, A. Chelny, A. Savchuk, Y. Ahmerov, O. Rabinovich, V. Murashev, S. Didenko, Y. Osipov, S. Sizov, M. Orlova, A. Aluyev, MOCVD growth GaN on sapphire, in: IOP Conf Ser Mater Sci Eng, Institute of Physics Publishing, 2019. https://doi.org/10.1088/1757-899X/617/1/012015.

[68] P. Tian, P.R. Edwards, M.J. Wallace, R.W. Martin, J.J.D. McKendry, E. Gu, M.D. Dawson, Z.J. Qiu, C. Jia, Z. Chen, G. Zhang, L. Zheng, R. Liu, Characteristics of GaN-based light emitting diodes with different thicknesses of buffer layer grown by HVPE and MOCVD, J Phys D Appl Phys 50 (2017). https://doi.org/10.1088/1361-6463/50/7/075101.

[69] R.D. Vispute, V. Talyansky, R.P. Sharma, S. Choopun, M. Downes, T. Venkatesan, K.A. Jones, A.A. Iliadis, M. Asif Khan, J.W. Yang, Growth of epitaxial GaN films by pulsed laser deposition, Appl Phys Lett 71 (1997) 102–104. https://doi.org/10.1063/1.119441.

[70] S. Oktyabrsky, K. Dovidenko, A.K. Sharma, V. Joshkin, J. Narayan, Cite this article as, 1999.

[71] T. Feng, H.D. Young, C. Zhang, A. Christou, Laser assisted molecular beam epitaxy (LAMBE) of compound semiconductor buffer layers and AlN, GaN structures for high electron mobility transistor, in: Conference on Optoelectronic and Microelectronic Materials and Devices, Proceedings, COMMAD, Institute of Electrical and Electronics Engineers Inc., 2002: pp. 37–40. https://doi.org/10.1109/COMMAD.2002.1237183.

[72] G.A. Garrett, C.J. Collins, A. V. Sampath, H. Shen, M. Wraback, S.F. LeBoeuf, J. Flynn, G. Brandes, Defect density dependence of carrier dynamics in A1GaN multiple quantum wells grown on GaN substrates and templates, in: Physica Status Solidi C: Conferences, 2005: pp. 2332–2336. https://doi.org/10.1002/pssc.200461600.

[73] A. Pandey, B.S. Yadav, D.V.S. Rao, D. Kaur, A.K. Kapoor, Dislocation density investigation on MOCVD-grown GaN epitaxial layers using wet and dry defect selective etching, Appl Phys A Mater Sci Process 122 (2016). https://doi.org/10.1007/s00339-016-0143-3.

[74] H.M. Smith, A.F. Turner, Vacuum Deposited Thin Films Using a Ruby Laser, n.d.

[75] D. Dijkkamp, T. Venkatesan, X.D. Wu, S.A. Shaheen, N. Jisrawi, Y.H. Min-Lee,

W.L. McLean, M. Croft, Preparation of Y-Ba-Cu oxide superconductor thin films using pulsed laser evaporation from high Tc bulk material, Appl Phys Lett 51 (1987) 619–621. https://doi.org/10.1063/1.98366.

[76] M. Kawwam, K. Lebbou, The influence of deposition parameters on the structural quality of PLD-grown GaN/sapphire thin films, Appl Surf Sci 292 (2014) 906–914. https://doi.org/10.1016/j.apsusc.2013.12.078.

[77] S. Inoue, K. Okamoto, N. Matsuki, T.W. Kim, H. Fujioka, Epitaxial growth of GaN on copper substrates, Appl Phys Lett 88 (2006). https://doi.org/10.1063/1.2213178.

[78] A. Zomorrodian, N.J. Wu, Y. Song, S. Stahl, A. Ignatiev, E. Brady Trexler, C.A. Garcia, Micro photo detector fabricated of ferroelectric-metal heterostructure, Japanese Journal of Applied Physics, Part 1: Regular Papers and Short Notes and Review Papers 44 (2005) 6105–6108. https://doi.org/10.1143/JJAP.44.6105.

[79] S. Hirata, K. Okamoto, S. Inoue, T.W. Kim, J. Ohta, H. Fujioka, M. Oshima, Epitaxial growth of AlN films on single-crystalline Ta substrates, J Solid State Chem 180 (2007) 2335–2339. https://doi.org/10.1016/j.jssc.2007.06.008.

[80] K. Okamoto, S. Inoue, N. Matsuki, T.W. Kim, J. Ohta, M. Oshima, H. Fujioka, A. Ishii, Epitaxial growth of GaN films grown on single crystal Fe substrates, Appl Phys Lett 93 (2008). https://doi.org/10.1063/1.3056117.

[81] T.W. Kim, N. Matsuki, J. Ohta, H. Fujioka, Characteristics of AlN/Ni(111) heterostructures and their application to epitaxial growth of GaN, Japanese Journal of Applied Physics, Part 2: Letters 45 (2006). https://doi.org/10.1143/JJAP.45.L396.

[82] J. Ohta, H. Fujioka, H. Takahashi, M. Oshima, Crystal Growth of GaN on (Mn, Zn)Fe 2 O 4 Substrates, n.d.

[83] M. Baseer Haider, M.F. Al-Kuhaili, S.M.A. Durrani, I. Bakhtiari, Effect of annealing on the optical properties of GaN films grown by pulsed laser deposition, J Mater Sci Technol 29 (2013) 752–756. https://doi.org/10.1016/j.jmst.2013.04.024.

[84] M. Khoury, O. Tottereau, G. Feuillet, P. Vennéguès, J. Zúñiga-Pérez, Evolution and prevention of meltback etching: Case study of semipolar GaN growth on patterned silicon substrates, J Appl Phys 122 (2017). https://doi.org/10.1063/1.5001914.

[85] R.D. Vispute, J. Narayan, H. Wu, K. Jagannadham, Epitaxial growth of AlN thin films on silicon (111) substrates by pulsed laser deposition, J Appl Phys 77 (1995) 4724–4728. https://doi.org/10.1063/1.359441.

[86] K. Jagannadham, A.K. Sharma, Q. Wei, R. Kalyanraman, J. Narayan, Structural characteristics of AlN films deposited by pulsed laser deposition and reactive magnetron sputtering: A comparative study, Journal of Vacuum Science & Technology A: Vacuum, Surfaces, and Films 16 (1998) 2804–2815. https://doi.org/10.1116/1.581425.

[87] J. Ohta, H. Fujioka, H. Takahashi, M. Oshima, Characterization of hetero-interfaces between group III nitrides formed by PLD and various substrates, n.d.

[88] X. Lu, J. Ma, H. Jiang, K. May Lau, Characterization of in situ SiNx thin film grown on AlN/GaN heterostructure by metal-organic chemical vapor deposition, Appl Phys Lett 104 (2014). https://doi.org/10.1063/1.4862664.

[89] H. Yang, W. Wang, Z. Liu, G. Li, Homogeneous epitaxial growth of AlN single-crystalline films on 2 inch-diameter Si (111) substrates by pulsed laser deposition, CrystEngComm 15 (2013) 7171–7176. https://doi.org/10.1039/c3ce40886h.

[90] N. Gopalakrishnan, B.C. Shin, H.S. Lim, G.Y. Kim, Y.S. Yu, Comparison of ZnO:GaN films on Si(1 1 1) and Si(1 0 0) substrates by pulsed laser deposition, in: Physica B Condens Matter, 2006: pp. 756–759. https://doi.org/10.1016/j.physb.2005.12.189.

[91] X.L. Tong, Q.G. Zheng, S.L. Hu, Y.X. Qin, Z.H. Ding, Structural characterization and optoelectronic properties of GaN thin films on Si(111) substrates using pulsed laser deposition assisted by gas discharge, Appl Phys A Mater Sci Process 79 (2004) 1959–1963. https://doi.org/10.1007/s00339-003-2106-8.

[92] T. Yamada, T. Tanikaway, Y. Honda, M. Yamaguchi, H. Amano, Growth of GaN on Si(111) substrates via a reactive-sputter-deposited AlN intermediate layer, Jpn J Appl Phys 52 (2013). https://doi.org/10.7567/JJAP.52.08JB16.

[93] H. Wang, H. Sodabanlu, Y. Daigo, T. Seino, T. Nakagawa, M. Sugiyama, Initial growth control of GaN on Si with physical-vapor-deposition-AlN seed layer for high-quality GaN templates, Applied Physics Express 9 (2016). https://doi.org/10.7567/APEX.9.055503.

[94] C. Ramesh, P. Tyagi, S. Singh, P. Singh, G. Gupta, K.K. Maurya, K.M.K. Srivatsa, M. Senthil Kumar, S.S. Kushvaha, Influence of growth temperature on structural and optical properties of laser MBE grown epitaxial thin GaN films on a-plane sapphire, Journal of Vacuum Science & Technology B, Nanotechnology and Microelectronics: Materials, Processing, Measurement, and Phenomena 36 (2018). https://doi.org/10.1116/1.5025126.

[95] V. Aggarwal, C. Ramesh, P. Tyagi, S. Gautam, A. Sharma, S. Husale, M.S. Kumar, S.S. Kushvaha, Controlled epitaxial growth of GaN nanostructures on sapphire (11–20) using laser molecular beam epitaxy for photodetector applications, Mater Sci Semicond Process 125 (2021). https://doi.org/10.1016/j.mssp.2020.105631.

[96] S.S. Kushvaha, M.S. Kumar, K.K. Maurya, M.K. Dalai, N.D. Sharma, Highly c-axis oriented growth of GaN film on sapphire (0001) by laser molecular beam epitaxy using HVPE grown GaN bulk target, AIP Adv 3 (2013). https://doi.org/10.1063/1.4821276.

[97] M.H. Kim, M. Oshima, H. Kinoshita, Y. Shirakura, K. Miyamura, J. Ohta, A. Kobayashi, H. Fujioka, Investigation of the initial stage of GaN epitaxial growth on 6H-SiC (0001) at room temperature, Appl Phys Lett 89 (2006). https://doi.org/10.1063/1.2227616.

[98] P. Sanguino, M. Niehus, L. V Melo, R. Schwarz, S. Koynov, T. Monteiro, J. Soares, H. Alves, B.K. Meyer, Characterisation of GaN films grown on sapphire by low-temperature cyclic pulsed laser deposition/nitrogen rf plasma, n.d. www.elsevier.com/locate/sse.

[99] R. Dixit, P. Tyagi, S.S. Kushvaha, S. Chockalingam, B.S. Yadav, N.D. Sharma, M.S. Kumar, Influence of growth temperature on laser molecular beam epitaxy and properties of GaN layers grown on c-plane sapphire, Opt Mater (Amst) 66 (2017) 142–148. https://doi.org/10.1016/j.optmat.2017.01.053.

[100] S. Dewan, M. Tomar, A.K. Kapoor, R.P. Tandon, V. Gupta, Luminescence studies of laser MBE grown GaN on ZnO nanostructures, in: SPIE-Intl Soc Optical Eng, 2017: p. 30. https://doi.org/10.1117/12.2272549.

[101] S. Dewan, M. Tomar, R.P. Tandon, V. Gupta, In-situ and post deposition analysis of laser MBE deposited GaN films at varying nitrogen gas flow, Vacuum 164 (2019) 72–76. https://doi.org/10.1016/j.vacuum.2019.02.053.

[102] S.S. Kushvaha, M. Senthil Kumar, B.S. Yadav, P.K. Tyagi, S. Ojha, K.K.

Maurya, B.P. Singh, Influence of laser repetition rate on the structural and optical properties of GaN layers grown on sapphire (0001) by laser molecular beam epitaxy, CrystEngComm 18 (2016) 744–753. https://doi.org/10.1039/c5ce02257f.

[103] K. Shimamura, H. Tabata, H. Takeda, V. V Kochurikhin, T. Fukuda, Growth and characterization of (La,Sr)(Al,Ta)O single crystals as substrates for GaN epitaxial growth, 1998.

[104] P. Vashishtha, P. Prajapat, A. Sharma, P. Goswami, S. Walia, G. Gupta, Self-driven and thermally resilient highly responsive nano-fenced MoS2 based photodetector for near-infrared optical signal, Mater Res Bull 164 (2023). https://doi.org/10.1016/j.materresbull.2023.112260.

[105] M.A. Sánchez-García, J.L. Pau, F. Naranjo, A. Jiménez, S. Fernández, J. Ristic, F. Calle, E. Calleja, E. Muñ Oz, Plasma-assisted MBE growth of group-III nitrides: from basics to device applications, n.d. www.elsevier.com/locate/mseb.

[106] Y. Kato, S. Kitamura, K. Hiramatsu, N. Sawaki, CRYSTAL GROWTH Selective growth of wurtzite GaN and Al~Ga 1_~N on GaN/sapphire substrates by metalorganic vapor phase epitaxy, 1994.

[107] W.K. Wang, D.S. Wuu, S.H. Lin, P. Han, R.H. Horng, T.C. Hsu, D.T.C. Huo, M.J. Jou, Y.H. Yu, A. Lin, Efficiency improvement of near-ultraviolet InGaN LEDs using patterned sapphire substrates, IEEE J Quantum Electron 41 (2005) 1403–1409. https://doi.org/10.1109/JQE.2005.857057.

[108] Y.J. Lee, J.M. Hwang, T.C. Hsu, M.H. Hsieh, M.J. Jou, B.J. Lee, T.C. Lu, H.C. Kuo, S.C. Wang, Enhancing the output power of GaN-based LEDs grown on wet-etched patterned sapphire substrates, IEEE Photonics Technology Letters 18 (2006) 1152–1154. https://doi.org/10.1109/LPT.2006.874737.

[109] J.J. Chen, Y.K. Su, C.L. Lin, S.M. Chen, W.L. Li, C.C. Kao, Enhanced output power of GaN-based LEDs with nano-patterned sapphire substrates, IEEE Photonics Technology Letters 20 (2008) 1193–1195. https://doi.org/10.1109/LPT.2008.924900.

[110] H. Park, K.J. Byeon, J.J. Jang, O. Nam, H. Lee, Enhancement of photo- and electro-luminescence of GaN-based LED structure grown on a nanometer-scaled patterned sapphire substrate, Microelectron Eng 88 (2011) 3207–3213. https://doi.org/10.1016/j.mee.2011.07.014.

[111] Y. Zhang, T. Wei, J. Wang, D. Lan, Y. Chen, Q. Hu, H. Lu, J. Li, The improvement of GaN-based light-emitting diodes using nanopatterned sapphire substrate with small pattern spacing, AIP Adv 4 (2014). https://doi.org/10.1063/1.4867091.

[112] X. Guo, J. Hu, Z. Zhuang, M. Deng, F. Wu, X. Li, B. Liu, C. Yuan, H. Ge, F. Li, Y. Chen, Fabrication of wafer-scale nanopatterned sapphire substrate by hybrid nanoimprint lithography, Journal of Vacuum Science & Technology B, Nanotechnology and Microelectronics: Materials, Processing, Measurement, and Phenomena 32 (2014). https://doi.org/10.1116/1.4898778.

[113] S.X. Jiang, Z.Z. Chen, X.Z. Jiang, X.X. Fu, S. Jiang, Q.Q. Jiao, T.J. Yu, G.Y. Zhang, Study on the morphology and shape control of volcano-shaped patterned sapphire substrates fabricated by imprinting and wet etching, CrystEngComm 17 (2015) 3070–3075. https://doi.org/10.1039/c4ce02452d.

[114] Y.C.S. Wu, A.P.S. Isabel, J.H. Zheng, B.W. Lin, J.H. Li, C.C. Lin, Crystal

quality and light output power of GaN-based LEDs grown on concave patterned sapphire substrate, Materials 8 (2015) 1993–1999. https://doi.org/10.3390/ma8041993.

[115] H. Hu, B. Tang, H. Wan, H. Sun, S. Zhou, J. Dai, C. Chen, S. Liu, L.J. Guo, Boosted ultraviolet electroluminescence of InGaN/AlGaN quantum structures grown on high-index contrast patterned sapphire with silica array, Nano Energy 69 (2020). https://doi.org/10.1016/j.nanoen.2019.104427.

[116] M.T. Wang, K.Y. Liao, Y.L. Li, Growth mechanism and strain variation of GaN material grown on patterned sapphire substrates with various pattern designs, IEEE Photonics Technology Letters 23 (2011) 962–964. https://doi.org/10.1109/LPT.2011.2147778.

[117] W. Tian, Y. Wu, T. Wu, L. Dou, X. Cao, J. Li, Mechanisms and Performance Analysis of GaN-Based Micro-LED Grown on Pattern Sapphire Substrate by Laser Lift-Off Process, ECS Journal of Solid State Science and Technology 11 (2022) 046001. https://doi.org/10.1149/2162-8777/ac63e5.

[118] H. Gao, F. Yan, Y. Zhang, J. Li, Y. Zeng, G. Wang, Improvement of the performance of GaN-based LEDs grown on sapphire substrates patterned by wet and ICP etching, Solid State Electron 52 (2008) 962–967. https://doi.org/10.1016/j.sse.2007.12.013.

[119] J.X. Zheng, K.S. Tian, J.Y. Qi, M.R. Guo, X.Q. Liu, Advances in fabrication of micro-optical components by femtosecond laser with etching technology, Opt Laser Technol 167 (2023). https://doi.org/10.1016/j.optlastec.2023.109793.

[120] G.Y. Mak, E.Y. Lam, H.W. Choi, Deep etch of GaN by laser micromachining, in: Physica Status Solidi (C) Current Topics in Solid State Physics, 2010: pp. 2151–2153. https://doi.org/10.1002/pssc.200983480.

[121] X. Li, P. Ma, X. Ji, T. Wei, X. Tan, J. Wang, J. Li, Implementation of slow and smooth etching of GaN by inductively coupled plasma, Journal of Semiconductors 39 (2018). https://doi.org/10.1088/1674-4926/39/11/113002.

[122] G.Y. Mak, E.Y. Lam, H.W. Choi, Precision laser micromachining of trenches in GaN on sapphire, Journal of Vacuum Science & Technology B, Nanotechnology and Microelectronics: Materials, Processing, Measurement, and Phenomena 28 (2010) 380–385. https://doi.org/10.1116/1.3359593.

[123] S. Wolter, H. Spende, J. Gülink, J. Hartmann, H.H. Wehmann, A. Waag, A. Lex, A. Avramescu, H.J. Lugauer, N. von Malm, J.J. Drolet, M. Strassburg, Size-dependent electroluminescence and current-voltage measurements of blue ingan/gan µleds down to the submicron scale, Nanomaterials 11 (2021). https://doi.org/10.3390/nano11040836.

[124] R. Kamimura, K. Furuta, Dry etching technologies of optical device and III-v compound semiconductors, IEICE Transactions on Electronics E100C (2017) 150–155. https://doi.org/10.1587/transele.E100.C.150.

[125] H. Hahn, J.B. Gruis, N. Ketteniss, F. Urbain, H. Kalisch, A. Vescan, Influence of mask material and process parameters on etch angle in a chlorine-based GaN dry etch, Journal of Vacuum Science & Technology A: Vacuum, Surfaces, and Films 30 (2012). https://doi.org/10.1116/1.4738848.

[126] H.W. Choi, C.W. Jeon, M.D. Dawson, Tapered sidewall dry etching process for GaN and its applications in device fabrication, Journal of Vacuum Science & Technology B: Microelectronics and Nanometer Structures Processing, Measurement, and Phenomena 23

(2005) 99–102. https://doi.org/10.1116/1.1839914.

[127] E.D. Le Boulbar, C.J. Lewins, D.W.E. Allsopp, C.R. Bowen, P.A. Shields, Fabrication of high-aspect ratio GaN nanostructures for advanced photonic devices, Microelectron Eng 153 (2016) 132–136. https://doi.org/10.1016/j.mee.2016.03.058.

[128] Y.T. Dai, G. Xu, X.L. Tong, Deep UV laser etching of GaN epilayers grown on sapphire substrate, J Mater Process Technol 212 (2012) 492–496. https://doi.org/10.1016/j.jmatprotec.2011.08.022.

[129] E. Gu, H. Howard, A. Conneely, G.M. O'Connor, E.K. Illy, M.R.H. Knowles, P.R. Edwards, R.W. Martin, I.M. Watson, M.D. Dawson, Microfabrication in free-standing gallium nitride using UV laser micromachining, Appl Surf Sci 252 (2006) 4897–4901. https://doi.org/10.1016/j.apsusc.2005.07.117.

[130] X.Q. Liu, B.F. Bai, Q.D. Chen, H.B. Sun, Etching-assisted femtosecond laser modification of hard materials, Opto-Electronic Advances 2 (2019) 1–14. https://doi.org/10.29026/oea.2019.190021.

[131] X.Q. Liu, L. Yu, S.N. Yang, Q.D. Chen, L. Wang, S. Juodkazis, H.B. Sun, Optical Nanofabrication of Concave Microlens Arrays, Laser Photon Rev 13 (2019). https://doi.org/10.1002/lpor.201800272.

[132] T. de Castro, H. Fares, A.A. Khalil, R. Laberdesque, Y. Petit, C. Strutinski, S. Danto, V. Jubera, S.J.L. Ribeiro, M. Nalin, T. Cardinal, L. Canioni, Femtosecond laser micro-patterning of optical properties and functionalities in novel photosensitive silver-containing fluorophosphate glasses, J Non Cryst Solids 517 (2019) 51–56. https://doi.org/10.1016/j.jnoncrysol.2019.04.012.

[133] M. Fleisch, S. Gao, D. Bošnjaković, X. Zhang, R.A. Rupp, I. Drevenšek-Olenik, Laser-written polymeric scaffolds for micro-patterned liquid crystal alignment, Liq Cryst 46 (2019) 2075–2084. https://doi.org/10.1080/02678292.2019.1631970.

[134] A. Keating, X. Sun, Selective Oxidation and Carbonization by Laser Writing into Porous Silicon, Adv Mater Technol 4 (2019). https://doi.org/10.1002/admt.201800334.

[135] R. Kumar, E. Joanni, R.K. Singh, E.T.S.G. da Silva, R. Savu, L.T. Kubota, S.A. Moshkalev, Direct laser writing of micro-supercapacitors on thick graphite oxide films and their electrochemical properties in different liquid inorganic electrolytes, J Colloid Interface Sci 507 (2017) 271–278. https://doi.org/10.1016/j.jcis.2017.08.005.

[136] K. Sugioka, Progress in ultrafast laser processing and future prospects, Nanophotonics 6 (2017) 393–413. https://doi.org/10.1515/nanoph-2016-0004.

[137] B.K. Nayak, M.C. Gupta, K.W. Kolasinski, Spontaneous formation of nanospiked microstructures in germanium by femtosecond laser irradiation, Nanotechnology 18 (2007). https://doi.org/10.1088/0957-4484/18/19/195302.

[138] Y.H.X. al Huang Gao, K. Ramasesha, C.D. Pemmaraju, S.A. Sato, D. Whitmore, A. Gandman, J.S. Prell, L.J. Borja, D. Prendergast, K. Yabana, D.M. Neumark, S.R. Leone, Large-scale nanoshaping of ultrasmooth 3D crystalline metallic structures, Science (1979) 346 (2014) 1348–1352. https://doi.org/10.1126/science.1260311.

[139] B.L.Y.W. et al. Luming Yu, ultra-smallsize (1 -20 μm) blue and green micro-LEDs fabricated by Iaser direct writing lithography, n.d.

[140] C. Momma, S. Nolte, B.N. Chichkov, F. V Alvensleben, A.T. Tunnermann¨, Precise laser ablation with ultrashort pulses, 1997.

[141] K. Ozono, M. Obara, A. Usui, H. Sunakawa, M. Obara, High-speed ablation etching of GaN semiconductor using femtosecond laser, 2001. www.elsevier.com/locate/optcom.

[142] T. Kim, H.S. Kim, M. Hetterich, D. Jones, J.M. Girkin, E. Bente, M.D. Dawson, Femtosecond laser machining of gallium nitride, 2001. www.elsevier.com/locate/mseb.

[143] G. Ricel, D. Jones2, K.S. Kim1, J.M. Girkin1, D. Jarozynski2, M.D. Dawson1, Micromachining of gallium nitride, sapphire and silicon carbide with ultrashort pulses, n.d. http://spiedl.org/terms.

[144] S. Nakashima, K. Sugioka, K. Midorikawa, Fabrication of microchannels in single-crystal GaN by wet-chemical-assisted femtosecond-laser ablation, Appl Surf Sci 255 (2009) 9770–9774. https://doi.org/10.1016/j.apsusc.2009.04.159.

[145] S. Nakashima, K. Sugioka, T. Ito, H. Takai, K. Midorikawa, Fabrication of periodic nano-hole array on GaN surface by fs laser for improvement of extraction efficiency in blue LED, in: Phys Procedia, Elsevier B.V., 2010: pp. 203–211. https://doi.org/10.1016/j.phpro.2010.08.138.

[146] G.F.B. Almeida, L.K. Nolasco, G.R. Barbosa, A. Schneider, A. Jaros, I. Manglano Clavero, C. Margenfeld, A. Waag, T. Voss, C.R. Mendonça, Incubation effect during laser micromachining of GaN films with femtosecond pulses, Journal of Materials Science: Materials in Electronics 30 (2019) 16821–16826. https://doi.org/10.1007/s10854-019-01373-2.

[147] L.K. Nolasco, G.F.B. Almeida, T. Voss, C.R. Mendonça, Femtosecond laser micromachining of GaN using different wavelengths from near-infrared to ultraviolet, J Alloys Compd 877 (2021). https://doi.org/10.1016/j.jallcom.2021.160259.

[148] H. Wei, C. Huang, H. Liu, D. Liu, P. Yao, D. Chu, Modeling and optimizing femtosecond laser process parameters for high-efficient and near damage-free micromachining of single-crystal GaN substrate, Mater Sci Semicond Process 153 (2023). https://doi.org/10.1016/j.mssp.2022.107123.

[149] K.H. Li, Y.F. Cheung, C.W. Tang, C. Zhao, K.M. Lau, H.W. Choi, Optical crosstalk analysis of micro-pixelated GaN-based light-emitting diodes on sapphire and Si substrates, Physica Status Solidi (A) Applications and Materials Science 213 (2016) 1193–1198. https://doi.org/10.1002/pssa.201532789.

[150] K.H. Li, Y.F. Cheung, W.S. Cheung, H.W. Choi, Confocal microscopic analysis of optical crosstalk in GaN micro-pixel light-emitting diodes, Appl Phys Lett 107 (2015). https://doi.org/10.1063/1.4934840.

[151] S.-H. Li, C.-P. Lin, Y.-H. Fang, W.-H. Kuo, M.-H. Wu, C.-L. Chao, R.-H. Horng, G.-D.J. Su, Performance analysis of GaN-based micro light-emitting diodes by laser lift-off process, Solid State Electronics Letters 1 (2019) 58–63. https://doi.org/10.1016/j.ssel.2019.06.001.

[152] V.W. Lee, N. Twu, I. Kymissis, Micro-LED technologies and applications, Inf Disp (1975) 32 (2016) 16–23. https://doi.org/10.1002/j.2637-496x.2016.tb00949.x.

[153] Z. Chen, S. Yan, C. Danesh, MicroLED technologies and applications: Characteristics, fabrication, progress, and challenges, J Phys D Appl Phys 54 (2021). https://doi.org/10.1088/1361-6463/abcfe4.

[154] C.C. Lin, Y.R. Wu, H.C. Kuo, M.S. Wong, S.P. DenBaars, S. Nakamura, A.

Pandey, Z. Mi, P. Tian, K. Ohkawa, D. Iida, T. Wang, Y. Cai, J. Bai, Z. Yang, Y. Qian, S.T. Wu, J. Han, C. Chen, Z. Liu, B.R. Hyun, J.H. Kim, B. Jang, H.D. Kim, H.J. Lee, Y.T. Liu, Y.H. Lai, Y.L. Li, W. Meng, H. Shen, B. Liu, X. Wang, K.L. Liang, C.J. Luo, Y.H. Fang, The micro-LED roadmap: status quo and prospects, JPhys Photonics 5 (2023). https://doi.org/10.1088/2515-7647/acf972.

[155] A. Fang, Z. Du, W. Guo, J. Liu, H. Xu, P. Tang, J. Sun, Advancements in Micro-LED Performance through Nanomaterials and Nanostructures: A Review, Nanomaterials 14 (2024) 940. https://doi.org/10.3390/nano14110940.

[156] M.K. Kelly, O. Ambacher, R. Dimitrov, R. Handschuh, M. Stutzmann, Optical process for lift of Group III-nitride films, (n.d.). https://doi.org/10.1002/1521-396X(199701)159:1.

[157] W.S. Wong, T. Sands, N.W. Cheung, Damage-free separation of GaN thin films from sapphire substrates, Appl Phys Lett 72 (1998) 599–601. https://doi.org/10.1063/1.120816.

[158] W.S. Wong, T. Sands, N.W. Cheung, M. Kneissl, D.P. Bour, P. Mei, L.T. Romano, N.M. Johnson, Fabrication of thin-film InGaN light-emitting diode membranes by laser lift-off, Appl Phys Lett 75 (1999) 1360–1362. https://doi.org/10.1063/1.124693.

[159] H.K. Cho, S.K. Kim, D.K. Bae, B.C. Kang, J.S. Lee, Y.H. Lee, Laser liftoff GaN thin-film photonic crystal GaN-based light-emitting diodes, IEEE Photonics Technology Letters 20 (2008) 2096–2098. https://doi.org/10.1109/LPT.2008.2006506.

[160] W.S. Wong, Y. Cho, E.R. Weber, T. Sands, K.M. Yu, J. Krüger, A.B. Wengrow, N.W. Cheung, Structural and optical quality of GaN/metal/Si heterostructures fabricated by excimer laser lift-off, Appl Phys Lett 75 (1999) 1887–1889. https://doi.org/10.1063/1.124861.

[161] C.F. Chu, F.I. Lai, J.T. Chu, C.C. Yu, C.F. Lin, H.C. Kuo, S.C. Wang, Study of GaN light-emitting diodes fabricated by laser lift-off technique, J Appl Phys 95 (2004) 3916–3922. https://doi.org/10.1063/1.1651338.

[162] T.S. Kang, X.T. Wang, C.F. Lo, F. Ren, S.J. Pearton, O. Laboutin, Y. Cao, J.W. Johnson, J. Kim, Simulation and experimental study of ArF 193 nm laser lift-off AlGaN/GaN high electron mobility transistors, Journal of Vacuum Science & Technology B, Nanotechnology and Microelectronics: Materials, Processing, Measurement, and Phenomena 30 (2012). https://doi.org/10.1116/1.3664283.

[163] R. Delmdahl, R. Pätzel, J. Brune, R. Senczuk, C. Goßler, R. Moser, M. Kunzer, U.T. Schwarz, Line beam processing for laser lift-off of GaN from sapphire, Physica Status Solidi (A) Applications and Materials Science 209 (2012) 2653–2658. https://doi.org/10.1002/pssa.201228430.

[164] S.H. Lee, S.Y. Park, K.J. Lee, Laser lift-off of GaN thin film and its application to the flexible light emitting diodes, in: Biosensing and Nanomedicine V, SPIE, 2012: p. 846011. https://doi.org/10.1117/12.964095.

[165] H.P. Ho, K.C. Lo, G.G. Siu', C. Surya, Raman spectroscopy study on free-standing GaN separated from sapphire substrates by 532nm Nd:YAG laser lift-off, n.d.

[166] V. Voronenkov, N. Bochkareva, R. Gorbunov, A. Zubrilov, V. Kogotkov, P. Latyshev, Y. Lelikov, A. Leonidov, Y. Shreter, Laser slicing: A thin film lift-off method for GaN-on-GaN technology, Results Phys 13 (2019).

https://doi.org/10.1016/j.rinp.2019.102233.

[167] Y. Gong, Z. Gong, Laser-Based Micro/Nano-Processing Techniques for Microscale LEDs and Full-Color Displays, Adv Mater Technol 8 (2023). https://doi.org/10.1002/admt.202200949.

[168] J. Chun, Y. Hwang, Y.S. Choi, T. Jeong, J.H. Baek, H.C. Ko, S.J. Park, Transfer of GaN LEDs from sapphire to flexible substrates by laser lift-off and contact printing, IEEE Photonics Technology Letters 24 (2012) 2115–2118. https://doi.org/10.1109/LPT.2012.2221694.

[169] T. Il Kim, Y.H. Jung, J. Song, D. Kim, Y. Li, H.S. Kim, I.S. Song, J.J. Wierer, H.A. Pao, Y. Huang, J.A. Rogers, High-efficiency, microscale GaN light-emitting diodes and their thermal properties on unusual substrates, Small 8 (2012) 1643–1649. https://doi.org/10.1002/smll.201200382.

[170] Y.F. Cheung, K.H. Li, H.W. Choi, Flexible Free-Standing III-Nitride Thin Films for Emitters and Displays, ACS Appl Mater Interfaces 8 (2016) 21440–21445. https://doi.org/10.1021/acsami.6b04413.

[171] G. Ezhilarasu, A. Hanna, S.S. Iyer, A. Paranjpe, High yield precision transfer and assembly of GaN μLEDs using laser assisted micro transfer printing, in: Proceedings - Electronic Components and Technology Conference, Institute of Electrical and Electronics Engineers Inc., 2019: pp. 1470–1474. https://doi.org/10.1109/ECTC.2019.00226.

[172] Z. Pan, C. Guo, X. Wang, J. Liu, R. Cao, Y. Gong, J. Wang, N. Liu, Z. Chen, L. Wang, M. Ishikawa, Z. Gong, Wafer-Scale Micro-LEDs Transferred onto an Adhesive Film for Planar and Flexible Displays, Adv Mater Technol 5 (2020). https://doi.org/10.1002/admt.202000549.

[173] G. Ezhilarasu, A. Paranjpe, J. Lee, F. Wei, S.S. Iyer, A Heterogeneously Integrated, High Resolution and Flexible Inorganic μlED Display using Fan-Out Wafer-Level Packaging, in: Proceedings - Electronic Components and Technology Conference, Institute of Electrical and Electronics Engineers Inc., 2020: pp. 677–684. https://doi.org/10.1109/ECTC32862.2020.00112.

[174] W. Tian, Y. Wu, T. Wu, L. Dou, X. Cao, J. Li, Mechanisms and Performance Analysis of GaN-Based Micro-LED Grown on Pattern Sapphire Substrate by Laser Lift-Off Process, ECS Journal of Solid State Science and Technology 11 (2022) 046001. https://doi.org/10.1149/2162-8777/ac63e5.

[175] L. Tang, Y. Wang, G. Cheng, M.J. Manfra, T.D. Sands, Free standing GaN nano membrane by laser lift-off method, Mater. Res. Soc. Symp. Proc 14 (2012). https://doi.org/10.1557/opl.2012.

[176] R. Delmdahl, Fabricating the Flexible Future: How UV laser systems enable the transition from rigid to flexible in microelectronics manufacturing, Optik & Photonik 11 (2016) 28–30. https://doi.org/10.1002/opph.201600039.

[177] X.L. Tong, L. Li, D.S. Zhang, Y.T. Dai, D.J. Lv, K. Ling, Z.X. Liu, P.X. Lu, G. Yang, Z.Y. Yang, H. Long, The influences of laser scanning speed on the structural and optical properties of thin GaN films separated from sapphire substrates by excimer laser lift-off, J Phys D Appl Phys 42 (2009). https://doi.org/10.1088/0022-3727/42/4/045414.

[178] A.D. Williams, T.D. Moustakas, Formation of large-area freestanding gallium nitride substrates by natural stress-induced separation of GaN and sapphire, J Cryst Growth

300 (2007) 37–41. https://doi.org/10.1016/j.jcrysgro.2006.10.224.

[179] J.-H. Cheng, Y.S. Wu, W.C. Peng, H. Ouyang, Effects of Laser Sources on Damage Mechanisms and Reverse-Bias Leakages of Laser Lift-Off GaN-Based LEDs, J Electrochem Soc 156 (2009) H640. https://doi.org/10.1149/1.3148251.

[180] M. Chen, J.Y. Zhang, X.Q. Lv, L.Y. Ying, B.P. Zhang, Effect of laser pulse width on the laser lift-off process of GaN films, Chinese Physics Letters 30 (2013). https://doi.org/10.1088/0256-307X/30/1/014203.

[181] T. Wang, Y. Fang, X. Guo, G. Shen, Z. Cui, Experimental and numerical investigation on GaN/Al2O3 laser lift-off technique, Thin Solid Films 515 (2007) 3854–3857. https://doi.org/10.1016/j.tsf.2006.10.110.

[182] T. Bret, V. Wagner, D. Martin, P. Hoffmann, M. Ilegems, A Mechanistic Study of GaN Laser Lift-Off, n.d.

[183] S. Krause, P.T. Miclea, G. Seifert, Selective femtosecond laser lift-off process for scribing in thin-film photovoltaics, Journal of Laser Micro Nanoengineering 10 (2015) 274–278. https://doi.org/10.2961/jlmn.2015.03.0007.

[184] J. Kim, J.H. Kim, S.H. Cho, K.H. Whang, Selective lift-off of GaN light-emitting diode from a sapphire substrate using 266-nm diode-pumped solid-state laser irradiation, Appl Phys A Mater Sci Process 122 (2016). https://doi.org/10.1007/s00339-016-9928-7.

[185] J. Park, Y.G. Sin, J.H. Kim, J. Kim, Dependence of adhesion strength between GaN LEDs and sapphire substrate on power density of UV laser irradiation, Appl Surf Sci 384 (2016) 353–359. https://doi.org/10.1016/j.apsusc.2016.05.078.

[186] S. Bornemann, N. Yulianto, H. Spende, Y. Herbani, J.D. Prades, H.S. Wasisto, A. Waag, Femtosecond Laser Lift-Off with Sub-Bandgap Excitation for Production of Free-Standing GaN Light-Emitting Diode Chips, Adv Eng Mater 22 (2020). https://doi.org/10.1002/adem.201901192.

[187] K. Ding, V. Avrutin, N. Izyumskaya, Ü. Özgür, H. Morkoç, Micro-LEDs, a manufacturability perspective, Applied Sciences (Switzerland) 9 (2019). https://doi.org/10.3390/app9061206.

[188] V.R. Marinov, Laser-Enabled Extremely-High Rate Technology for μLED Assembly, in: Dig Tech Pap, John Wiley and Sons Inc, 2018: pp. 692–695. https://doi.org/10.1002/SDTP.12352.

[189] 84, (n.d.).

[190] M.A. Meitl, Z.T. Zhu, V. Kumar, K.J. Lee, X. Feng, Y.Y. Huang, I. Adesida, R.G. Nuzzo, J.A. Rogers, Transfer printing by kinetic control of adhesion to an elastomeric stamp, Nat Mater 5 (2006) 33–38. https://doi.org/10.1038/nmat1532.

[191] S.H. Ahn, L.J. Guo, Large-area roll-to-roll and roll-to-plate Nanoimprint Lithography: A step toward high-throughput application of continuous nanoimprinting, ACS Nano 3 (2009) 2304–2310. https://doi.org/10.1021/nn9003633.

[192] B.K. Sharma, B. Jang, J.E. Lee, S. Bae, T.W. Kim, H. Lee, J. Kim, J. Ahn, Stretchable Electronics: Load-Controlled Roll Transfer of Oxide Transistors for Stretchable Electronics (Adv. Funct. Mater. 16/2013), Adv Funct Mater 23 (2013) 1977–1977. https://doi.org/10.1002/adfm.201370078.

[193] I. Zergioti, S. Mailis, N.A. Vainos, C. Fotakis, S. Chen, C.P. Grigoropoulos,

Microdeposition of metals by femtosecond excimer laser, 1998.

[194] R. Fardel, M. Nagel, F. Nüesch, T. Lippert, A. Wokaun, Laser-induced forward transfer of organic LED building blocks studied by time-resolved shadowgraphy, Journal of Physical Chemistry C 114 (2010) 5617–5636. https://doi.org/10.1021/jp907387q.

[195] Z. Yan, T. Pan, M. Xue, C. Chen, Y. Cui, G. Yao, L. Huang, F. Liao, W. Jing, H. Zhang, M. Gao, D. Guo, Y. Xia, Y. Lin, Thermal Release Transfer Printing for Stretchable Conformal Bioelectronics, Advanced Science 4 (2017). https://doi.org/10.1002/advs.201700251.

[196] R. Li, Y. Li, C. Lü, J. Song, R. Saeidpourazar, B. Fang, Y. Zhong, P.M. Ferreira, J.A. Rogers, Y. Huang, Axisymmetric thermo-mechanical analysis of laser-driven non-contact transfer printing, Int J Fract 176 (2012) 189–194. https://doi.org/10.1007/s10704-012-9744-9.

[197] J. Eisenhaure, S. Kim, Laser-Driven Shape Memory Effect for Transfer Printing Combining Parallelism with Individual Object Control, Adv Mater Technol 1 (2016). https://doi.org/10.1002/admt.201600098.

[198] S. Bornemann, N. Yulianto, H. Spende, Y. Herbani, J.D. Prades, H.S. Wasisto, A. Waag, Femtosecond Laser Lift-Off with Sub-Bandgap Excitation for Production of Free-Standing GaN Light-Emitting Diode Chips, Adv Eng Mater 22 (2020). https://doi.org/10.1002/adem.201901192.

[199] R. Miller, V. Marinov, O. Swenson, Z. Chen, M. Semler, Noncontact selective laser-assisted placement of thinned semiconductor dice, IEEE Trans Compon Packaging Manuf Technol 2 (2012) 971–978. https://doi.org/10.1109/TCPMT.2012.2183594.

[200] N.S. Karlitskaya, J. Meijer, D.F. de Lange, H. Kettelarij, Laser propulsion of microelectronic components: releasing mechanism investigation, in: High-Power Laser Ablation VI, SPIE, 2006: p. 62612P. https://doi.org/10.1117/12.673815.

[201] J. Bian, L. Zhou, X. Wan, C. Zhu, B. Yang, Y.A. Huang, Laser Transfer, Printing, and Assembly Techniques for Flexible Electronics, Adv Electron Mater 5 (2019). https://doi.org/10.1002/aelm.201800900.

[202] H. Luo, C. Wang, C. Linghu, K. Yu, C. Wang, J. Song, Laser-driven programmable non-contact transfer printing of objects onto arbitrary receivers via an active elastomeric microstructured stamp, Natl Sci Rev 7 (2020) 296–304. https://doi.org/10.1093/nsr/nwz109.

[203] R. Saeidpourazar, R. Li, Y. Li, M.D. Sangid, C. Lu, Y. Huang, J.A. Rogers, P.M. Ferreira, Laser-driven micro transfer placement of prefabricated microstructures, Journal of Microelectromechanical Systems 21 (2012) 1049–1058. https://doi.org/10.1109/JMEMS.2012.2203097.

[204] C. Linghu, S. Zhang, C. Wang, K. Yu, C. Li, Y. Zeng, H. Zhu, X. Jin, Z. You, J. Song, Universal SMP gripper with massive and selective capabilities for multiscaled, arbitrarily shaped objects, 2020. http://advances.sciencemag.org/.

[205] C. Wang, C. Linghu, S. Nie, C. Li, Q. Lei, X. Tao, Y. Zeng, Y. Du, S. Zhang, K. Yu, H. Jin, W. Chen, J. Song, Programmable and scalable transfer printing with high reliability and efficiency for flexible inorganic electronics, 2020. http://advances.sciencemag.org/.

[206] J. Bohandy, B.F. Kim, F.J. Adrian, Metal deposition from a supported metal film

using an excimer laser, J Appl Phys 60 (1986) 1538–1539. https://doi.org/10.1063/1.337287.

[207] D.P. Banks, C. Grivas, J.D. Mills, R.W. Eason, I. Zergioti, Nanodroplets deposited in microarrays by femtosecond Ti:sapphire laser-induced forward transfer, Appl Phys Lett 89 (2006). https://doi.org/10.1063/1.2386921.

[208] M. Feinaeugle, P. Gregorčič, D.J. Heath, B. Mills, R.W. Eason, Time-resolved imaging of flyer dynamics for femtosecond laser-induced backward transfer of solid polymer thin films, Appl Surf Sci 396 (2017) 1231–1238. https://doi.org/10.1016/j.apsusc.2016.11.120.

[209] T. Sano, H. Yamada, T. Nakayama, I. Miyamoto, Experimental investigation of laser induced forward transfer process of metal thin ®lms, n.d.

[210] J.M. Fitz-Gerald, A. Piqué, D.B. Chrisey, P.D. Rack, M. Zeleznik, R.C.Y. Auyeung, S. Lakeou, Laser direct writing of phosphor screens for high-definition displays, Appl Phys Lett 76 (2000) 1386–1388. https://doi.org/10.1063/1.126040.

[211] R. Fardel, M. Nagel, F. Nüesch, T. Lippert, A. Wokaun, Laser forward transfer using a sacrificial layer: Influence of the material properties, Appl Surf Sci 254 (2007) 1322–1326. https://doi.org/10.1016/j.apsusc.2007.08.091.

[212] J. Bian, F. Chen, B. Yang, J. Hu, N. Sun, D. Ye, Y. Duan, Z. Yin, Y. Huang, Laser-Induced Interfacial Spallation for Controllable and Versatile Delamination of Flexible Electronics, ACS Appl Mater Interfaces 12 (2020) 54230–54240. https://doi.org/10.1021/acsami.0c18951.

[213] R. Miller, V. Marinov, O. Swenson, Z. Chen, M. Semler, Noncontact selective laser-assisted placement of thinned semiconductor dice, IEEE Trans Compon Packaging Manuf Technol 2 (2012) 971–978. https://doi.org/10.1109/TCPMT.2012.2183594.

[214] J. Hong, Thermo-Mechanical Analysis of Blister Formation on a Rigid Substrate in Blister-Actuated Laser-Induced Forward Transfer, IEEE Trans Compon Packaging Manuf Technol 10 (2020) 637–643. https://doi.org/10.1109/TCPMT.2019.2959708.

[215] V.R. Marinov, Laser-Enabled Extremely-High Rate Technology for μLED Assembly, in: Dig Tech Pap, John Wiley and Sons Inc, 2018: pp. 692–695. https://doi.org/10.1002/SDTP.12352.

[216] B. Zhang, O. Haupt, Microled-high throughput laser based mass transfer technology, in: Dig Tech Pap, John Wiley and Sons Inc, 2021: p. 664. https://doi.org/10.1002/sdtp.15241.

[217] D. Young, R.C.Y. Auyeung, A. Pique Â, D.B. Chrisey, D.D. Dlott, Plume and jetting regimes in a laser based forward transfer process as observed by time-resolved optical microscopy, n.d.

[218] R. Saeidpourazar, M.D. Sangid, J.A. Rogers, P.M. Ferreira, A prototype printer for laser driven micro-transfer printing, in: J Manuf Process, 2012: pp. 416–424. https://doi.org/10.1016/j.jmapro.2012.09.014.

[219] R. Li, Y. Li, C. Lü, J. Song, R. Saeidpouraza, B. Fang, Y. Zhong, P.M. Ferreira, J.A. Rogers, Y. Huang, Thermo-mechanical modeling of laser-driven non-contact transfer printing: Two-dimensional analysis, Soft Matter 8 (2012) 7122–7127. https://doi.org/10.1039/c2sm25339a.

[220] D. Iqbal, M.H. Samiullah, Photo-responsive shape-memory and shape-

changing liquid-crystal polymer networks, Materials 6 (2013) 116–142. https://doi.org/10.3390/ma6010116.

[221] J.D. Eisenhaure, S. Il Rhee, A.M. Al-Okaily, A. Carlson, P.M. Ferreira, S. Kim, The use of shape memory polymers for microassembly by transfer printing, Journal of Microelectromechanical Systems 23 (2014) 1012–1014. https://doi.org/10.1109/JMEMS.2014.2345274.

[222] Y. Huang, N. Zheng, Z. Cheng, Y. Chen, B. Lu, T. Xie, X. Feng, Direct Laser Writing-Based Programmable Transfer Printing via Bioinspired Shape Memory Reversible Adhesive, ACS Appl Mater Interfaces 8 (2016) 35628–35633. https://doi.org/10.1021/acsami.6b11696.

[223] S. Kim, J. Wu, A. Carlson, S.H. Jin, A. Kovalsky, P. Glass, Z. Liu, N. Ahmed, S.L. Elgan, W. Chen, P.M. Ferreira, M. Sitti, Y. Huang, J.A. Rogers, Microstructured elastomeric surfaces with reversible adhesion and examples of their use in deterministic assembly by transfer printing, (n.d.). https://doi.org/10.1073/pnas.1005828107/-/DCSupplemental.

[224] R.H. Horng, Y.F. Chen, C.H. Wang, H.Y. Chen, Development of Metal Bonding for Passive Matrix Micro-LED Display Applications, IEEE Electron Device Letters 42 (2021) 1017–1020. https://doi.org/10.1109/LED.2021.3078778.

[225] W. Guo, H. Meng, Y. Chen, T. Sun, Y. Li, Wafer-Level Monolithic Integration of Vertical Micro-LEDs on Glass, IEEE Photonics Technology Letters 32 (2020) 673–676. https://doi.org/10.1109/LPT.2020.2991672.

[226] C.M. Kang, J.Y. Lee, D.J. Kong, J.P. Shim, S. Kim, S.H. Mun, S.Y. Choi, M. Do Park, J. Kim, D.S. Lee, Hybrid Full-Color Inorganic Light-Emitting Diodes Integrated on a Single Wafer Using Selective Area Growth and Adhesive Bonding, ACS Photonics 5 (2018) 4413–4422. https://doi.org/10.1021/acsphotonics.8b00876.

[227] O.B. Shchekin, J.E. Epler, T.A. Trottier, T. Margalith, D.A. Steigerwald, M.O. Holcomb, P.S. Martin, M.R. Krames, High performance thin-film flip-chip InGaN-GaN light-emitting diodes, Appl Phys Lett 89 (2006). https://doi.org/10.1063/1.2337007.

[228] X.L. Hu, J. Zhang, H. Wang, X.C. Zhang, High-luminous efficacy white light-emitting diodes with thin-film flip-chip technology and surface roughening scheme, J Phys D Appl Phys 49 (2016). https://doi.org/10.1088/0022-3727/49/44/445102.

[229] K. Lee, H.J. Kim, M.J. Yim, K.W. Paik, Ultrasonic bonding using anisotropic conductive Films (ACFs) for flip chip interconnection, IEEE Transactions on Electronics Packaging Manufacturing 32 (2009) 241–247. https://doi.org/10.1109/TEPM.2009.2027894.

[230] M.H. Hong, S.C. Kim, Y.H. Kim, Ultra-fine pitch chip-on-glass (COG) bonding with metal bumps having insulating layer in the side walls using anisotropic conductive film (ACF), Current Applied Physics 12 (2012) 612–615. https://doi.org/10.1016/j.cap.2011.07.016.

[231] C. Liou, F. Shih, Y. Huang, Z. Hu, C. Tsou, W. Fang, The Implementation of Sapphire Microreflector for Monolithic Micro-LED Array, IEEE Trans Compon Packaging Manuf Technol 11 (2021) 181–190. https://doi.org/10.1109/TCPMT.2021.3049563.

[232] C. Linghu, S. Zhang, C. Wang, H. Luo, J. Song, Mass transfer for Micro-LED display: Transfer printing techniques, in: Semiconductors and Semimetals, Academic Press

Inc., 2021: pp. 253–280. https://doi.org/10.1016/bs.semsem.2020.12.002.

[233] K.S. Choi, J. Joo, K.S. Jang, Y.S. Eom, G.M. Choi, H.G. Yun, S.H. Moon, J.S. Kim, M. Oh, J.H. Choi, J.W. Choi, S.Y. Cho, S. Choi, S.H. Park, G.C. Kim, S.K. Kim, J.S. Kim, S. Yoo, Development of Digital Signage Modules composed of Mini-LEDs using Laser-Assisted Bonding (LAB) Technology, in: Proceedings - Electronic Components and Technology Conference, Institute of Electrical and Electronics Engineers Inc., 2020: pp. 1031–1036. https://doi.org/10.1109/ECTC32862.2020.00167.

[234] K.-S. Choi, J. Joo, K. Jang, G.-M. Choi, H.-G. Yun, S.H. Moon, Y.-S. Eom, Laser-Assisted Bonding (LAB), Its Bonding Materials, and Their Applications, Journal of Welding and Joining (2020). https://doi.org/10.5781/jwj.2020.38.2.2.

[235] K. Schricker, L. Samfaß, M. Grätzel, G. Ecke, J.P. Bergmann, Bonding mechanisms in laser-assisted joining of metal-polymer composites, Journal of Advanced Joining Processes 1 (2020). https://doi.org/10.1016/j.jajp.2020.100008.

[236] K.S. Choi, J. Joo, Y.S. Eom, G.M. Choi, K.S. Jang, C. Lee, S.H. Moon, H.G. Yun, J.H. Choi, J.W. Choi, Simultaneous Transfer and Bonding (SITRAB) Process for Micro-LEDs Using Laser-Assisted Bonding with Compression (LABC) Process and SITRAB Adhesive, in: Proceedings - Electronic Components and Technology Conference, Institute of Electrical and Electronics Engineers Inc., 2021: pp. 1607–1613. https://doi.org/10.1109/ECTC32696.2021.00255.

[237] J. Joo, C. Lee, I.S. Kye, Y.S. Eom, K.S. Jang, G.M. Choi, S.H. Moon, H.G. Yun, K.S. Choi, Development of simultaneous transferring and bonding (SITRAB) process for LED arrays using Anisotropic Solder Paste (ASP) and Laser-Assisted Bonding (LAB) Technology, in: Proceedings - Electronic Components and Technology Conference, Institute of Electrical and Electronics Engineers Inc., 2021: pp. 687–692. https://doi.org/10.1109/ECTC32696.2021.00119.

[238] Y.S. Eom, G.M. Choi, K.S. Jang, J. Joo, C. mi Lee, J.H. Oh, S.H. Moon, K.S. Choi, Process window of simultaneous transfer and bonding materials using laser-assisted bonding for mini- and micro-LED display panel packaging, ETRI Journal 46 (2024) 347–359. https://doi.org/10.4218/etrij.2022-0471.

[239] W. Tian, Z. Ma, X. Cao, J. Lin, Y. Cui, X. Huang, Application of metal interconnection process with micro-LED display by laser-assisted bonding technology, Journal of Materials Science: Materials in Electronics 34 (2023). https://doi.org/10.1007/s10854-023-11549-6.

[240] K. Kim, G. Jung, J. Kim, Y. Sung, J. Kang, W.J. Lee, Y. Moon, T. Jeong, J.H. Song, Correlation between photoluminescence and electroluminescence in GaN-related micro light emitting diodes: Effects of leakage current, applied bias, incident light absorption and carrier escape, Opt Mater (Amst) 120 (2021). https://doi.org/10.1016/j.optmat.2021.111448.

[241] N. Kokubo, Y. Tsunooka, F. Fujie, J. Ohara, S. Onda, H. Yamada, M. Shimizu, S. Harada, M. Tagawa, T. Ujihara, Nondestructive visualization of threading dislocations in GaN by micro raman mapping, Jpn J Appl Phys 58 (2019). https://doi.org/10.7567/1347-4065/ab0acf.

[242] K.R. Bagnall, E.A. Moore, S.C. Badescu, L. Zhang, E.N. Wang, Simultaneous measurement of temperature, stress, and electric field in GaN HEMTs with micro-Raman

spectroscopy, Review of Scientific Instruments 88 (2017). https://doi.org/10.1063/1.5010225.

[243] H. Yamamoto, K. Agui, Y. Uchida, S. Mochizuki, T. Uruma, N. Satoh, T. Hashizume, Evaluation of carrier concentration reduction in GaN-on-GaN wafers by Raman spectroscopy and Kelvin force microscopy, Jpn J Appl Phys 56 (2017). https://doi.org/10.7567/JJAP.56.08LB07.

[244] T. Passow, M. Kunzer, A. Pfeuffer, M. Binder, J. Wagner, Ultraviolet laser ablation as technique for defect repair of GaN-based light-emitting diodes, Appl Phys A Mater Sci Process 124 (2018). https://doi.org/10.1007/s00339-018-1681-7.

[245] M. Mikulics, P. Kordoš, D. Gregušová, Z. Sofer, A. Winden, S. Trellenkamp, J. Moers, J. Mayer, H. Hardtdegen, Conditioning nano-LEDs in arrays by laser-micro-annealing: The key to their performance improvement, Appl Phys Lett 118 (2021). https://doi.org/10.1063/5.0038070.

[246] B.S. Zheng, C.L. Ho, K.Y. Cheng, C.L. Liao, M.C. Wu, K.C. Hsieh, Improved contact characteristics of laser-annealed p-GaN coated with Ni films, J Appl Phys 118 (2015). https://doi.org/10.1063/1.4929522.

[247] H.W. Jang, T. Sands, J.L. Lee, Effects of KrF excimer laser irradiation on metal contacts to n-type and p-type GaN, J Appl Phys 94 (2003) 3529–3535. https://doi.org/10.1063/1.1594814.

[248] Y.C. Cheng, C.C. Liao, S.W. Feng, C.C. Yang, Y.S. Lin, M. Kung-Jeng, C.C. Chou, C.M. Lee, J.I. Chyi, Laser-induced activation of p-type GaN with the second harmonics of a Nd:YAG laser, Japanese Journal of Applied Physics, Part 1: Regular Papers and Short Notes and Review Papers 40 (2001) 2143–2145. https://doi.org/10.1143/jjap.40.2143.

[249] S. Zhang, H. Zheng, L. Zhou, H. Li, Y. Chen, C. Wei, T. Wu, W. Lv, G. Zhang, S. Zhang, Z. Gong, B. Jia, H. Lin, Z. Gao, W. Xu, H. Ning, Research Progress of Micro-LED Display Technology, Crystals (Basel) 13 (2023). https://doi.org/10.3390/cryst13071001.

[250] T. Paskova, D.A. Hanser, K.R. Evans, GaN substrates for III-nitride devices, in: Proceedings of the IEEE, Institute of Electrical and Electronics Engineers Inc., 2010: pp. 1324–1338. https://doi.org/10.1109/JPROC.2009.2030699.

[251] Chen ZZ, Pan ZJ, et al. Micro-Raman combined photoluminescence detection device for micro-LED chip and method thereof. China Patent, 111443073.B, 2021-06-01

[252] Chen ZZ, Pan ZJ, et al. Raman enhancement detection method and Raman enhancement detection device for micro-LED chip. China Patent, 111610177.A, 2020-09-01